New Hampshire DOT

Research Record

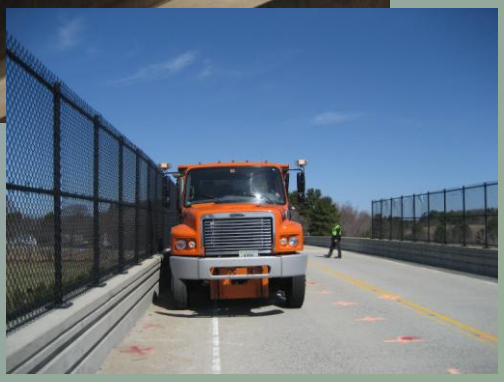

In-Service Performance Monitoring of a CFRP Reinforced HPC Bridge Deck

Final Report

Prepared by the University of New Hampshire Department of Civil Engineering for the New Hampshire Department of Transportation, in cooperation with the U.S. Department of Transportation, Federal Highway Administration

Technical Report Documentation Page

1. Report No. FHWA-NH-RD-14282I	**2. Gov. Accession No.**	**3. Recipient's Catalog No.**
4. TITLE AND SUBTITLE IN-SERVICE PERFORMANCE MONITORING OF A CFRP REINFORCED HPC BRIDGE DECK		**5. Report Date** August 2010 **6. Performing Organization Code**
7. Author(s) Erin Santini Bell, Ph.D., P.E. and Jesse Sipple		**8. Performing Organization Report No.**
9. Performing Organization Name and Address Department of Civil Engineering University of New Hampshire W141 Kingsbury Hall Durham, NH 03824		**10. Work Unit No. (TRAIS)** **11. Contract or Grant No.** 14282I, X-A000(655)
12. Sponsoring Agency Name and Address New Hampshire Department of Transportation 7 Hazen Drive, PO Box 483 Concord, NH 03302-0483		**13. Type of Report and Period Covered** FINAL REPORT **14. Sponsoring Agency Code**

15. Supplementary Notes
In cooperation with the U. S. Department of Transportation, Federal Highway Administration

16. Abstract

The Rollins Road Bridge in Rollinsford, New Hampshire was constructed in part with funding from the FHWA's Innovative Bridge Research and Construction (IBRC) program and opened to traffic in December, 2000. A requirement of the IBRC program is the use of high performance and innovative materials and the implementation of an instrumentation and evaluation plan. The FHWA provided funds for the instrumentation and data acquisition system on the bridge, but not for the long-term post-processing of the collected data. Of the originally installed 80 sensors, over 50 temperature and strain gauges are currently operational. The response recorded by these gauges is used for performance monitoring of the innovative bridge deck and overall condition assessment of the Rollins Road Bridge.

The health of the US infrastructure is on the minds of everyone following the August 1, 2007 collapse of the I-35W Bridge in Minneapolis, Minnesota. The safety of bridges nationwide should be a top priority for both our citizens and government since they are the backbone of this nation's economy, with 73% of all traffic and 90% of all truck traffic traveling over state-owned bridges. Performing nondestructive load tests, collecting structural response data, and structural modeling techniques allow bridge owners an objective insight into the health of a bridge. This report includes the Special Topics Studies required to create a structural modeling that can be used to evaluate collected data. The art of reconciling the structural model to reflect collected field data also allows bridge owners to have an up-to-date analytical model of the bridge for condition assessment, decision-making, and asset management. The results from the Rollins Road Bridge load test accurately show that a model can be updated to match measured structural response from a nondestructive load test.

17. Key Words Structural equation modeling, Load test, Dynamic loads, Live loads, Structural health monitoring, Bridge construction, Bridge superstructure, Bridge decks, High performance concrete, Data collection, Technological innovation, Demonstration project, New Hampshire	18. Distribution Statement No restrictions. This document is available to the public through the National Technical Information Service, Springfield, Virginia, 22161

19. Security Classif. (of this report)	**20. Security Classif. (of this page)**	**21. No. of Pages**	**22. Price**
Unclassified	Unclassified	172	

DISCLAIMER

This document is disseminated under the sponsorship of the New Hampshire Department of Transportation (NHDOT) and the U.S. Department of Transportation Federal Highway Administration (FHWA) in the interest of information exchange. The NHDOT and FHWA assume no liability for the use of information contained in this report. The document does not constitute a standard, specification, or regulation.

The NHDOT and FHWA do not endorse products, manufacturers, engineering firms, or software. Products, manufacturers, engineering firms, software, or proprietary trade names appearing in this report are included only because they are considered essential to the objectives of the document.

In-Service Performance Monitoring of a CFRP Reinforced HPC Bridge Deck

Final Research Report

Submitted to:
New Hampshire Department of Transportation
RAC Project No. 142821

By:

Erin Santini Bell, Ph.D., P.E.
Assistant Professor of Civil Engineering
University of New Hampshire
Principal Investigator
Ph: (603) 862-3850
Fax: (603) 862-2364
Email: erin.bell@unh.edu

Jesse Sipple
Former Graduate Research Assistant
Department of Civil Engineering
University of New Hampshire

Initial Submission: June 2009
Resubmission: August 2010

Executive Summary:

The Rollins Road Bridge in Rollinsford, New Hampshire was constructed in part with funding from the FHWA's Innovative Bridge Research and Construction (IBRC) program and opened to traffic in December, 2000. A requirement of the IBRC program is the use of high performance and innovative materials and the implementation of an instrumentation and evaluation plan. *The FHWA provided funds for the instrumentation and data acquisition system on the bridge, but not for the long-term post-processing of the collected data.* Of the originally installed 80 sensors, over 50 temperature and strain gauges are currently operational. The response recorded by these gauges is used for performance monitoring of the innovative bridge deck and overall condition assessment of the Rollins Road Bridge.

The health of the US infrastructure is on the minds of everyone following the August 1, 2007 collapse of the I-35W Bridge in Minneapolis, Minnesota. The safety of bridges nationwide should be a top priority for both our citizens and government since they are the backbone of this nation's economy, with 73% of all traffic and 90% of all truck traffic traveling over state-owned bridges. Performing nondestructive load tests, collecting structural response data, and structural modeling techniques allow bridge owners an objective insight into the health of a bridge. This report includes the Special Topics Studies required to create a structural modeling that can be used to evaluate collected data. The art of reconciling the structural model to reflect collected field data also allows bridge owners to have an up-to-date analytical model of the bridge for condition assessment, decision-making, and asset management. The results from the Rollins Road Bridge load test accurately show that a model can be updated to match measured structural response from a nondestructive load test.

TABLE OF CONTENTS

LIST OF FIGURES

LIST OF TABLES

LIST OF EQUATIONS

CHAPTER I

INTRODUCTION

1.1 – Social Need

Bridging the Gap, published by the American Association of State Highway and Transportation Officials (AASHTO) in July 2008, addressed the issues with our nation's aging infrastructure in response to the one year anniversary of the Interstate-35W Bridge collapse (Petroski, 2007). Five major problems of our nation's bridges are age and deterioration, congestion, soaring construction costs, maintaining bridge safety, and the need for new bridges. Five proposed solutions for our nation's bridges are investment, research and innovation, systematic maintenance, public awareness, and financial options (AASHTO, 2008). The collapse of the I-35W Bridge was a tragedy, however, it did bring the safety of our aging infrastructure into the public eye. The *2006 Status of the Nation's Highways, Bridges, and Transit* report published by the U.S. Department of Transportation states that of the 594,101 bridges in the National Bridge Inventory, 13.1% are rated as structurally deficient and 13.6% are rated as functionally obsolete. The terms structurally deficient and functionally obsolete mean "deteriorated conditions of significant bridge elements and reduced load-carrying capacity" and "function of the geometrics of the bridge not meeting the current design standards" respectively (U.S. Department of Transportation, 2006). In other words, structurally deficient means the

bridge cannot properly support the design or required loading and functionally obsolete means the current bridge geometric configuration does not meet current standards for the traffic using the bridge.

Prioritization of New Hampshire's red listed bridges in an efficient manner will be required to bridge the gap between the problem and the solution (NHDOT, 2008). The decision to replace or repair, and how to repair each individual bridge structure, is a common and difficult management issue for bridge owners (Farhey, 2005). The New Hampshire Section of the American Society of Civil Engineers (NHASCE) published the *2006 Report Card for New Hampshire's Infrastructure*, which states that out of the 2,113 state and 1,621 municipality owned bridges, 145 and 363 bridges, respectively, are on the red list. The red listed bridges have known deficiencies, load capacity reductions, or geometric configurations which require inspection more frequently that the standard biannual inspection routine. 167 state and 226 municipal bridges are listed as either structurally deficient or functionally obsolete. These numbers represent an overall 10% decrease in red listed bridges but a 2% increase in structurally deficient or functionally obsolete bridges with respect to the *NHASCE 2002 Report Card*. New Hampshire has been successful in removing an average of 10 state and 16 municipal owned bridges from the red list per year for the last 10 years. The report states that there is a substantial need for investment to maintain this trend (NHASCE, 2006).

Currently, the top priority for bridge owners is corrosion in the concrete deck, according to a recent study conducted by the Federal Highway Administration's (FHWA's) Long Term Bridge Performance (LTBP) Program (to be published). New Hampshire uses salt and sand for ice management on roads and bridges. It is these salts and sands that impart chlorides into the concrete deck. These chlorides permeate through the concrete and eventually cause corrosion in

the reinforcing steel. Once the steel corrodes and expands, delamination in the deck can begin. The delaminating concrete decks lose structural integrity and need replacement. Using carbon fiber reinforced polymer (CFRP) reinforcing in the deck, eliminates the fear of corrosion in the deck. During the construction of the Rollins Road Bridge with CFRP, the estimated increase in total project cost was approximately 3%. The performance of the CFRP will be evaluated as part of the research for consideration in future NHDOT and other state departments of transportation bridge construction and rehabilitation projects.

1.2 – Current State of Bridge Inspection

Several state departments of transportations (DOTs) use the PONTIS (AASHTO, 2008) program distributed by AASHTO. PONTIS is a comprehensive tool that is used to store and manage bridge information that is collected during inspection to evaluate the needs of all bridges in the specific network (Hearn, 2007). The way to gather information into PONTIS is through FHWA's National Bridge Inspection Program (NBIP). This program was developed in 1967 in response to the Silver Bridge collapse in Ohio (Phares, Rolander, Graybeal, & Washer, 2000). In 2000, Brent Phares polled state and county DOTs, as well as inspection contractors, and found that most common form of nondestructive evaluation is through visual inspection (Phares, Rolander, Graybeal, & Washer, 2000). Visual inspections are typically scheduled to be performed every 24 months.

1.3 – Visual Inspection and Structural Health Monitoring

The information bridge owners need to obtain through visual inspections is threefold; to identify any change to the serviceability of the bridge or the load capacity, what the reliability of the bridge is, and how long the structure will operate at its current capacity. Due to these needs and given that public safety and resource management are important issues to bridge

owners, an inexpensive continuous bridge monitoring system that can provide useful information relating to the condition of the bridge, the deterioration over time, damage indices, and early warning of unsafe conditions, would be an invaluable tool. This continuous monitoring along with the strategy and methodology of its implementation is the goal of structural health monitoring (Guan, Karbhari, & Sikorsky, 2007).

Visual inspections are performed by highly trained personnel that have the knowledge and experience to identify areas of concern that could lead to potential problems or that need to be investigated further. However, a more objective method of bridge assessment may be possible through the use of structural health monitoring (SHM) techniques. This method is more objective because it collects numerical data which can be correlated to the health of the bridge. Data is collected from sensors via data acquisition systems, the data is analyzed to provided measurements of structural health, which in turn will determine if a reduced bridge load rating or other immediate attention is warranted. The Rollins Road Bridge was instrumented during construction so it is an ideal candidate for inclusion in a state-wide SHM managed through the ITS Center of the NHDOT. A detailed list of other instrumentation plans and SHM methodologies developed and deployed throughout the world are included in Appendix A.

1.4 – Case Studies

The Rollins Road Bridge (RRB) Research Project is not the first in-service bridge to have instrumentation that can be used for SHM. It was the first exclusively CRFP-reinforced deck in the U.S. The instrumentation was designed to validate and assess the performance of the CFRP reinforced grid in the deck. It is this same instrumentation that this now used for SHM. In fact, there is an increasing popularity to integrate SHM into existing and new bridge projects as aging infrastructure becomes a top priority to the U.S. traveling public.

One specific case, similar to the RRB project, was a successful test on the Morristown Bridge, located on Route 100 in Vermont, U.S. The bridge was instrumented with internal temperature and fiber optic strain gauges on the glass fiber reinforced polymers (GFRP) reinforcement and in the concrete deck. A theodolite was used to measure deflections on the girder and deck during the load tests. In this specific application, the analysis of load test data concluded that the strain in the GFRP bars was significantly less than the ultimate and the tensile strain in the concrete and was well below the cracking strain for concrete. Slab and deck deflections were significantly less than AASHTO limits (Benmokrane, El-Salakawy, El-Ragaby, & Lackey, 2006). The Morristown Bridge Project did not correlate the load test data to any model. They looked directly at the stresses experienced by the material in which the gauges were attached and compared that with known material properties; element behavior as opposed to overall system response. Another project was done on the Wotton Bridge in Wotton, Quebec with similar results, again, with no use of a comparative model, parameter estimation, or model updating (Benmokrane, El-Salakawy, El-Ragaby, & Lackey, 2006).

Previous research on the Rollins Road Bridge was performed and a data-to-data comparison was examined by Martha Bowman in 2002 (Bowman M. M., 2002) (Bowman, Yost, Steffen, & Goodspeed, 2003). Initial testing on the RRB showed that transverse strains in the carbon fiber reinforced polymers (CFRP) grid could be estimated using conventional ACI design methods and the CFRP properties. There was a variation between predicted and measured strains that was attributed to temperature effects. The stress on the CFRP was less than 1% of the grid's ultimate tensile capacity and less than 2% of the grid's ultimate compressive capacity during the load test. Future work for this research project suggested that tests to determine

deflections due to only temperature change would provide insight into how the bridge globally responds to those temperature changes (Bowman M. M., 2002).

Nationally, there are several projects focused on instrumentation and evaluation of in-service structures. Once the funding for those projects expires, the continuation of retrieval and analysis of this data is limited by availability of future funding and personnel. SHM with parameter estimation can be performed with this data to create and continuously update a model that evolves as the bridge ages. This model may be able to capture loads applied and deterioration experienced. This process could aid in the tracking of the bridge as it ages and give objective information related to bridge asset management needs.

1.6 – Monitoring Model Creation

The goal of a monitoring based model is to capture accurate structural behavior. Structural models for structural health monitoring have different requirements than structural models for design. Bridges are typically designed according to design codes to produce a safe bridge design in a practical time frame. SHM modeling involves the selection of appropriate software where characteristics can be easily added, such as the modeling of elastomeric bearing pads, carbon fiber reinforced polymers, prestressing tendons, and bridge girder geometry.

1.6.1 – Modeling

With the current advancements in bridge modeling programs, such as SAP2000® (Computer & Structures Inc., Berkeley, CA) and GT Strudl® (Georgia Tech – CASE Center, Atlanta, GA), finite element modeling has often become part of the bridge design process. The SAP2000® Bridge Information Modeler can be used to compute influence lines and bridge response due to applied vehicle loads, dynamic loads, moving vehicle loads, self weight, and several other load applications including thermal loads (Computer Structures, Inc., 2007).

Programs like SAP2000® and other structural analysis and design programs are used mainly as an aid in the design process in conjunction with local and national codes.

The type of model used in a SHM program has different characteristics and areas of focus than a model used for design purposes. The SHM model must be accurate enough to capture the behavior of the bridge and be used in parameter estimation and model updating. Boundary conditions are an important and sensitive detail in modeling, such as those associated with accurately modeling elastomeric bearing pads. All loads applied to the bridge during a load test, whether they are vehicle, temperature, or wind must be included in the SHM model. All structural properties and components of the bridge during load testing such as elastomeric bearing pads, carbon fiber reinforcement polymers, the New England Bulb Tee girder, bridge rails, and temperature effects must also be included in the SHM model.

1.6.2 – Elastomeric Bearing Pads

Elastomeric bearings are recently the most common type of bearing used in bridge construction in the U.S. and have been used in bridge construction since the 1950s (Stanton, Roeder, Mackenzie-Helnwein, White, Kuester, & Craig, 2008). Figure 1 shows the steel reinforced elastomeric bearing pad used at Rollins Road Bridge. Elastomeric material is used in the bearing pad which is commonly about ⅝-inch thick layers of neoprene often separated by thin (~⅛-inch) plates of steel. These types of bearing are so popular because they resist typical bridge loads and allow for deformations without the need for machined or moving parts. This adds to the fact that they are economically feasible and are favorable when it comes to seismic codes. Simplicity of construction, economical feasibility, and favorability in seismic areas has made the elastomeric bearings the conventional type of bearing for bridges in the U.S. (Stanton, Roeder, Mackenzie-Helnwein, White, Kuester, & Craig, 2008).

Figure 1: Steel reinforced elastomeric bearing pad at Rollins Road Bridge

One specific type of elastomeric bridge bearing pad is the steel-reinforced elastomeric bearing pad, which is typically used for the highest loads. These steel-reinforced bearings contain layers of rubber and steel that are bonded together forming an alternating layered bearing. These bearing pads are stronger and stiffer in compression than non-reinforced pads, while still allowing the same shear deformations. The current methods of handling steel-reinforced elastomeric bearing in the AASHTO code are based on limited research or theoretical results. Rotation of the bearing pad was not considered a high-priority issue when the elastomeric design limits were developed, and the research done for tension limits used limited laboratory samples done almost 60 years ago. The design standards are viewed to be highly conservative and to not be verified experimentally (Stanton, Roeder, Mackenzie-Helnwein, White, Kuester, & Craig, 2008).

The difference between the requirements for design models and monitoring models can be seen with elastomeric bearing pads. The *NCHRP Report 596 – Rotation Limits for Elastomeric Bearings* goes into extensive detail on how to calculate the rotational and axial stiffness values from experimentally determined equations. Conservative bearing stiffness

values are suitable for design since they work and do not cause the structure to be under-designed. In SHM models, the behavior must be accurately captured, so a conservative estimate could cause misleading results.

1.6.3 – Carbon Fiber Reinforced Polymers

Using carbon fiber reinforced polymers (CFRP) as the primary reinforcement in a concrete bridge deck is fairly new to civil engineering structures. The increased use of these products is due to advancements in technology making it feasible in today's construction market. Composite materials, such as CFRP, use the strength of the base material, carbon fibers, held together and given stability by a polymer resin. These materials have been widely used in other industries such as transportation, marine, and aircraft. Advantages to using CFRP composites are that it is lightweight, nonmagnetic, corrosion resistant, and weather resistant. CFRP also has a high strength to weight ratio and a low maintenance requirement. CFRP is favorable for civil structures because it increases service life, reduces maintenance costs due to corrosion resistance from deicing salts, reduces time in field installation due to less weight, and decreases construction time due to ease of installation.

One disadvantage for the use of CFRP is the high initial cost of the fiber and polymer resins. CFRP reinforced bridges are beginning to be viewed as financially viable due to the life-cycle advantages that CFRP offers (Nystrom, Watkins, Antonio, & Murray, 2003). However, the lack of a well-established database for the use of fiber reinforced polymers in civil engineering structures causes designers to be reluctant to use the material (Karbhari, et al., 2003).

The CFRP is modeled in SAP2000® by using the layered shell element type. This allows for the user to input different material types and thicknesses throughout the depth of the shell element.

1.6.4 – New England Bulb Tee

The New England Bulb Tee (NEBT) girder was developed by the Precast/Prestressed Concrete Institute (PCI) New England Technical Committee for Bridges, which is a partnership between all northeast states highway departments, private consultants, and area precast fabricators. This specific beam was developed because the use of the standard AASHTO I-girder was limited in the Northeastern US. Local precast concrete fabricators did not own the forms to support deeper sections needed for long spans and structural steel was already competitive in the construction market. The goal of this committee was to establish a precast girder that would be competitive to steel in New England and the northeast (Bardow, Seraderian, & Culmo, 1997).

In order for the precast girder to survive in the Northeast markets as a viable structural element for bridge construction, it had to be capable of spanning long distances, while depth, weight, and shipping length were kept to a minimum. These limitations are necessary because most of the roads in the region were built for horse drawn vehicles, therefore when they are reconstructed, the vertical clearance under the bridges must be able to handle the vertical clearance of the taller modern railroad and/or truck traffic underneath the bridge while allowing for the higher traffic and truck loads on the deck of the of the bridge. The transportation and installation of these precast girders is complicated by the geometric configuration of a majority of the roads in the Northeast. Roads in the Northeast are, on average, very narrow and have a tight turning radii. Precast beam installation requires the use of large cranes, which also poses a problem in the Northeast region due to utility lines, private boundary limits, and small roads (Bardow, Seraderian, & Culmo, 1997).

The end results from the PCI New England Technical Committee for Bridges was a bulb tee shaped girder that would work for both pretensioning and post-tensioning by having a web width of 7-inches with five variable depths depending on the overall depth of the beam. The prestress tendon configuration commonly consists of 10 draped 13-mm (0.5 in) or 15-mm (0.6 in) strands and 21 straight 13-mm (0.5 in) or 15-mm (0.6 in) strands in the base. The NEBT can have 13-mm (0.5 in) or 15-mm (0.6 in) strands and can hold up to 52 strands, with as many as 10 draped. The NEBT girder has been used in different projects in New England since its development in the early 1990s (Bardow, Seraderian, & Culmo, 1997).

1.6.5 – Environmental Effects

Few researchers have addressed the environmental effects, specifically thermal impact, on bridge structural responses. (Sohn, Dzwonczyk, Straser, Kiremidjian, Law, & Meng, 1999) (Wipf, 1991). Research has shown that temperature can have an effect on boundary conditions (Peeters & De Roeck, 2001). A large focus and impediment in the research of thermal movements is getting accurate bridge material temperatures from ambient air temperatures (Branco & Mendes, 1993).

AASHTO does take longitudinal thermal expansion of the bridge into account in their bridge code (Moorty & Roeder, 1992). These movements are typically accounted for by the installation of bearing pads and expansion joints in order to minimize the large forces that could develop if not properly accounted for. The equation that AASHTO suggests to use for these movements is seen in Equation 1. This equation raises an important question; what is used as the coefficient of thermal expansion of the entire bridge assembly? Secondly, as mentioned before bearing pads and bridge joints are typically used to account for thermal movements, but how can one be sure if they are working properly?

Equation 1: Axial strain caused by uniform change in temperature (Hibbler, 2005)

$$\varepsilon_T = \alpha * \Delta T$$

1.7 – Research Goals and Activities

The Rollins Road Bridge (RRB) Project builds upon previous research in instrumentation done to expand the field of SHM and monitoring model creation as described above. The project began where the previous project terminated, after the completion of two successful load tests, and an analysis of the behavior of carbon fiber polymer reinforcement in the cast-in-place concrete deck. This project specifically addresses the durability of the CFRP in the RRB via data-to-data comparison as seen in Chapter IV: Data Quality Assurance and Data Quality Control and provides the NHDOT with accessible and objective data to gage the performance of the CFRP for use in future projects. A load test was performed in April 2008, and the collected data was compared to the data collected during the December 2000 and August 2001 load tests.

This research also goes a step further by creating an analytical structural model and correlating the field measured structural response and predicted structural of the analytical model. A model has been created and updated to the most current conditions of the bridge, using information from an April 2008 load test and as shown in Chapter VI: Manual Model Updating; and submitted to the New Hampshire Department of Transportation (NHDOT) to be used for bridge management and to aid in developing their SHM program. This research project will also transfer information relating how the NHDOT can use tools they currently possess to enhance their current bridge management program by adding SHM, instrumentation, parameter estimation and model updating. These additions will provide a value-added aspect to their asset management and condition assessment programs.

These new methods will also be tied into the current NHDOT practice of visual inspection, bridge assessment, load rating and special permitting. For this project, the visual

inspection report was used to develop the criteria for model creation and updating for the RRB. The goal is that the model will utilize all information received through visual inspection and instrumentation to enhance that visual inspection report with objective data. Even though the instrumentation plan for the RRB was not designed specifically for SHM and model updating, a goal of this research project is to determine the level of information, relating to the bridge health that can be drawn from the collected bridge data. Another goal of this project is to gage the performance of the CFRP-reinforced concrete as a metric for future use of this and other innovative materials.

CHAPTER II

INTRODUCTION OF ROLLINS ROAD BRIDGE

2.1 - Location

Rollins Road Bridge is located in Rollinsford, New Hampshire. Rollinsford is in southeastern New Hampshire about 12 miles from the Atlantic Ocean, see Figure 2. The bridge is not considered to be located in a coastal region, which would add considerations associated with being close to saltwater. The bridge serves as an overpass to carry Rollins Road over Main Street and an active B&M Railroad (NHDOT Bureau of Bridge Design, 1999). The weather in the area is typical of New England, with an annual snowfall of 60 inches, as recorded in Concord, NH about 35 miles west of the bridge (National Climatic Data Center). Such harsh winters mean a heavy use of deicing agents on the road surface throughout the winter months. The effects from the use of these harsh chemicals can be seen in the deck of the previous 70-year old RRB. The deck had to be replaced/repaired several times due to deterioration accelerated by use of deicing agents (Bailey & Murphy, 2008).

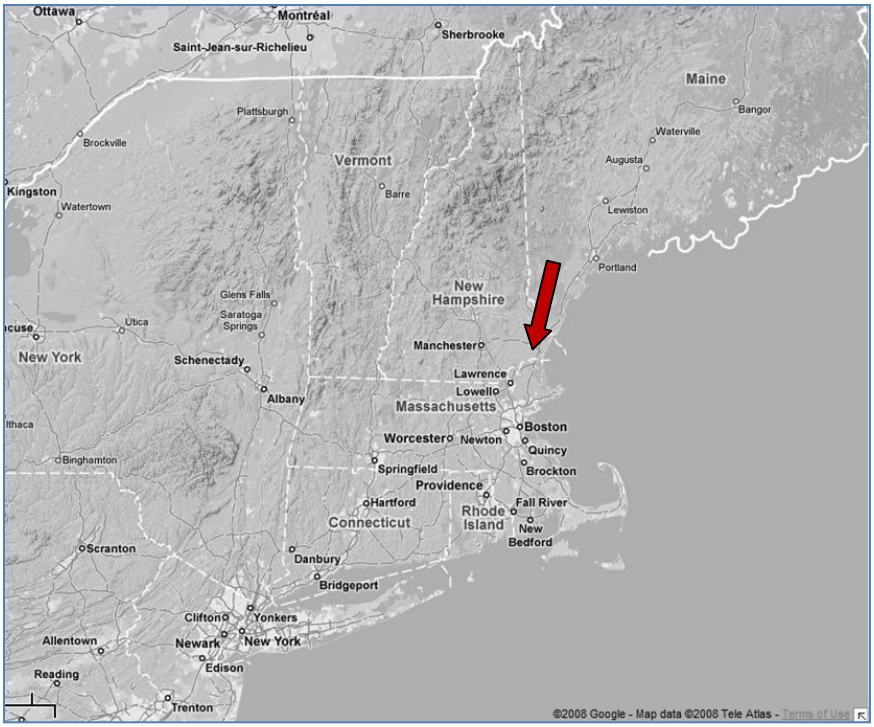

Figure 2: Location of Rollins Road Bridge (Image Courtesy of Google Maps©)

2.2 - History of the Rollins Road Bridge

The original Rollins Road Bridge was a two lane, 172-foot long bridge. Steel stringers supported a reinforced concrete deck over four simple spans, see Figure 3. The NHDOT decided that due to corrosion of both the steel reinforcement in the concrete deck and the steel stringers, the bridge needed immediate repair or replacement (Bowman, Yost, Steffen, & Goodspeed, 2003). The last inspection report of the old RRB was done during the construction of the new bridge, shown in Table 1. The report notes that there were several problems with the bridge, including a rating of 3 indicating a serious deck condition.

Figure 3: Rollins Road Bridge prior to new bridge construction (Bowman M. M., 2002)

Table 1: Excerpt of the 2000 Rollins Road Bridge Inspection Report (NHDOT Bureau of Bridge Design, 2007)

26 October 2000 Bridge Inspection Report		
Deck	3	Serious
Superstructure	4	Poor
Substructure	6	Satisfactory

The NHDOT planned to remove the old Rollins Road Bridge and construct a new bridge in its place to open in the year 2000. The new Rollins Road Bridge was designed and constructed with funding from the Innovative Bridge Research and Construction (IBRC) program which is administered by the FHWA. The new Rollins Road Bridge, referred to from this point forward as Rollins Road Bridge, is the focus of this research project on SHM for the NHDOT. The purpose of the IBRC program is "to reduce congestion associated with bridge construction and maintenance projects, to increase productivity by lowering the life-cycle costs of bridges, to keep Americans and America's commerce moving, and to enhance safety" (Office of Bridge Technology, 2008).

Two requirements of the IBRC program are the bridge is to be constructed with high performance and innovative materials and the results are to be disseminated to others. Many bridges in this program used instrumentation to objectively capture these results. The focus of the IBRC program is the use innovative techniques and materials during the bridge design and construction to reduce construction time and cost and to require less maintenance over the bridge's service life. The goal of the instrumentation in the RRB is to follow the progress of the new materials used in the bridge, again not for SHM. However, even though the instrumentation plan was not specifically designed for SHM, this research project was able to successfully utilize some of the sensors, including strain and temperature, to capture the behavior of the bridge during NDT load tests.

Rollins Road Bridge, which opened in December 2000, as seen in Figure 4, is a simply supported single span of 110-feet with a concrete beam and concrete deck superstructure. The center pier was also not included in the new bridge design for safety purposes. The bridge has a rating of 99-tons (Fu, Feng, & Dekelbab, 2003) and is in very good condition, as seen in the most recent inspection report shown in Table 2.

Figure 4: New Rollins Road Bridge, opened in 2000

Table 2: Excerpt from the 2007 Rollins Road Bridge Inspection Report (NHDOT Bureau of Bridge Design, 2007)

09 July 2007 Bridge Inspection Report		
Deck	9	Excellent
Superstructure	9	Excellent
Substructure	9	Excellent

2.3 – Rollins Road Bridge Specifics

A large part of the SHM protocol is the development of an accurate bridge model in order to capture the bridge behavior in a useful manner. In order to create that model, the structural properties of the bridge must be known with a high level of confidence and modeled accurately. Details of the bridge are presented in the Master of Science Thesis of Martha Bowman, entitled *Load Testing of the Carbon FRP Bridge Reinforce Concrete Bridge Deck on the Rollins Road Bridge, Rollinsford, New Hampshire* (Bowman M. M., 2002). Researchers at the University of New Hampshire (UNH) were actively involved in the design and construction of RRB. Researchers were present at stressing and pouring of the girders, the pouring of the concrete bridge deck, and at several other times during the construction of the bridge. Due to this presence of researchers, and excellent support from the NHDOT designers and construction personnel during the entire process, much care was taken to ensure the bridge was constructed to specification and instrumentation installed properly.

As previously mentioned, in order to obtain funding from the IBRC, the bridge needed to contain high performance and innovative materials which ended up being carbon fiber reinforcement polymers (CFRP) in the deck and high performance concrete (HPC) in the girders. The bridge also needed to be instrumented, so fiber optic strain sensors in the CFRP, deck, and girder as well as temperature sensors were included in the design. The cross section of the bridge, as seen in Figure 5, is described in detail in section 2.3.1.

Several bridge components were specifically looked at for inclusion in the bridge model, including the CFRP reinforced bridge deck, New England Bulb Tee girders, steel-reinforced elastomeric bearing pads, the bridge rail, and the instrumentation plan, see Figure 5. Accurate modeling of these components plays an important role in creating a monitoring-based analytical model.

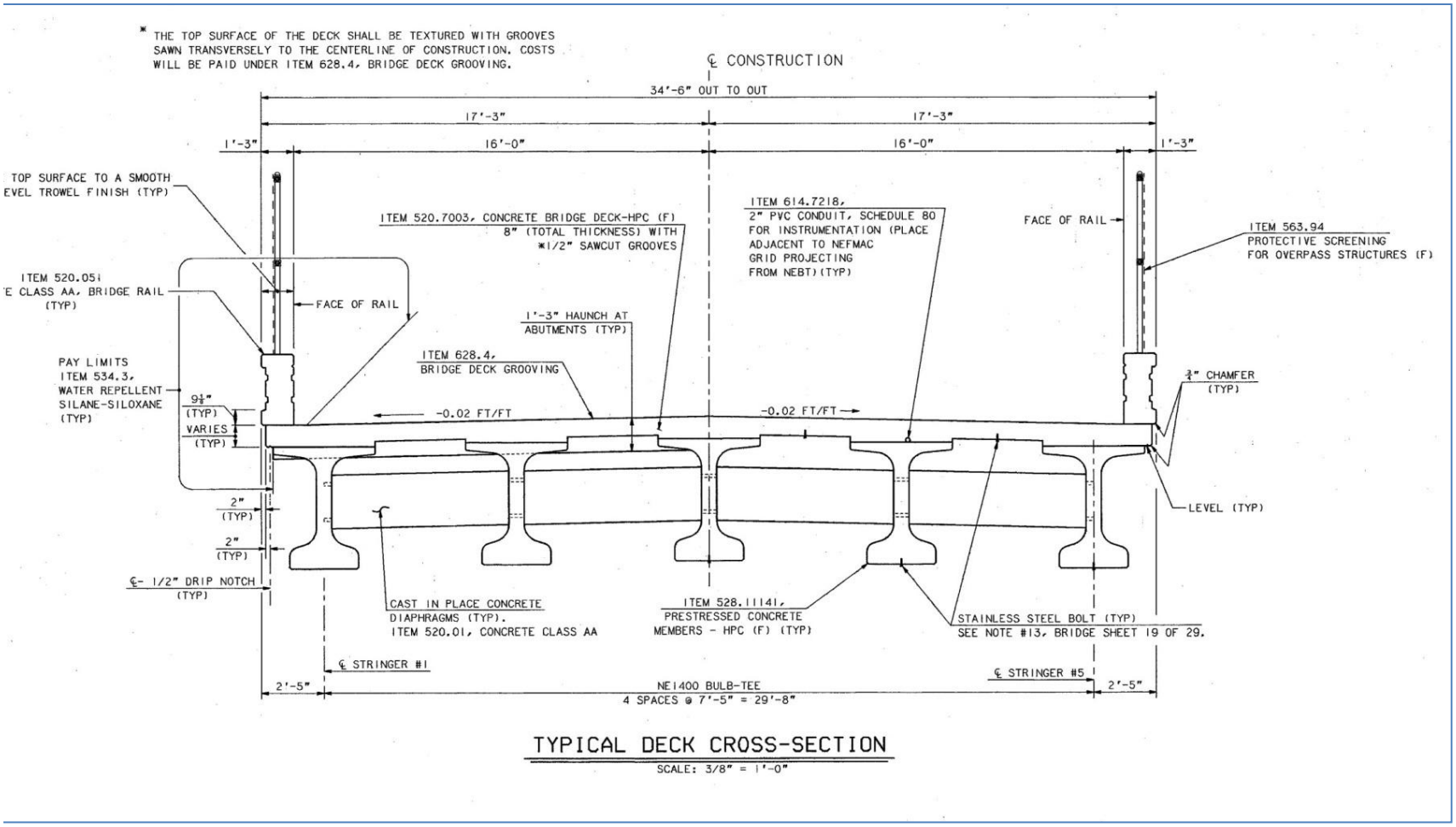

Figure 5: Typical cross-section of Rollins Road Bridge (NHDOT Bureau of Bridge Design, 1999)

2.3.1 – Bridge Deck

The bridge deck is an 8-inch cast-in-place (CIP) concrete deck. Even though there are 0.5-inch saw cuts shown on the design drawings they were not installed during construction. The concrete deck strength can be seen in Table 3. There are also three CIP diaphragms, one at each end and one in the midspan. A typical concrete bridge deck is reinforced with steel rebar; however, in order to take advantage of the IBRC program and due to increased use of deicing salts in New Hampshire, carbon fiber reinforced polymers, commercially known as NEFMAC, was used instead of steel. The CFRP has a tensile strength, f_{fu}, of 190-ksi and an elastic modulus, E_f, of 10,400-ksi. Some advantages of the CFRP include its high tensile strength, reduced unit weight, non-corrosiveness in salt environment, attractive life cycle performance, and ease of installation. Some disadvantages are the higher initial cost and lack of contractor familiarity with the material. After speaking with NHDOT construction personnel about the use of the material, the construction workers were happy using the material since they could pick up a section by themselves and easily install it on the bridge, using zip-ties as connectors.

Table 3: Deck concrete strength (Bowman M. M., 2002)

Days	f'_c
28	5.67
56	6.44
365	6.99

2.3.2 – Girders

The CFRP-reinforced deck is supported by five precast, prestressed New England Bulb Tee girders, cast with high performance concrete. Composite action between the deck and girders is achieved via 13-inch portions of the CFRP grid that function as shear transfer devices. The prestressing strand pattern is a draped strand pattern, as shown in Figure 6.

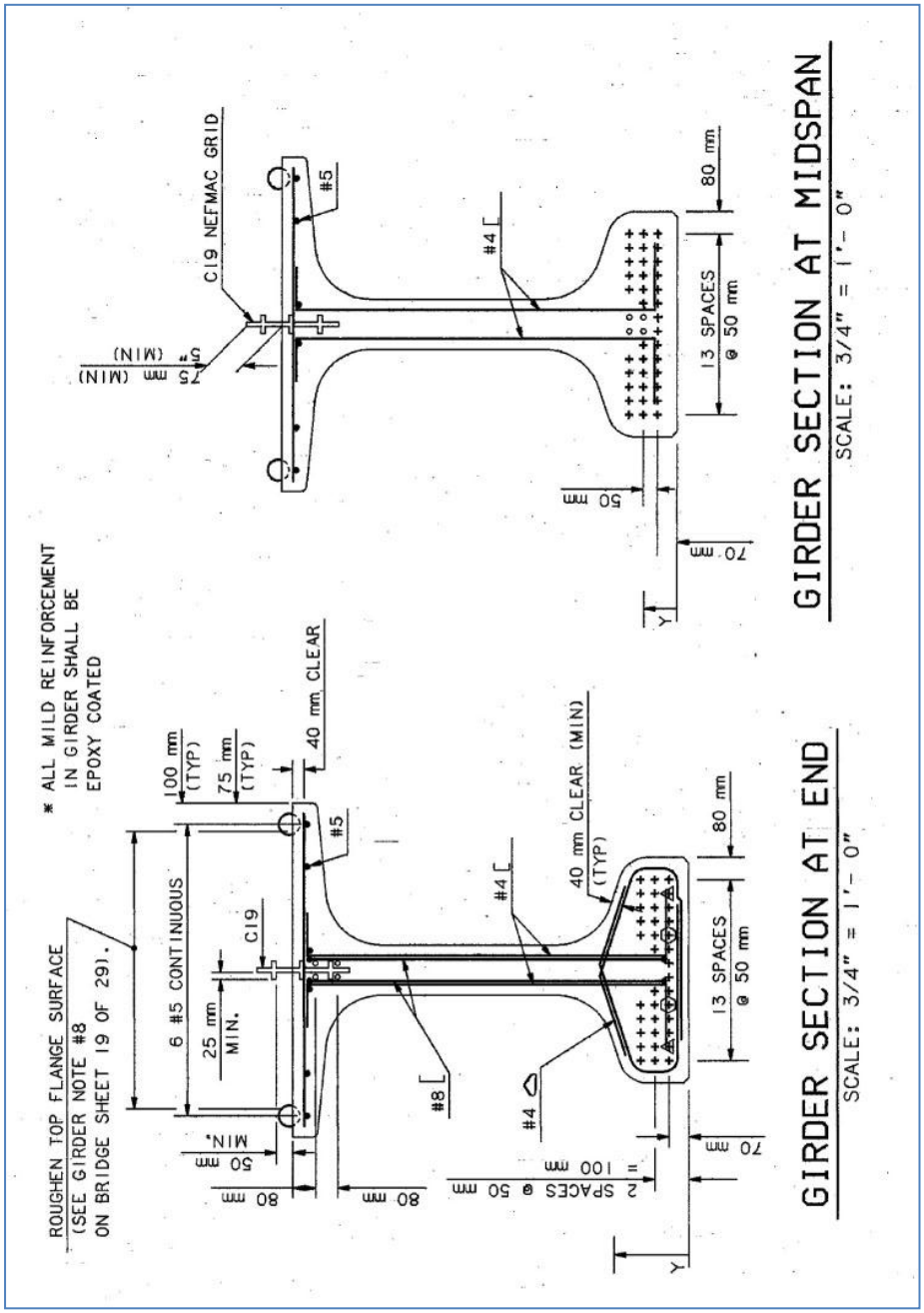

Figure 6: NEBT Section at end and midspan, showing prestressing steel (NHDOT Bureau of Bridge Design, 1999)

2.3.3 – Bearing Pads

Each NEBT girder sits on two, cylindrical, 16-inch diameter, steel reinforced, elastomeric bearing pads located at each end of the girder. The bearing pads were manufactured by The D.S. Brown Company (The D.S. Brown Company, 2008) and are commercially known as Versiflex

Elastomeric Bearings. They have a total thickness of 5-⅛ inches, contain seven ⅛-inch steel reinforcing plates, have 60-durometer neoprene as the base material, and can be seen in plan and section in Figure 7. According to the AASHTO LRFD Bridge Design Specification Third Edition 2004, the elastomeric bearing pads are used to resist lateral movement due to temperature changes and load application (AASHTO, 2004). The bearing pads influence the boundary conditions for the model and obtaining the actual stiffness value of the bearing pads was important to the global behavior of the bridge model.

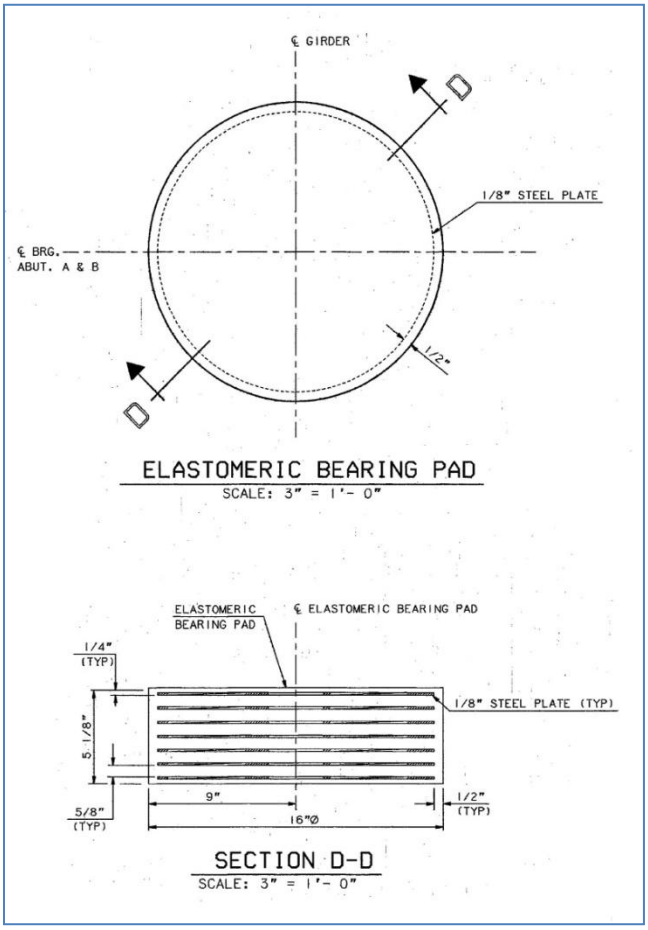

Figure 7: Elastomeric bearing pad details from Rollins Road Bridge Plans (NHDOT Bureau of Bridge Design, 1999)

2.3.4 – Abutments

The types of abutments used at RRB are classified as heavy abutments (Taly, 1998). Visual inspections prior to load test noted no change to the abutment that would require modeling to capture changes in bridge behavior.

2.4 – Instrumentation Plan

As part of the IBRC, the RRB was instrumented in order to capture the behavior of the CFRP and the bridge deck which contained an innovative material. All of the sensors in the deck are oriented in the lateral direction, perpendicular to the flow of traffic. This was done in order to understand the behavior of the deck as it bends over the girder when a load is applied. The only gauges oriented in the longitudinal direction, with the flow of traffic, were gauges in the precast, prestressed, high performance concrete NEBT girders. The purpose of these gauges was for researchers from the University of Nebraska at Lincoln to quantify the loss of prestress in the high performance concrete girders. These longitudinally oriented gauges proved to be most beneficial for the SHM program since they capture the global bending behavior of the bridge. The instrumentation plan was not designed for SHM, yet full advantage was taken of the gauges for research in SHM.

The fiber optic concrete strain sensors used in this project are Fabry-Perot strain gauges for embedment in concrete (EFO). The actual Fabry-Perot strain sensor is mounted inside a stainless steel envelope with two end flanges to ensure durability and protection of the sensor for long term monitoring projects, such as RRB. The two end flanges also ensure proper adherence to the concrete. The fiber optic sensors are also small in size, lightweight, non-conductive, resistant to corrosion, and immune to electromagnetic noise and radio frequencies, which eliminates the need for shielding and lightening protection (Choquet, Juneau, & Bessette, 2000).

The robustness of these fiber optic strain gauges justifies the extra cost of the gauge since they are still operational after being in service for eight years.

Conventional strain gauges, seen in Figure 8, measure the time it takes for an electrical current to pass over a known distance. If there is a change in the time it takes to get from point A to point B, the change in time is correlated to a change in distance, therefore strain. A similar idea is used for fiber optic strain gauges; however light is used instead of an electrical current. Two mirrors are separated by a known length, and the change in time it takes for the light to travel between the mirrors is correlated to strain. A photo of the fiber optic strain gauges can be seen in Figure 9.

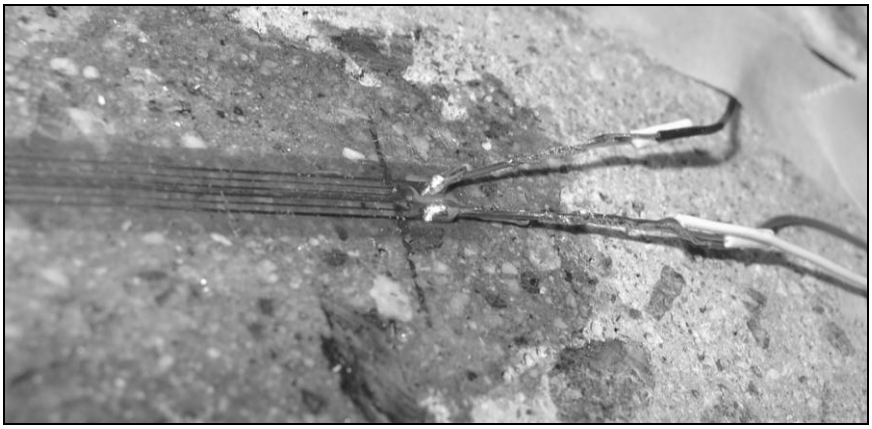

Figure 8: Conventional strain gauge attached to concrete

Figure 9: FISO EFO fiber optic strain gauge (FISO, 2008)

The deck gauges, Figure 10, were installed by researchers before the concrete deck was poured. The presence of researchers during the installation and the deck placement could be a contributing factor to the success of the entire instrumentation plan. The gauges were connected to fiberglass studs, arranged in a planned depth throughout the deck. In the RRB, all of these strain gauges are concentrated between girders 3 and 4, near the longitudinal midspan. Temperature sensors were also installed in the deck to obtain internal concrete temperatures.

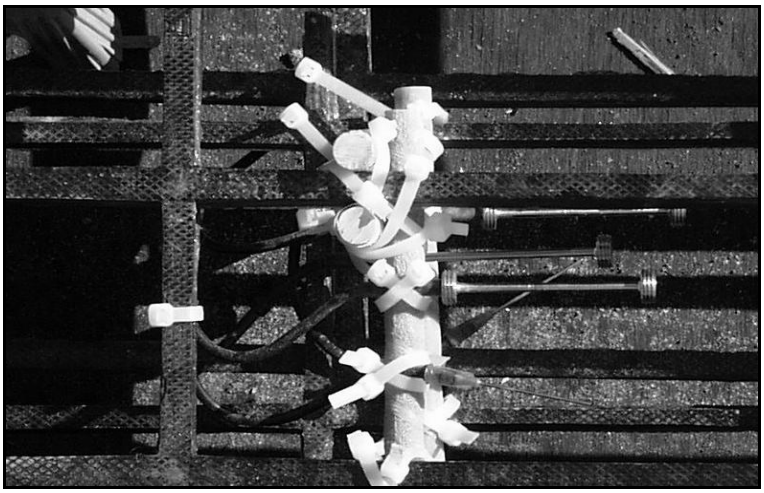

Figure 10: Deck temperature and concrete strain sensors (Adapted from (Bowman M. M., 2002))

Fiber optic strain gauges were embedded into the CFRP grid. Figure 11 shows the strain gauge being inserted between the carbon layers during the manufacturing process. A Kevlar reinforced polyurethane jacket was used around the fiber optic gable for protection. The process of embedding gauges into the CFRP allows for a unique strain reading, being inside the CFRP as opposed to a strain gauge being installed to the outside of a reinforcement bar.

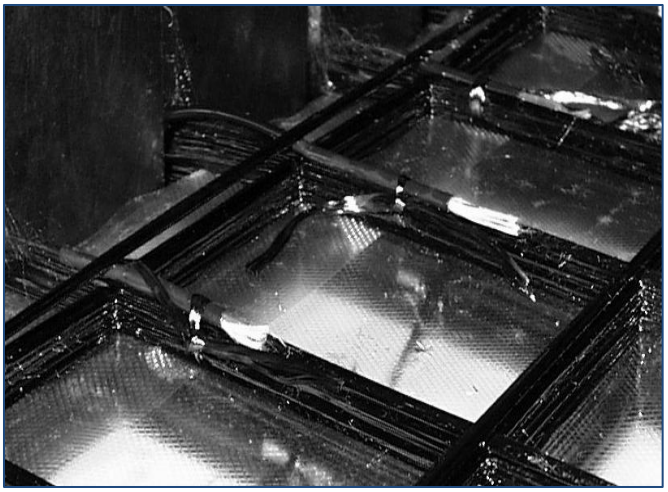

Figure 11: Strain sensors embedded in NEFMAC grid (Adapted from (Bowman M. M., 2002))

The girder sensors are the main focus of instrumentation for this research project. As mentioned before, they are the only sensors in the longitudinal direction allowing bending and axial stresses experienced by the bridge due to traffic to be observed. Longitudinally oriented gauges are best suited for SHM and parameter estimation program. The sensors in the girders are identical to the sensors in the deck. The purpose of these sensors was originally to instrument and observe the prestress loss in the high performance concrete girders. These results were used to create the structural model and are located in *NCHRP Report 496* (Tadros & Al-Omaishi, 2003). Girders 3, 4, and 5 have strain sensors installed at the longitudinal midspan of the bridge and at three different depths throughout the girder. These sensors were placed after tendon prestressing but before concrete placement, as seen in Figure 12. Figure 13 shows which gauges were used for analysis in this project. Only four out of the nine girder gauges were used because they were the four that had readings from all load tests and were still working in 2008.

Figure 12: Strain gauges in NEBT girder before prestressing (Adapted from (Bowman M. M., 2002))

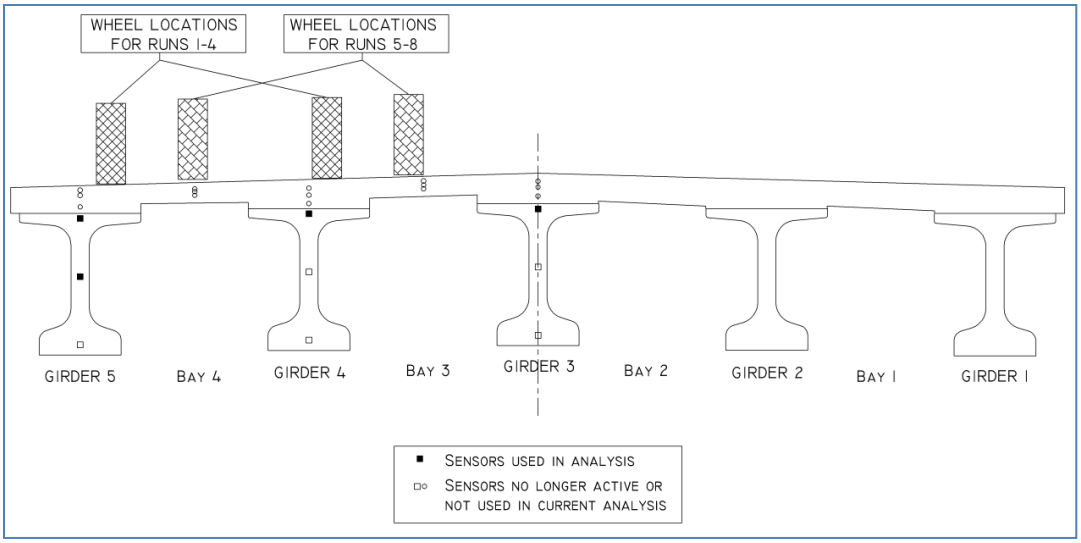

(a)

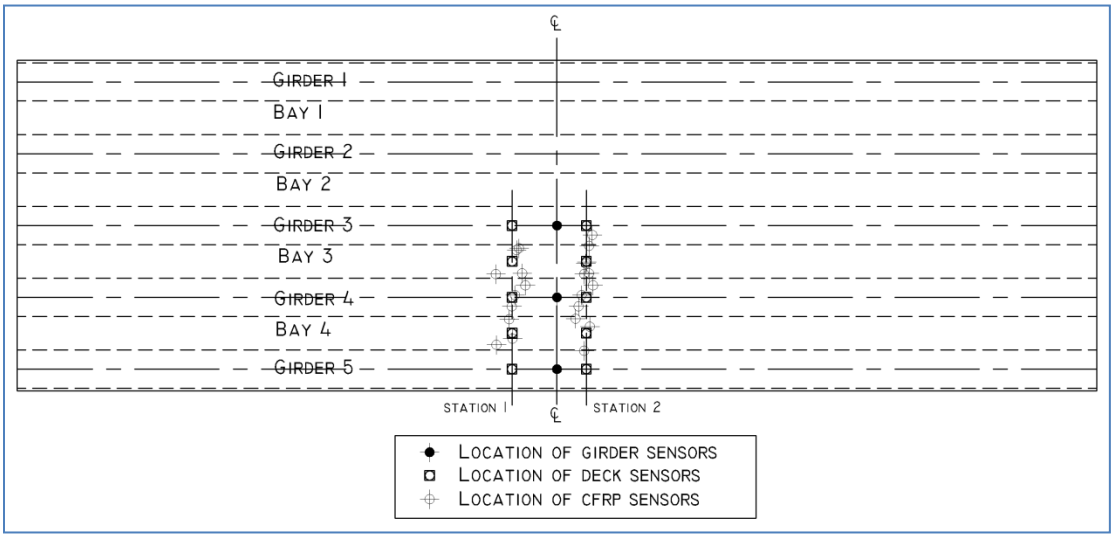

(b)

Figure 13: Graphic of sensors used in Rollins Road Bridge analysis, (a) shows the sensors in section view and (b) shows the sensors in plan view

The data management instrument (DMI) is located on-site and is in good working condition. The DMI is a 32-channel fiber optic data acquisition system provided by FISO Technologies, Inc. This particular DMI model has the ability to record continuous data or be calibrated for a controlled static load test. Since the start of the research project, continuous temperature and strain data has been downloaded from the bridge for use by future researchers to investigate the long term performance of the CFRP and concrete deck through trends and

examining material properties. For the continuous, long term temperature and strain data, the DMI is configured to take 60 readings over the period of one hour and average those values to produce a single data point for that one hour. This allows for two weeks of data to be collected without filling the memory capacity of the device. The DMI is also attached to a modem, allowing researchers to remotely call the bridge to download data or see current conditions. One downfall of collecting this continuous data is that there is no traffic camera or weigh-in-motion sensor at the bridge to determine the amount of traffic during the recording time.

The on-site DMI has a 32-channel capability. For the RRB Research Project 2008 Load Test, a second 32-channel DMI was rented from FISO Technologies, Inc. to be able to take full advantage of all working sensors. Of the 81 sensors originally installed in the bridge, 53 were operational in April 2008. The two DMIs allowed all 53 sensors to be recorded. The DMIs were configured to record every 4.8 seconds, which was the maximum sampling rate possible. Figure 14 shows two UNH researchers setting up the DMI on the morning of the load test.

Figure 14: Load test researchers with DMI

2.5 - Previous Work at Rollins Road Bridge

Two previous load tests were performed at RRB, one in December 2000 and the other in August 2001 (Bowman, Yost, Steffen, & Goodspeed, 2003). Bowman's (2002) research

investigated the performance of the CFRP and concrete deck. Small, single-span beam models were used to get transverse forces and moments over the beams. Data-to-data comparison was exclusively used in her research. This project is the first time that a structural model of the entire bridge has been created. Data from the previous research did not give "initial" strain gauge readings, as this was not needed at the time. This proved to be an issue when trying to compare the data to a predictive model. As future work in Bowman, M. M. (2002), a study on the thermal effects on the bridge's structural response was recommended.

CHAPTER III

FIELD TESTING PROTOCL AND PROCEDURES

An important part of SHM, with parameter estimation and model updating, is performing nondestructive load tests at the bridge to capture structural behavior. Nondestructive testing techniques apply a load to the bridge while keeping the response in the linear elastic range. This loading limit ensures that there is no damage to the structure caused by the testing and that there is no acceleration to any existing deterioration. While loads are being applied, measurements of structural response are recorded. These measurements are taken by a variety of different methods including strain, displacement, rotation, and acceleration.

3.1 - Previous Load Tests

Two load tests have been conducted at the RRB as part of previous research (Bowman M. M., 2002). One load test was conducted 56 days after pouring the concrete in December 2000 to establish a comparative baseline for the analysis of the CFRP and deck behavior. Another load test was performed in August 2001 to observe the performance of the CFRP in the deck after eight months of service. Both tests were conducted by UNH with the cooperation of the NHDOT. Since the tests were performed to observe CFRP and deck performance, the sensors in those locations became the focus of the load tests. Girder gauge data was also captured for

future use and prestress loss research. The type of analysis done on the measured response was data-to-data comparison, without comparing to a predictive model.

The truck used in the December 2000 load test had a gross weight of 75.6-kips (37.8-tons) while the August 2001 load test truck had a gross weight of 76.9-kips (38.45-tons). Actual wheel distributions can be seen in Table 4. Both of these trucks had three-axles, with each of the two rear axles containing four wheels. It was noted by the New Hampshire State Police personnel that the truck weight would have been over the legal limit for their configuration.

Table 4: Load test wheel weights for all three years

	2000		2001		2008	
	Driver Side	Passenger Side	Driver Side	Passenger Side	Driver Side	Passenger Side
Front Tires *kips*	11.20	11.80	10.45	10.10	5.25	5.25
Front Duals *kips*	13.50	12.90	13.55	14.60	N/A	N/A
Rear Duals *kips*	13.40	12.80	15.10	13.10	12.93	13.95

3.2 - April 2008 Load Test

The load test for the Rollins Road Bridge Research Project was conducted on the 18th of April, 2008. The purpose of this load test was to collect data in a similar fashion to the previous load tests, while also collecting data to be used for SHM. The biggest change between the 2000/2001 and the 2008 load test programs was the spacing between stop locations on the bridge. The 2000/2001 stop locations had to be close to the CFRP and the deck gauges to get accurate readings. The 2008 load test was not as concerned with the local measurements and wanted to capture the global response. The difference between the two load test programs resulted in the omission of a few stop locations. When researchers went to paint markings on the bridge for the 2008 load test, the old stop markings were still visible and a majority of the 2008

load test markings correlated to previous markings. The Rollinsford Police Department provided traffic control during the load test. No traffic was allowed to pass while strain readings were collected. Traffic was allowed to pass when the truck was being relocated to a new loading position. Three zero-load readings were also taken during the duration of the load test. This information proved to be crucial in relating measured response to the structural model's predicted response (as detailed in Chapter 5). The NHDOT Survey Crew used differential leveling to obtain displacement readings during the load test.

3.2.1 – Truck Specifications

This load test, like the previous two load tests, was conducted in collaboration with the NHDOT. A two axle NHDOT Sand Truck, as seen in Figure 15 and Figure 16, was used for load application to the bridge. The wheel weights of the truck were taken in similar fashion to the previous load tests by the New Hampshire State Police Mobile Weigh Station, seen in Figure 16. The gross weight of the truck was 37.4-kips (18.69-tons). This truck weighed less than the requested weight of 35-tons, however, the quality of the recorded data was acceptable.

Figure 15: NHDOT sand truck as load application during April 2008 load test

Figure 16: Trooper Huddleston (NH State Police) taking NHDOT wheel load measurements

The distribution of wheel loads can be seen in Table 4. Trooper Huddleston, the representative from the State Police, noted this truck would have been sighted as overloaded due to its current configuration, but was exempt because it is a NHDOT truck and part of a research project load test. Even though the truck was overloaded, it was still within the linear elastic range of behavior for RRB. Trooper Huddleston noted that the Haenni Scales, model #WL 101 (Haenni, 2008), have a variance of less than 1% as tested and certified by the NH State Police.

The truck dimensions were 14-feet 9-inches between the center of the front and rear wheel. The rear dual had a width of 1-foot 8-½-inches. The rear axle, measured from the center of the dual wheels to the center of the opposing dual wheels, had a width of 6-feet 2-inches. The front wheel had a width of 8-inches and the length of the front axle measured from the center of wheel to the center of wheel was 7-feet.

3.2.2 – Testing Plan

The truck testing runs included four in the north-west direction and four in the south-east direction. Two separate stop location sets were marked out on the bridge. One set placed the

wheel directly on the girder and the other set placed the center of gravity of the truck on the girder, meaning the wheels straddled the girder. Each stop location set was traveled four times, twice in each direction. In runs one through four, the trucks wheels were on girders five and four. For runs five through eight, the trucks wheels straddled girder 4, as seen in Figure 17.

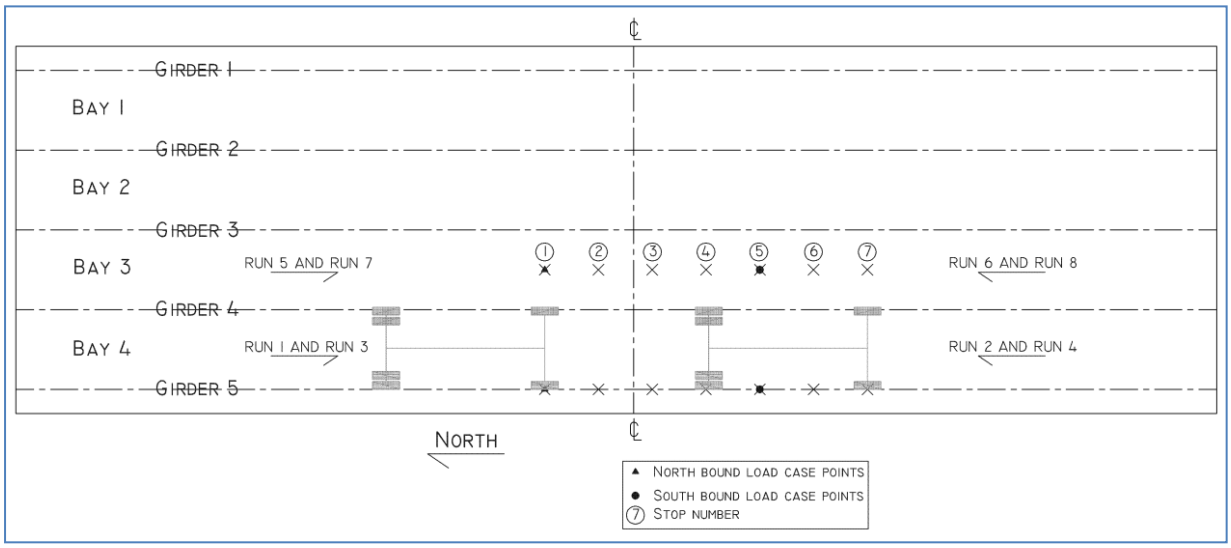

Figure 17: April 2008 load test truck stop/analysis diagram

3.2.3 – Snapshot Quality Assessment

The reason for having two runs in each direction for each set of stop locations was for statistical evaluation of collected measurements. However, examination of these data sets showed a difference in response when the truck load was identical indicating the impact of environmental loads. Figure 18, Figure 19, and Figure 20 show CFRP, deck, and girder gauge strain values respectively for different truck load runs using the same set of stop location traveling in the same direction. The CFRP and deck readings show there is a difference of 10-microstrain, while the girder gauge shows a 5-microstrain difference between the two runs. Without environmental loads, these two data sets should be nearly identical. The environmental effects on strain will be discussed in Chapter IV: Data Quality Assurance and Data Quality Control.

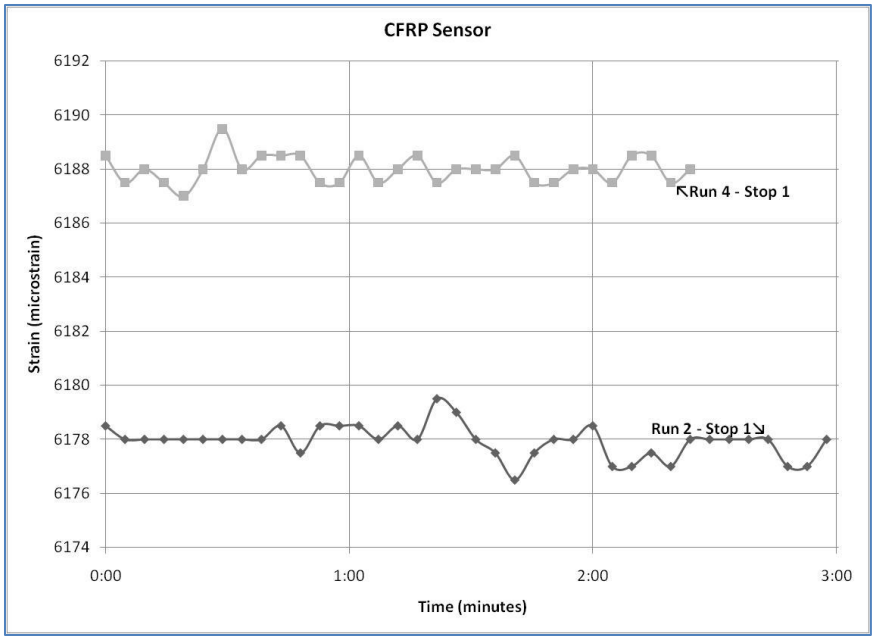

Figure 18: CFRP sensor recorded strain for two passes at same location, different time

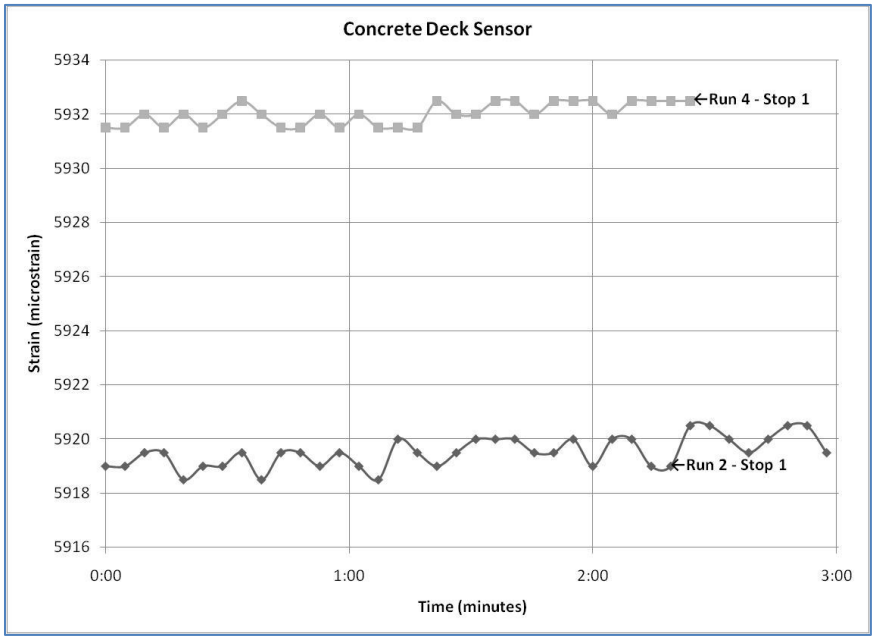

Figure 19: Concrete deck sensor recorded strain for two passes at same location, different time

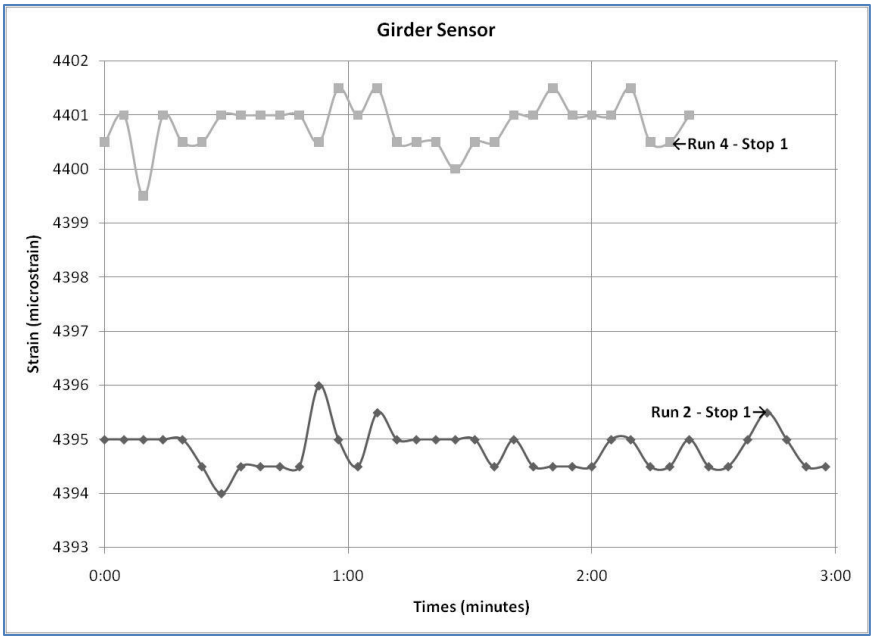

Figure 20: Girder sensor recorded strain for two passes at same location, different time

Out of the 56 stop locations during the April 2008 load test, four locations were used as the four modeled load cases. These stop points correlate to times when temperature, strain, and deflection readings were collected. The resulting load cases for the April 2008 load test are shown in Figure 21, Figure 22, Figure 23, and Figure 24. Similar methodology was done to make four load cases for both the December 2000 and August 2001 load tests, which all can be seen in Appendix c – Load Cases for All Years.

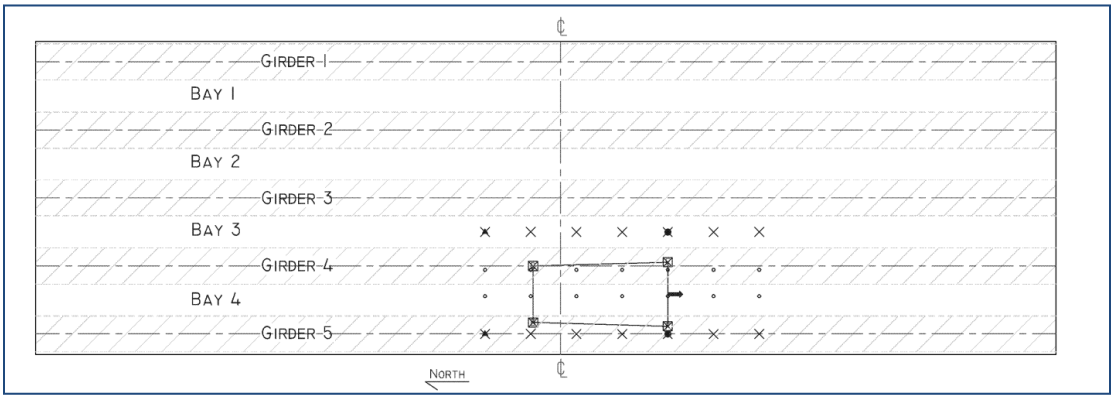

Figure 21: Load case 1 April 2008 load test

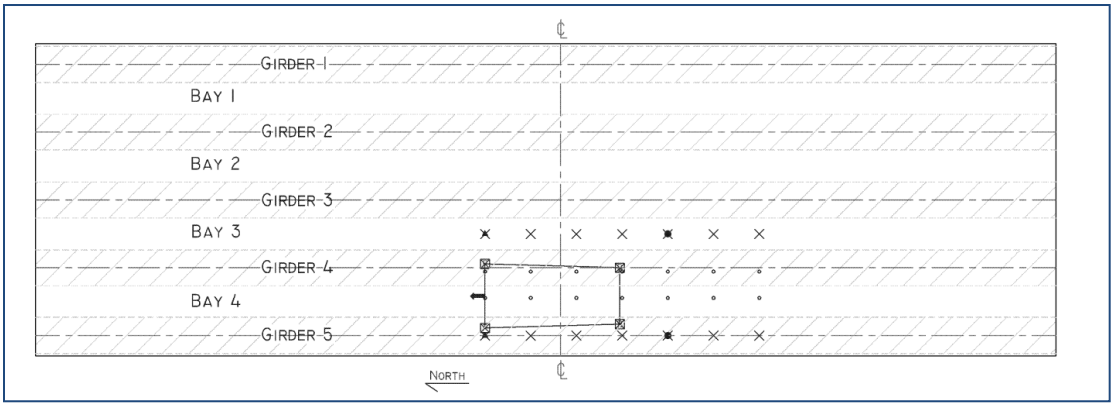

Figure 22: Load case 2 April 2008 load test

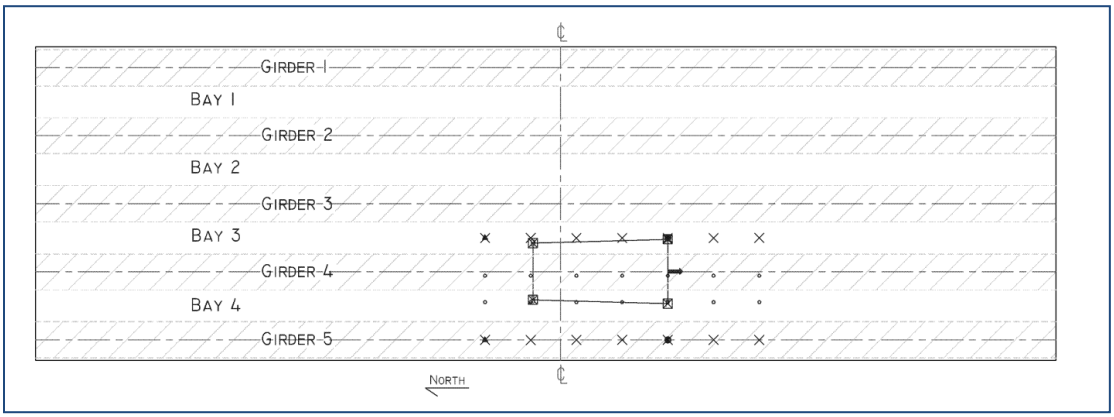

Figure 23: Load case 3 April 2008 load test

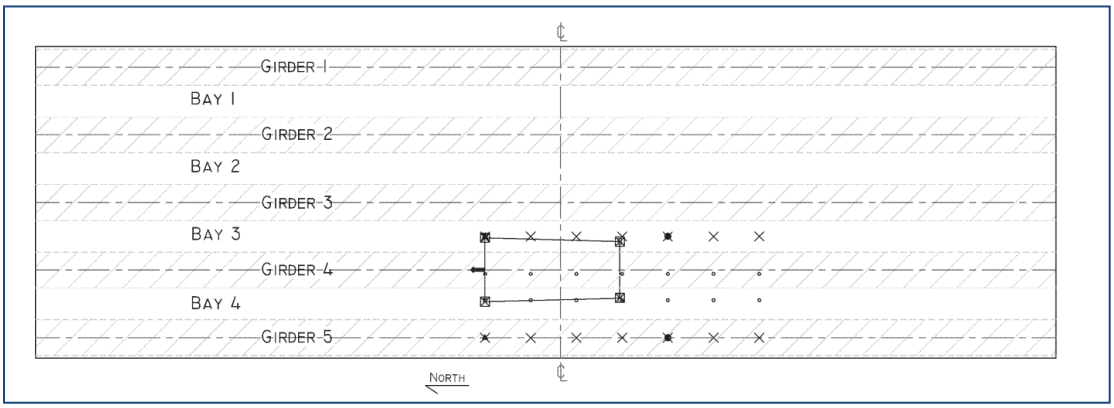

Figure 24: Load case 4 April 2008 load test

3.2.4 – Ambient Temperature Measurements

Ambient air temperature and deck surface temperatures were taken during the duration of the load test. Ambient temperature measurements were included when creating the load test program in case, and as proved to be, temperature played an important role in the structural

response of the bridge. Ambient temperature, above the deck and below the deck, was recorded at 15-minute intervals. Figure 25 shows the ambient temperature readings versus the time, on a 24-hour clock, during the duration of the April 2008 load test. At the end of the load test there was about a 25°F temperature difference between above and below the bridge deck.

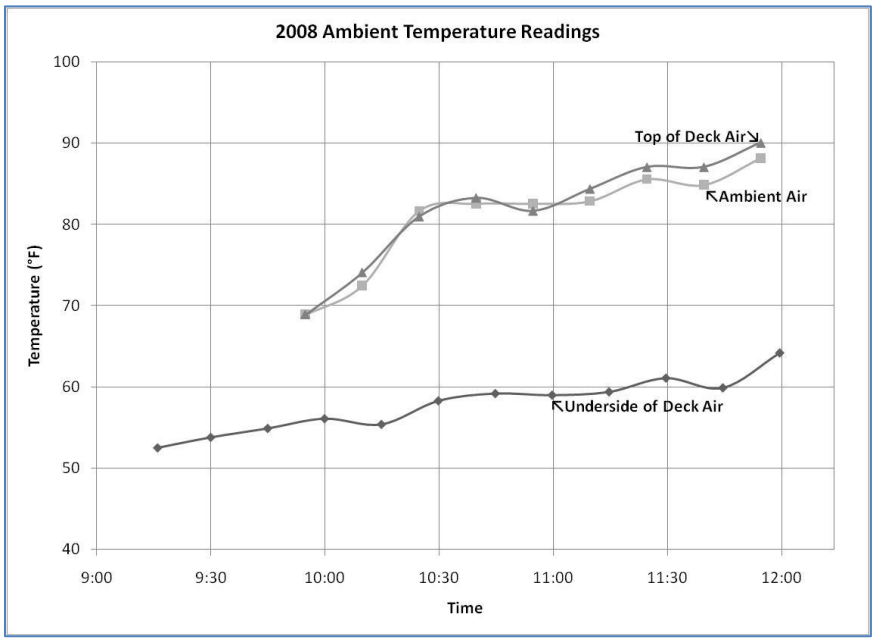

Figure 25: Rollins Road Bridge 2008 load test ambient temperature readings

3.2.5 – Optical Displacement Measurements

Optical displacement techniques were implemented during the load test. Several researchers from industry, as well as two undergraduate researchers, performed optical displacement field measurements. The two undergraduate researchers, Patrick Nearing and Peter Krauklin, used this opportunity as a field test for their senior project. Rick Farad from River City Software in Exeter, NH and Ronald Gamache, formerly of Transtech Systems, Inc., from Schenectady, NY were the industry researchers. The information collected by these groups is not included in this research report; however, these teams will use the survey displacement measurements and structural model predictions to verify the displacement collected via digital image correlation. The goal of the optical displacement research is to find a financially viable

and accurate way to capture a series of digital images during the load test that, after post-processing, produces accurate displacement measurements.

The undergraduate researchers from UNH had success in the laboratory and some difficulty with the field measurements. This difficulty could be due to field variables such as heat shimmer, settlement, and train vibrations. The optical displacement research has continued at UNH in conjunction with NSF-funded projects to deploy digital image correlation processes on multiple bridge tests. The measured results from the industry research partners were published (Gamache and Santini-Bell, 2009) and their research in this area continues as well.

3.2.6 – Global Displacement Measurements

The Rollins Road Bridge has bolts installed to the underside of the girder and deck for purposes of taking displacement measurements. When planning the load test, researchers determined when the center of mass of the truck would be closest to the midspan of the bridge, therefore having the largest deflections on the single span structure. Displacement measurements were taken at five locations at the midspan of the bridge, on girder 5, bay 4, girder 4, bay 3, and girder 3. The NHDOT Survey Crew used a digital leveling rod to take the measurements. A NHDOT bucket truck was used to get a survey crew member up to the underside of the bridge, as seen in Figure 26.

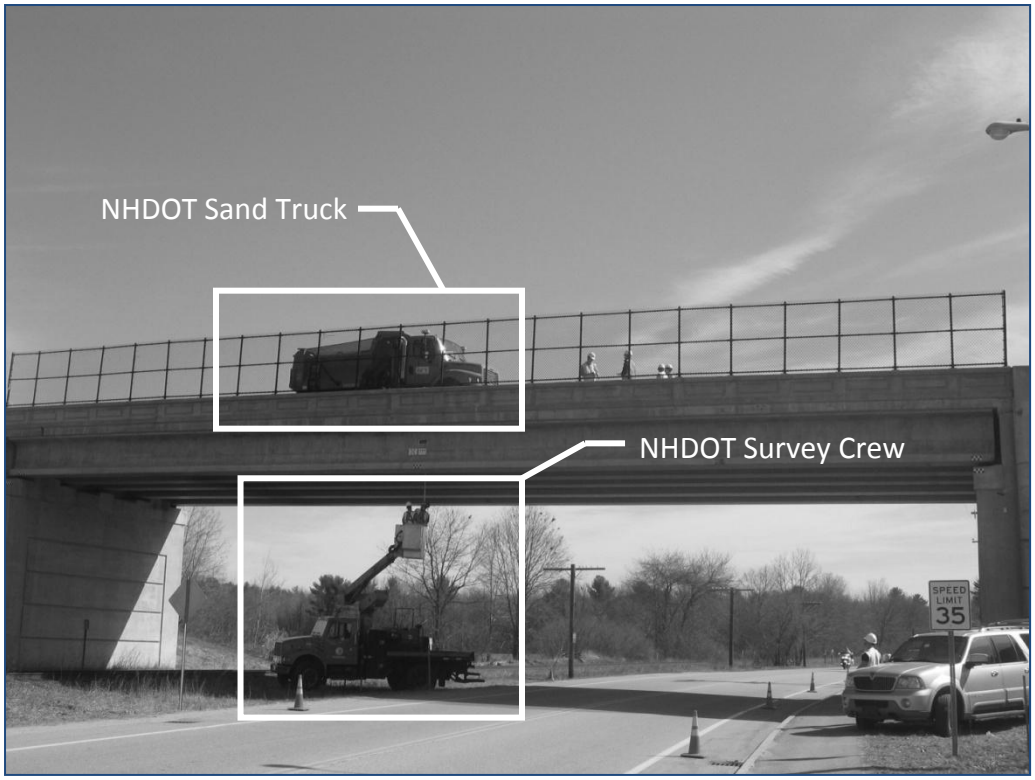

Figure 26: Photo of load test while survey crew takes displacement reading

Displacement readings are easily implemented into a SHM program, as they are reference dependent measurements. Strain and rotation are typically used to obtain structural response because they are not reference dependent. The repeatability of the deflection readings, collected via surveying technology at RRB, is limited due to factors including load truck vibration, wind, adjacent train traffic, and bucket lift stability. The deflection data can be seen below in Table 5, Table 6, and Table 7 and will be used for verification of the manually updated model as seen in Chapter VI: Manual Model Updating.

Table 5: December 2000 load test elevations (Bowman M. M., 2002)

December 2000 Elevation (feet)									
	No Load	*Girder 5 Front Wheel*	*Girder 5 Rear Wheel*	*Bay 4 Rear Wheel*	*Girder 4 Rear Wheel*	*Bay 3 Front Wheel*	*Bay 3 Rear Wheel*	*Girder 3 Front Wheel*	*Girder 3 Rear Wheel*
Girder 3	151.7338	151.7254	151.7254	151.7235	151.7419	151.7365	151.7274	151.7311	151.7242
Bay 3	156.6243	156.6326	156.6233	156.6205	156.6635	156.6225	156.6246	156.6252	156.6234
Girder 4	151.6632	151.6518	151.6417	151.6448	151.6485	151.6474	151.6427	151.6443	151.6643
Bay 4	156.4805	156.4725	156.4591	156.4589	156.4662	156.4704	156.4678	156.4767	156.4660
Girder 5	151.5077	151.4863	151.4944	151.4925	151.5043	151.4986	151.4866	151.5274	151.5058

Table 6: August 2001 load test elevations (Bowman M. M., 2002)

August 2001 Elevation (feet)									
	No Load	*Girder 5 Front Wheel*	*Girder 5 Rear Wheel*	*Bay 4 Front Wheel*	*Girder 4 Front Wheel*	*Bay 3 Front Wheel*	*Bay 3 Rear Wheel*	*Girder 3 South Direction*	*Girder 3 Rear Wheel*
Girder 3	151.6776	151.6692	--------	151.6684	151.6705	151.6704	--------	151.6736	151.6749
Bay 3	156.5754	156.5573	--------	156.5634	156.5620	156.5732	--------	156.5597	156.5635
Girder 4	151.6090	151.5902	--------	151.5889	151.5914	151.6034	--------	151.5924	151.5976
Bay 4	156.4220	156.3997	--------	156.4112	156.4087	156.4117	--------	156.4033	156.4112
Girder 5	151.4622	151.4328	--------	151.4352	151.4402	151.4436	--------	151.4461	151.4489

Table 7: April 2008 load test elevations

April 2008 Elevation (feet)									
Run #	*No Load*	*1*	*2*	*3*	*4*	*5*	*7*	*No Load*	*8*
Girder 3	151.6552	151.6471	151.6553	151.6540	151.6490	151.6713	151.6480	151.6574	151.6537
Bay 3	156.5472	156.5521	156.5347	156.5350	156.5347	156.5436	156.5682	156.5485	156.5481
Girder 4	151.5794	151.5798	151.5862	151.5828	151.5868	151.5835	151.5871	151.6003	151.5761
Bay 4	156.3835	156.3952	156.3970	156.4063	156.4018	156.3856	156.4060	156.4209	156.3954
Girder 5	151.4224	151.4125	151.4169	151.4184	151.4191	151.4219	151.4112	151.4404	151.4231

CHAPTER IV

DATA QUALITY ASSURANCE AND DATA QUALITY CONTROL

Almost 2,000 data points were measured per channel on the two DMIs (data management instruments) at the RRB for the April 2008 Load Test. Approximately 120,000 data points were recorded over the duration of a three hour load test. This is an overwhelming amount of data, however the load test plan was organized to facilitate effective and efficient data management. There were two goals for the data collected from this field test. The first goal was to perform a data-to-data comparison, following work of previous researchers and assessing the performance of the CFRP. The second and primary goal was to process the data for SHM and manual parameter estimation and modal updating.

4.1 - Data-to-data CFRP/Deck Analysis

The data-to-data comparison was conducted to assess the health of the CFRP, deck, and girder after eight years of service. This comparison method, used by Martha Bowman (Bowman, 2002) was also used for this research project, as requested by the NHDOT, to ensure that the visual inspection report correlates with the measured structural response of the RRB. Strain data was graphed with respect to time and can be seen in sections 4.1.1, 4.1.2 and 4.1.3. Three gauges from each the structural element including the CFRP grid, the concrete deck, and the precast girders were chosen to provide a representative sample of the bridge response. For all

Figures in this Chapter, the x-axis is the time of day for each day on a 24-hour clock. It should be noted that all three tests began between 9:30AM and 10:30AM. Also the initial strain reading collected on each day ranges between 5250 με and 6550 με. These values have no bearing on the performance of the structural elements during the load test. The evaluation of the structural integrity of the element is based on the differential strain caused by the truck loading and environmental effects.

4.1.1 – CFRP Reinforcement Data-to-Data Comparison

Figure 27, Figure 28, and Figure 29 show the data-to-data comparison of the strain sensors in the CFRP. These results could not be compared to a visual inspection report due to the fact that the CFRP grid is not visible and is not included in a standard biannual visual inspection. Each figure in this section shows a recorded microstrain differential of approximately 100 με for the 2001 and 2008 load test and approximately 50 με for the 2000 load test. The range change between load tests can be associated with the +6°F temperature change for December 2000, +16°F temperature change for August 2001, and the +19°F temperature change for April 2008. The difference in ambient temperature during the load tests correspond to the 2008 line having the greatest slope, followed by the 2001 line, and the 2000 line with the smallest slope. These results are consistent with satisfactory behavior of the CFRP.

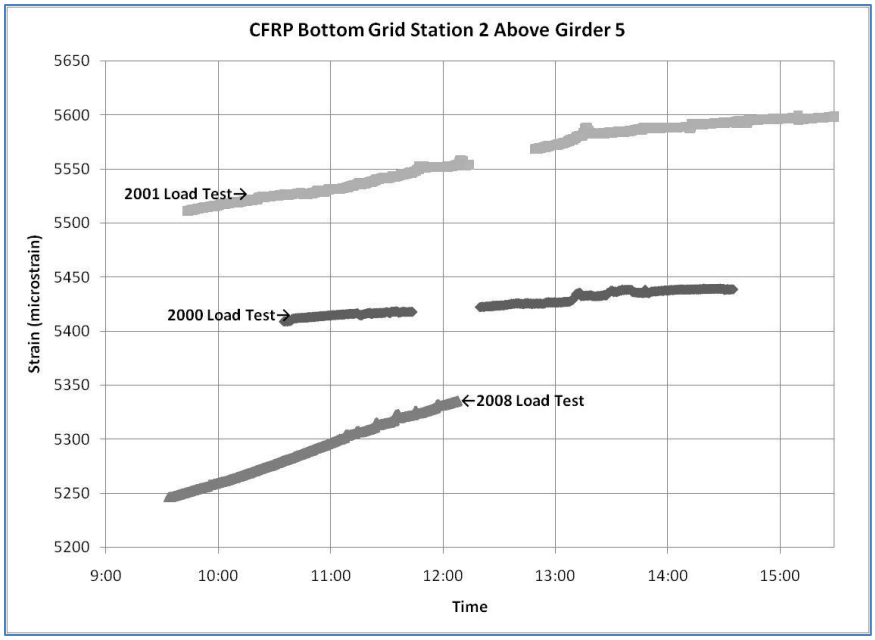

Figure 27: CFRP bottom grid station 2 above girder 5 strain readings for all three load tests

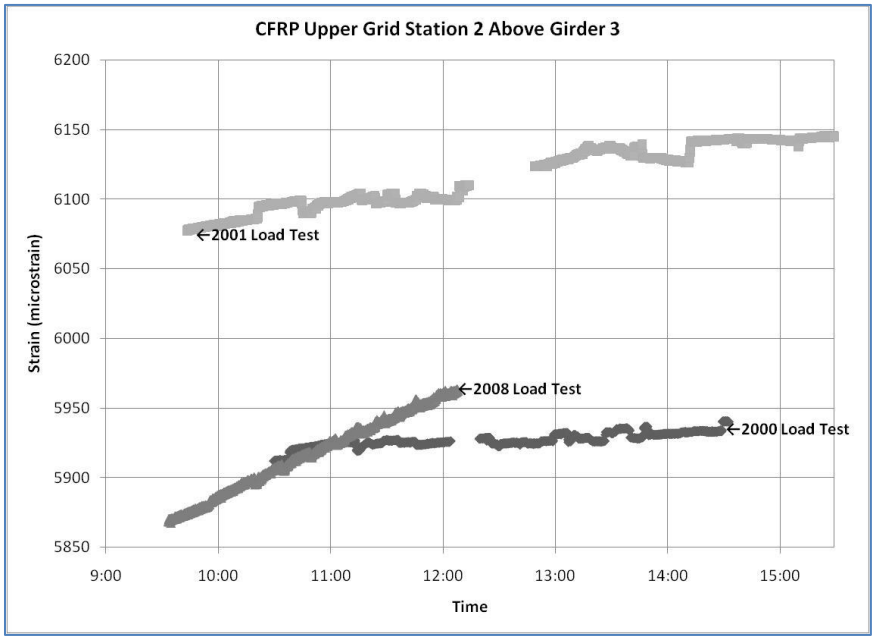

Figure 28: CFRP upper grid station 2 above girder 3 strain readings for all three load tests

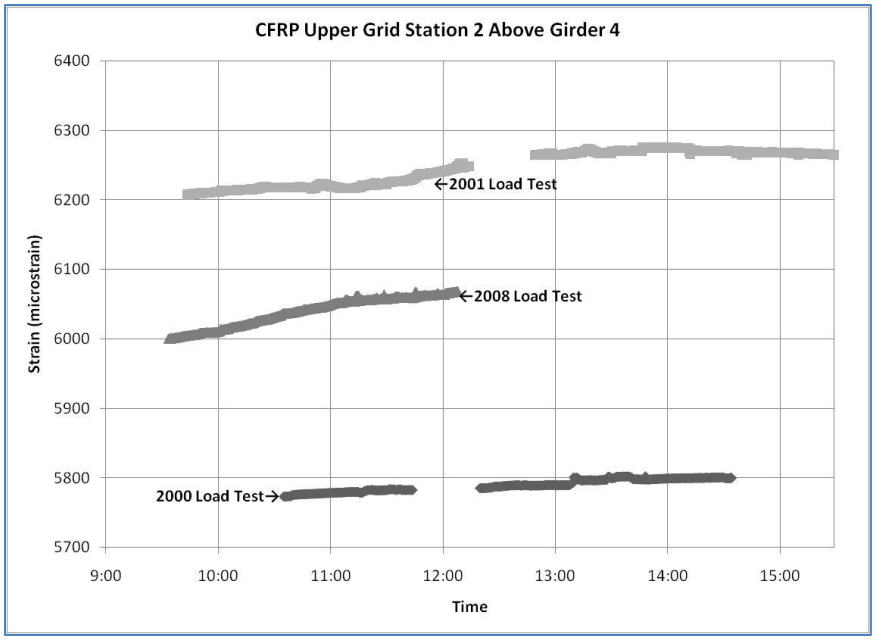

Figure 29: CFRP upper grid station 2 above girder 4 strain readings for all three load tests

4.1.2 – Concrete Deck Data-to-Data Comparison

Figure 30, Figure 31, and Figure 32 show the data-to-data comparison for strain gauges embedded in the concrete deck. The concrete deck gauges, shown here are for the bottom of the concrete deck, Figures 30 and 32 and the top of the concrete deck, Figure 31. The range of collected micro-strain for all three figures correlates to the change in temperature recorded for each load test. The range of strain reading shown in Figure 30 is about approximately half of the range in Figures 31 and 32, which is expected since the strain readings shown in Figure 30 were collected from a gauge located over a girder while the readings in Figures 31 and 32 were collected from gauges located in a bay.

A similar relationship between the December 2000 load test and the data collected from both the August 2001 and April 2008 is observed in the deck gauges and seen in the CFRP grid data, Figure 27-29. This behavior due to environmental and truck loads is consistent with the excellent rating assigned to the deck elements in the 2008 visual inspection report.

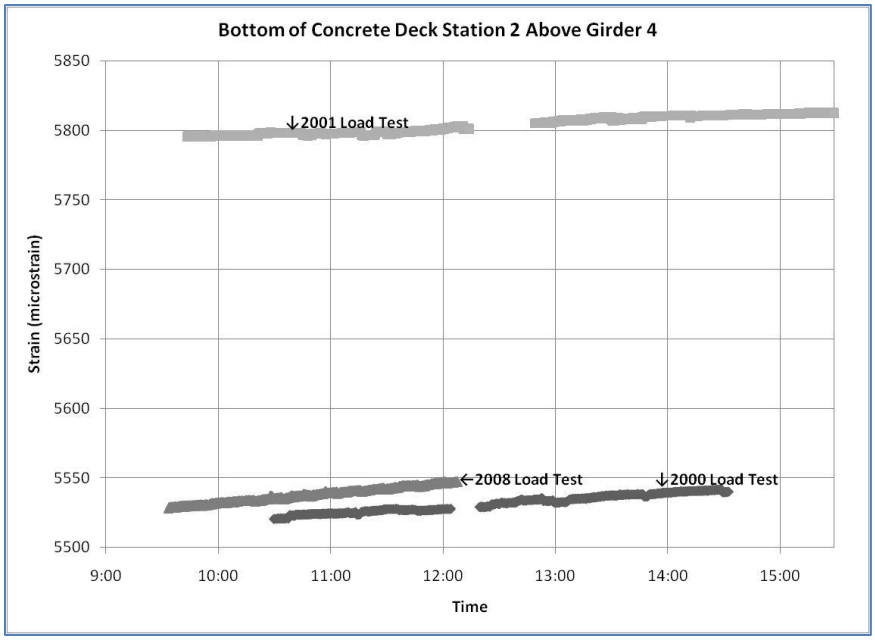

Figure 30: Bottom of concrete deck gauge station 2 above girder 4 strain readings for all three load tests

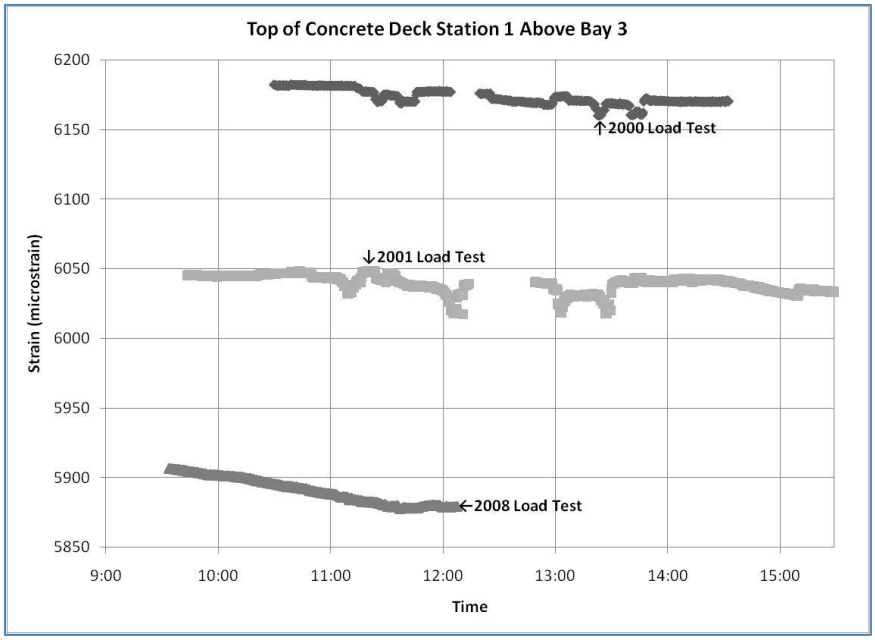

Figure 31: Top of concrete deck gauge station 1 above bay 3 strain readings for all three load tests

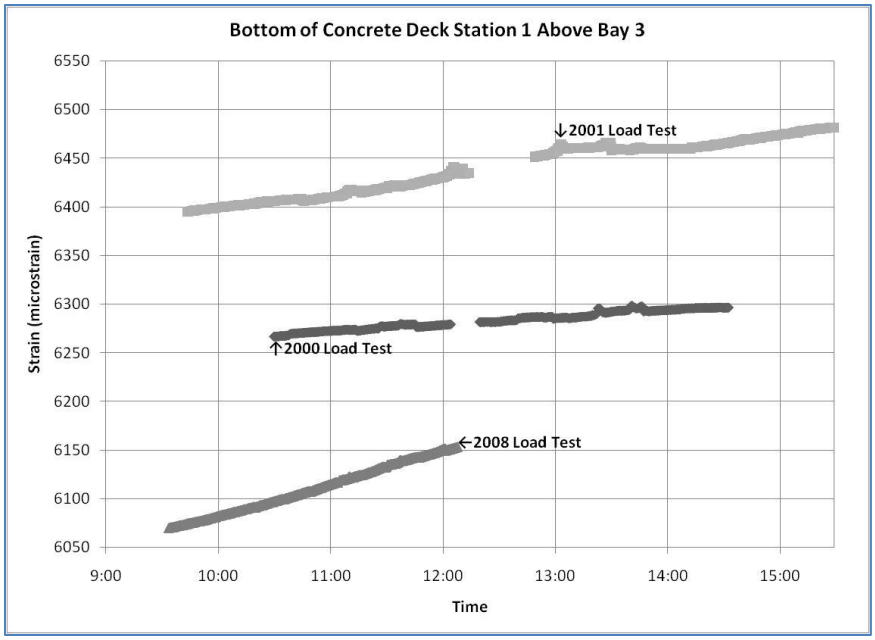

Figure 32: Bottom of concrete deck gauge station 1 above bay 3 strain readings for all three load tests

4.1.3 – Girder Data-to-Data Comparison

Figure 33, Figure 34, and Figure 35 show the strain values for the December 2000, August 2001, and April 2008 load tests in the HPC NEBT Girders 3, 4 and 5, respectively. The range in strain values from the three load tests is consistent with the behavior of the CFRP grid and the concrete deck. The range of strain measurements collected during the December 2000 load is approximately 25 με, while the range of strain measurements collected during the August 2001 and April 2008 is about 50 με, which is expected given the temperature ranges for the three load tests. This comparison also for supports the 2008 visual inspection report rating of excellent.

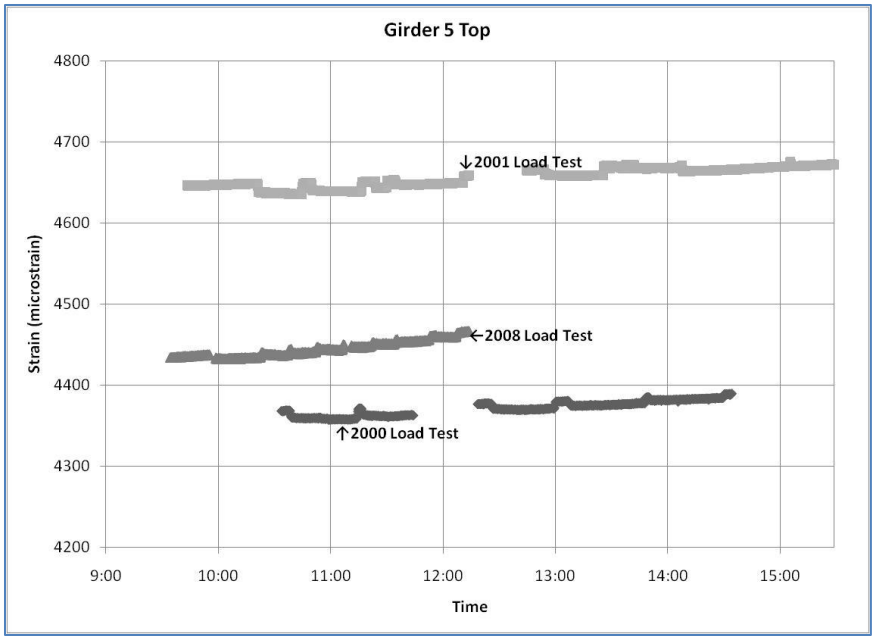

Figure 33: Girder 5 top gauge strain readings for all three load tests.

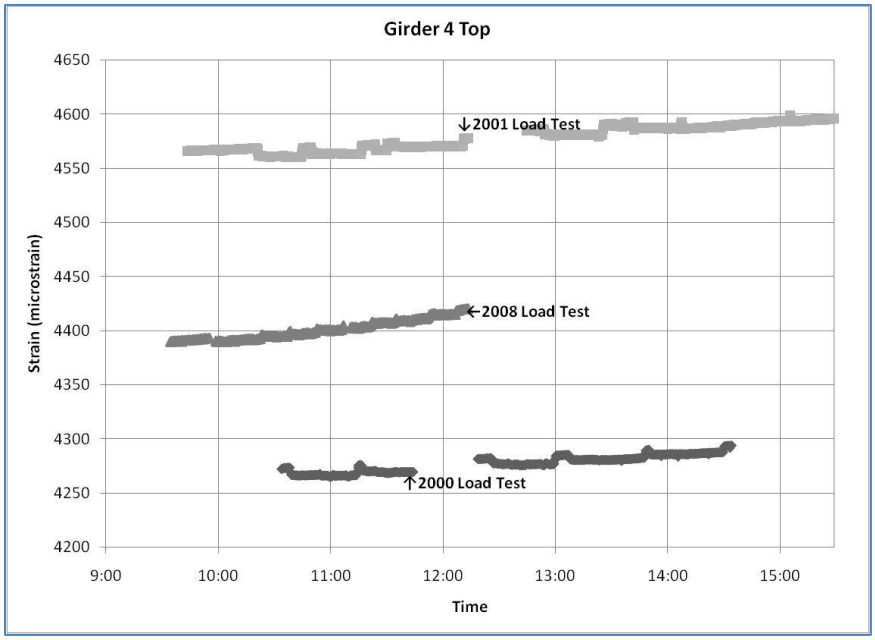

Figure 34: Girder 4 top gauge strain readings for all three load tests

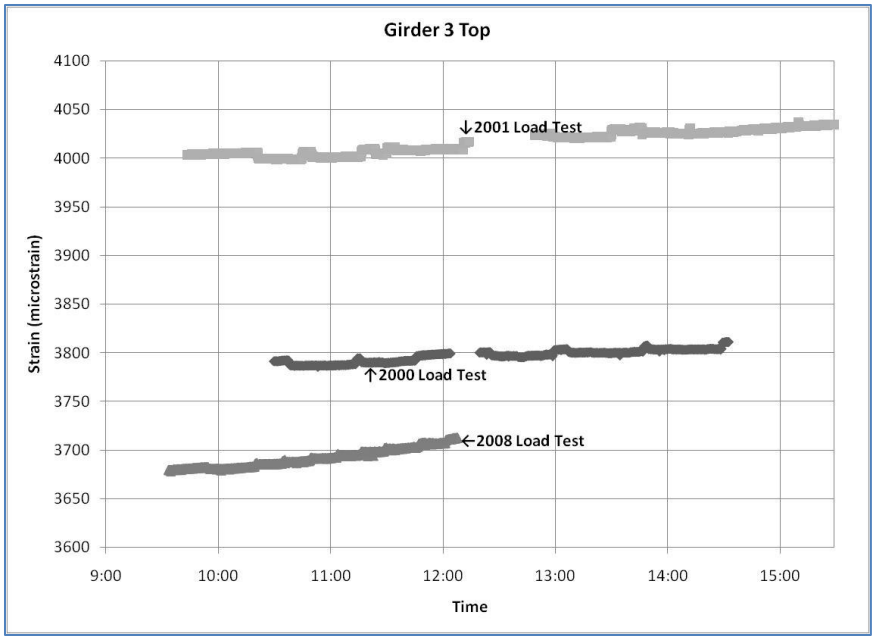

Figure 35: Girder 3 top gauge strain readings for all three load tests

4.2 – Discussion of Data-to-Data Comparison

The measured strain data ranges shows the April 2008 strain readings are consistent with the ranges collected by the previous two load tests. It is difficult to do a more comprehensive data-to-data comparison, because so many factors changed between the 2000/2001 and 2008 load tests: (1) the gross weight of the truck used for the April 2008 load test was approximately half the weight of the truck used in the previous two tests, (2) the stopping locations between the 2000/2001 and the 2008 tests were similar but not exactly the same, and (3) environmental influences the measured structural response of the bridge.

The change in ambient temperature in the December 2000 load test was +6°F, while the change during the August 2001 load test was +16°F, and change during the April 2008 load test was +19°F. This temperature differential between the beginning and end of load test and resulting range in collected strain data can be seen in the data-to-data comparison graphs, Figures 27 through 35. Figure 36 provides a graphical representation of the ambient temperatures recorded during all three load tests, 2000, 2001 and 2008.

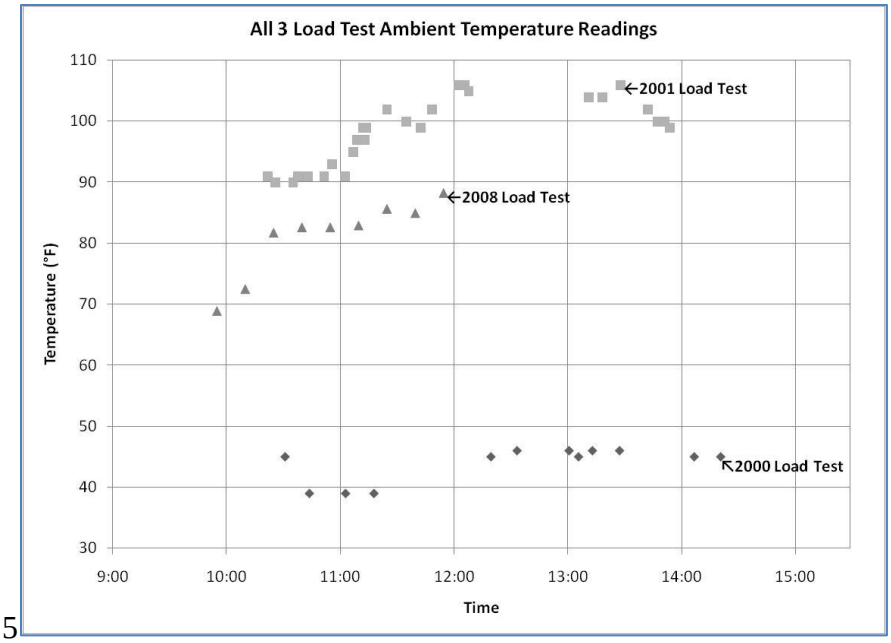

Figure 36: Ambient temperature readings for all three load tests

4.3 - Environmental Effects on Bridge Response

Visual assessment of the data-to-data comparison of strain values shows the significant environmental impact on strain reading. Figure 37 shows the strain readings for girder 3 and girder 4 during the December 2000 load test. Figure 37 shows peaks when the truck was on the bridge, causing a change of about 6-microstrain. However, over the 4-hour duration of the load test there is a change of 20-microstrain.

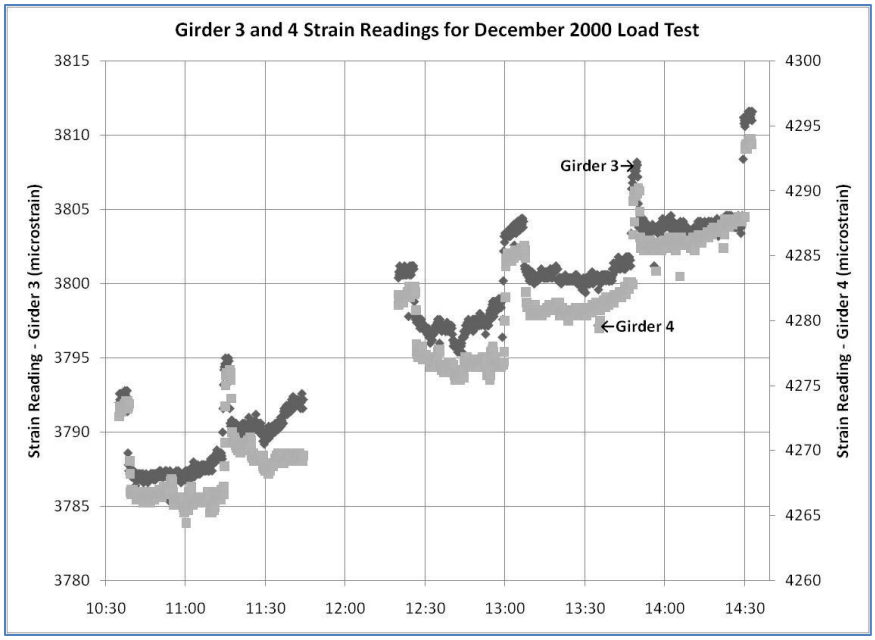

Figure 37: Strain readings from girder 3 and girder 4 over the duration of the December 2000 load test to show difference between thermal effects and load application

A similar trend is seen in the April 2008 load test data. With the smaller truck load, there was a change in strain of 3-mircostrain while the change in strain during the 2.5-hour duration of the load test was approximately 25-microstrain. This shows that the environmental effect, mainly temperature, overshadows the impact due to a 19-ton, technically overloaded, truck passing over and resting on the bridge.

An additional resource at the RRB is the temperature sensors that are installed in the bridge deck and girders. As discussed in the introduction, changing ambient temperature with respect to material temperature is a source of research and ambiguity in SHM. At the RRB, the temperature throughout the depth of the deck can be measured directly and then correlated to strain values. Given the significant environmental impact on the collected strain measurements, there were two options for accurate SHM. Environmental effects must either be included in the SAP2000® model of the bridge or be removed from the data to allow an accurate modeling of behavior and response for the RRB.

4.3.1 – Removal of Strain Caused by Environmental Factors

One option for dealing with environmental strain, including thermal strain, was to remove it from the data, leaving strain caused solely by load application. Removing strain caused by environmental effects, including temperature, removes any ambiguity on what the values for material coefficient of thermal expansion are, how to accurately model the behavior of temperature and humidity, how to accurately capture that behavior, and any modeling errors associated with modeling temperature change. During the April 2008 load test, zero-load readings were included in the load test plan. These zero-load readings were included to record the impact of environmental effects during the duration of the load test. Due to time constraints, only three points were taken, two towards the beginning of the load test and one at the end. For each zero-load reading all traffic, including the load truck, was removed from the bridge prior to and during data collection. The purpose of these three points is to identify change in response caused only by environmental factors, such as temperature and humidity.

One strain gauge from girder 3 and one strain gauge from girder 4 will be used in the demonstration on how environmental effects can be removed from the data. Figure 38 and Figure 39 show the girder 3 and girder 4 strain values, respectively, during the duration of the 2008 load test with a linear trend line connecting the three zero-load points.

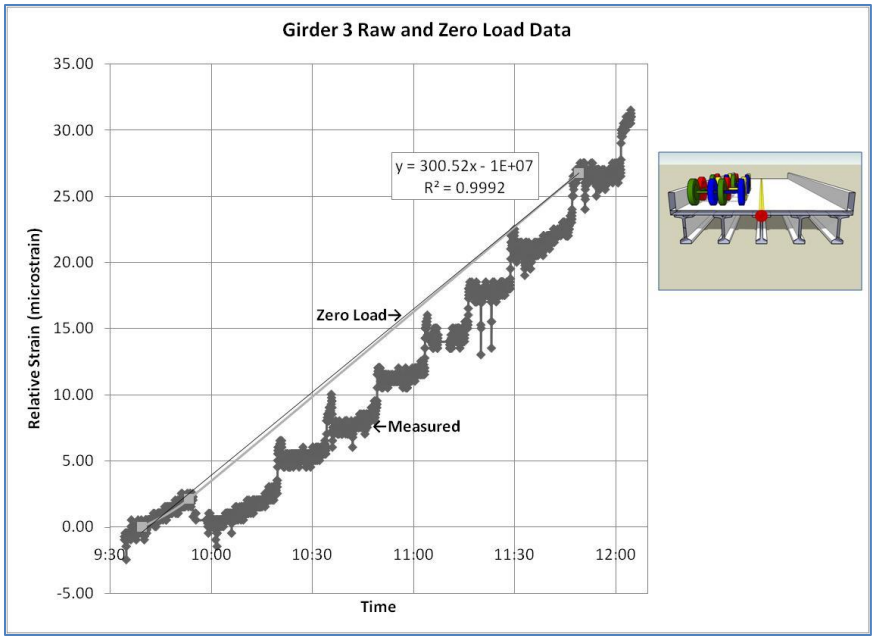

Figure 38: Girder 3 top sensor raw data from April 2008 load test, with three zero-load data points and trend line included

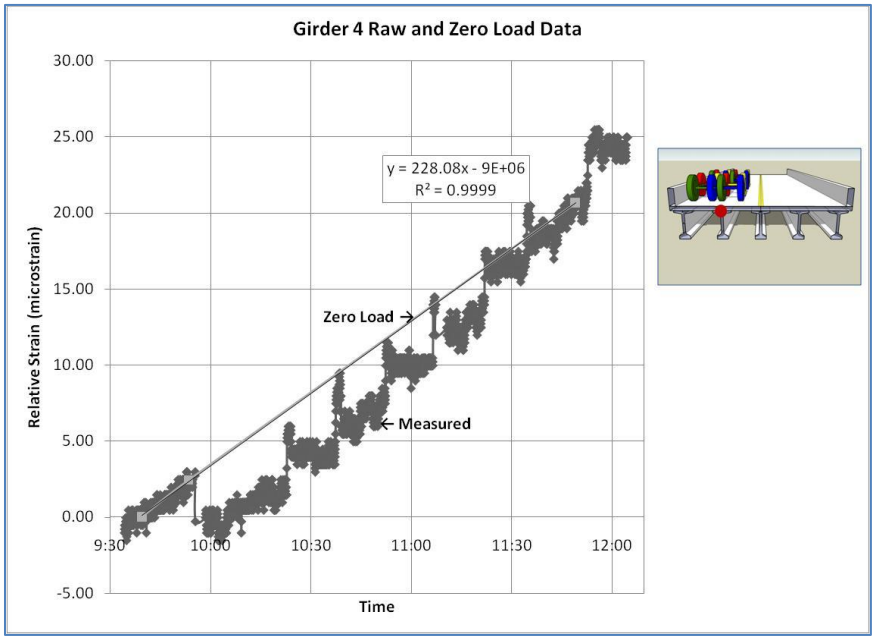

Figure 39: Girder 4 top sensor raw data from April 2008 load test, with three zero-load data points and trend line included

Table 8 shows the three the zero-load readings and coordinating strain values. From this point forward, all data will be plotted as relative strain for ease of comparison between conventional corrected, empirically corrected strain, and raw data. This means a point was

chosen as a baseline, and all data was compared to that value for each gauge. The strain values in Table 8 are caused solely by environmental change, mainly temperature, since no other load is applied at those times. Once environmental effects are removed from the data, all three strain readings should read zero.

Table 8: Girder 3 and Girder 4 strain readings at point of zero-load

Relative Zero Points G3	
Time	*Strain (με)*
9:39:30	0.00
9:53:30	2.12
11:49:30	26.80

Relative Zero Points G4	
Time	*Strain (με)*
9:39:30	0.00
9:53:30	2.42
11:49:30	20.68

4.3.2 – Conventional Thermal Correction

The conventional thermal strain equation can be seen in Equation 2, where α is the linear coefficient of thermal expansion, ΔT is the change in temperature, L is the original length of the member, and δ_T is the algebraic change in length of the member (Hibbler, 2005).

Equation 2: Conventional thermal change in length equation (Hibbler, 2005)

$$\delta_T = \alpha \Delta T L$$

Bowman (2002) examined the difference between the compensated and non-compensated strain gauges. The coefficient of thermal expansion of the compensated gauge is similar to the substrate in which it is embedded. All of the gauges used in this research project are non-compensated, meaning a slight correction must be performed to remove the expansion of the gauge due to temperature change. Bowman, M. M. (2002) obtained the equation for this correction from ROCTEST, seen in Equation 3.

Equation 3: ROCTEST correction equation (Bowman M. M., 2002)

$$\varepsilon_{LOAD} = (L_1 - L_0) + (\alpha_g - \alpha_s)(T_1 - T_0)$$

where,

ε_{LOAD}: Real strain, mechanic strain due to applied load (relative strain)

L_1: Reading from strain gauge

L_0: Initial reading from strain gauge

α_g: Thermal expansion coefficient for the gauge (0, if gauge is not compensated)

α_s: Thermal expansion coefficient for substrate on which gauge is fixed (4.4×10^{-6} /°F (Bowman, 2002))

T_1: Temperature reading of structure

T_0: Initial temperature reading of structure

Equation 2 is used to calculate change in the structure as a whole. Equation 3 is used to provide a numerical quantification for the difference in thermal expansion of the stainless steel gauge material and the concrete in which it is embedded.

Using Equation 3, the internal temperature readings from the temperature sensors and taking the first zero-load reading for L_0 and T_0, the conventional thermal correction is applied. The results from the correction can be seen in Figure 40 and Figure 41.

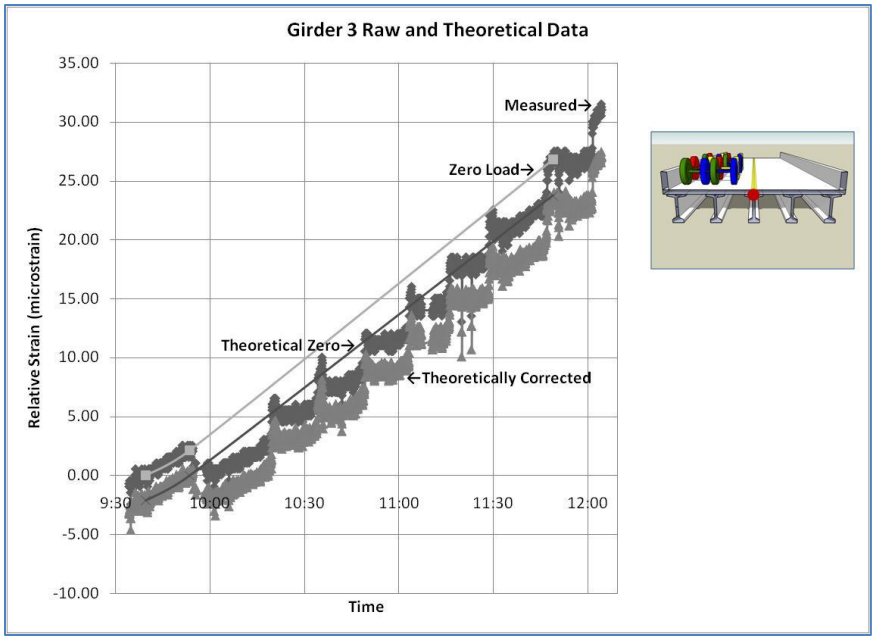

Figure 40: Girder 3 top sensor raw and theoretical data from April 2008 load test, with three zero-load data points and trend lines included

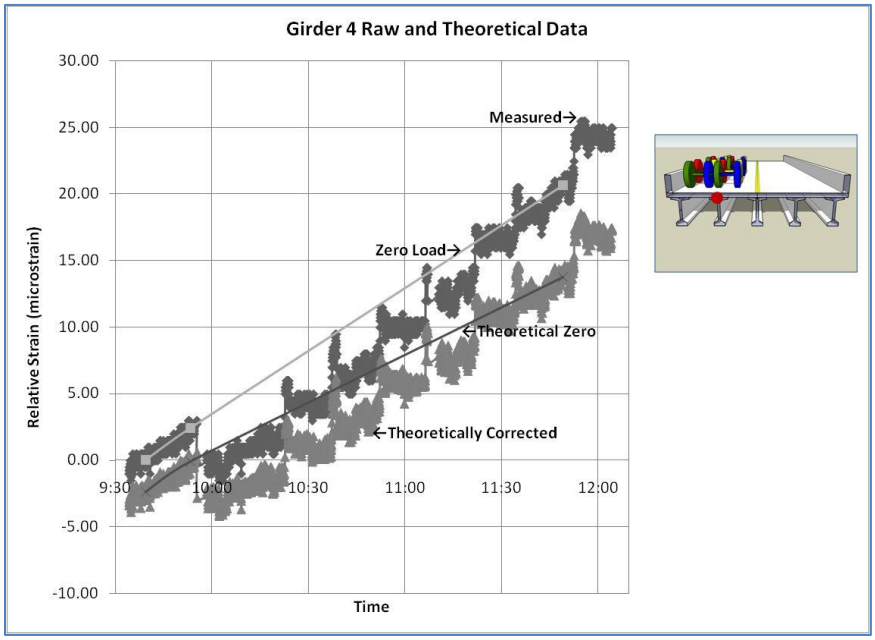

Figure 41: Girder 4 top sensor raw and theoretical data from April 2008 load test, with three zero-load data points and trend lines included

In the graphs above, it can still be seen that environmental effects are masking load application. Table 9 shows a similar table as shown before of the strain readings at the three zero-load times. There has been a reduction in strain values because if all environmental effects

were properly removed, these values should all read zero. Also, if the environmental effects were removed, the trend line for zero-load points shown in the graphs should lay along the x-axis (time axis).

Table 9: Girder 3 and Girder 4 conventionally corrected strain readings at point of zero-load

Conventionally Corrected Zero Points G3	
Time	*Strain (με)*
9:39:30	-2.13
9:53:30	-0.02
11:49:30	23.77

Conventionally Corrected Zero Points G4	
Time	*Strain (με)*
9:39:30	-2.39
9:53:30	-0.09
11:49:30	13.75

4.3.3 – Empirical Environmental Correction

Since the conventional thermal correction did not obtain the desired results, researchers investigated a more empirical method to account for environmental effects. This method was fairly simple to formulate since there were three zero-load points recorded for the April 2008 load test. Using these three points, the data can be accurately corrected to remove environmental effects and show the bridge response caused only by applied loads. The idea behind the correction is simple and goes along with the desired results from the previous correction. The three zero-load strain values are desired to be zero and the slope of the trend line for the zero-load strain readings should be zero. Using these two basic ideas, the effects of the slope, temperature, can be removed from the data and all the desired results should be achieved.

Using statistical methods, a confidence interval (CI) of 95% on the mean reading during the zero-load times, the correction was applied and the results can be seen in Figure 42 and Figure 43. The previous correction data was included in these graphs to show the change in data.

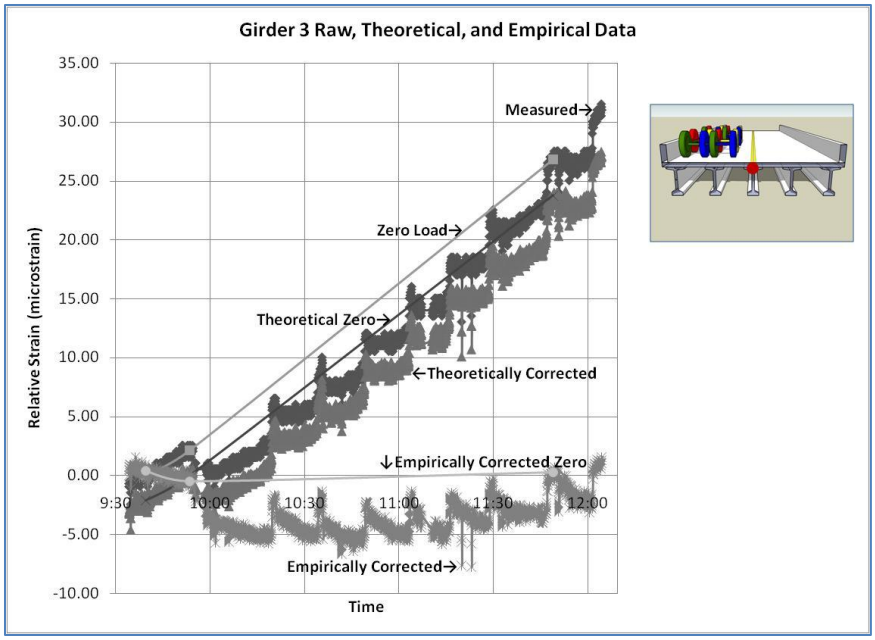

Figure 42: Girder 3 top sensor raw, theoretical, and empirical data from April 2008 load test, with three zero-load data points and trend lines included

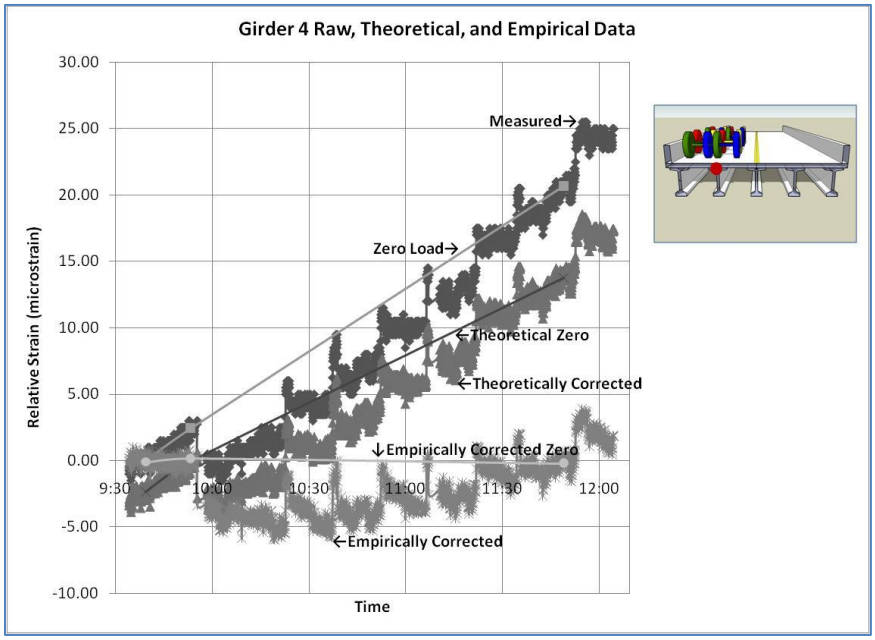

Figure 43: Girder 4 top sensor raw, theoretical, and empirical data from April 2008 load test, with three zero-load data points and trend lines included

These graphs show the reduced overall slope of the zero-load trend line as well as a much clearer visual representation of load application over the duration of the load test. Table 10 numerically confirms that the environmental effect was properly removed from the data, as the

strain values are close to zero. If more zero-load points were taken, the accuracy of the technique would improve.

Table 10: Girder 3 and Girder 4 empirically corrected strain readings at point of zero-load

Empirically Corrected Zero Points G3	
Time	*Strain (με)*
9:39:30	0.42
9:53:30	-0.50
11:49:30	0.29

Empirically Corrected Zero Points G4	
Time	*Strain (με)*
9:39:30	-0.13
9:53:30	0.15
11:49:30	-0.22

Further verification of the method can be seen in Figure 44 and Figure 45, where the truck position is included in the strain plots. There are two spikes seen in the data between 11:00 and 11:30 where it was noted by researchers that two large 18-wheeler trucks passed over the bridge. This spike is seen higher on girder 3 than girder 4 because the truck passed over girders 1 and 2.

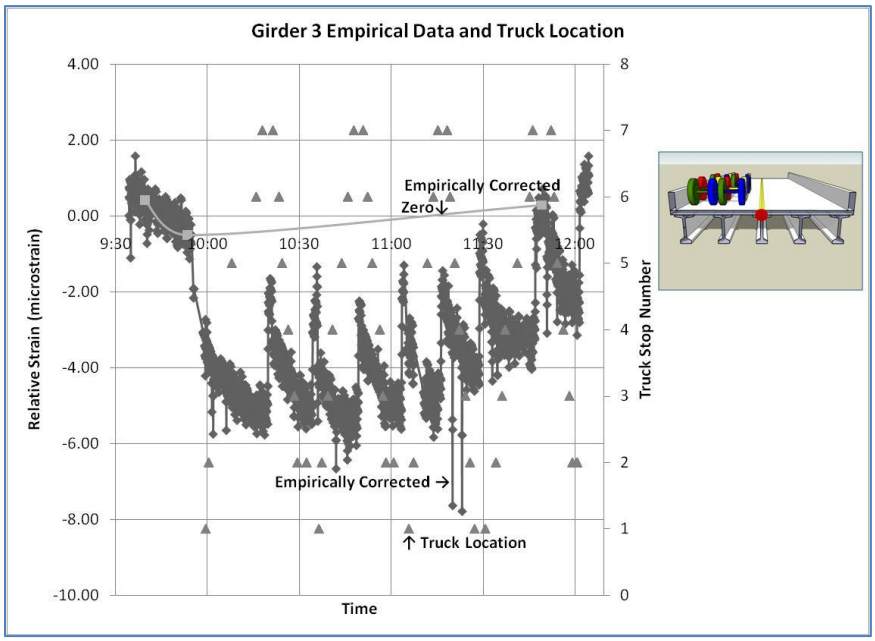

Figure 44: Girder 3 top sensor empirical data with truck position from April 2008 load test

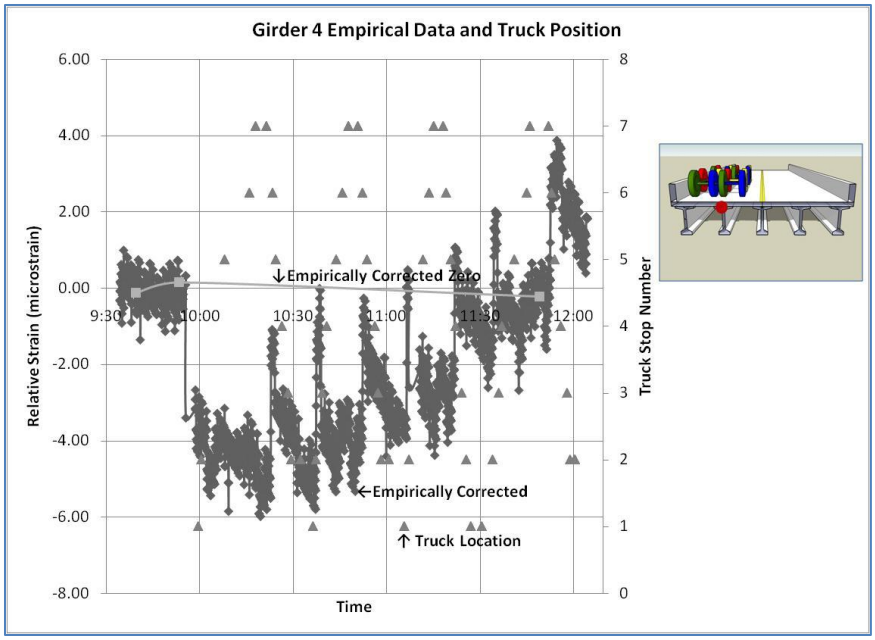

Figure 45: Girder 4 top sensor empirical data and truck position from April 2008 load test

4.3.4 – Discussion of Environmental Effect Correction Techniques

The theoretical thermal correction, presented here, accounts for axial effects only. The empirical environmental correction uses the actual response of the bridge to quantify the total environmental impact, including thermal effects. The equation for the conventional correction requires a coefficient of thermal expansion. The value used in the analysis was the coefficient of thermal expansion for the high performance concrete where the gauge was installed. Like with any bridge component and the analysis of that component, applied loads are not just taken by one part of the bridge, they are taken by the entire bridge as a whole. Instead of calculating participation factors and a coefficient of thermal expansion for the entire bridge, empirical correction methods can successfully be used to account for all environmental effects, not just temperature, from the collected strain data.

The empirical correction more accurately reflects actual conditions at the bridge and removes unknown components associated with theoretical assumptions. Performing the empirical correction also takes into account all possible environmental effects that could cause a

change in structural behavior at the bridge, such as humidity and even soil conditions as the temperature changes throughout the day. The empirical method can be done with little calculation and only requires having several zero-load readings included in the load test program. Once all environmental effects are properly accounted for in the load test data, a more effective model updating and parameter estimating process can occur.

Unfortunately, only the April 2008 load test took advantage of recording several zero-load readings during the load test. The December 2000 and August 2001 load test did have a zero-load reading, although not enough to get an accurate trend of temperature throughout the load test. For this reason, only the April 2008 load test data will be used to update the bearing pad stiffness values for the manual model updating portion of this research.

Figure 46 and Figure 47 show the raw and empirically corrected data along with the four load cases removed for manual model updating. These four load cases correspond to when the truck is located close to the center of the bridge and where survey measurements were recorded.

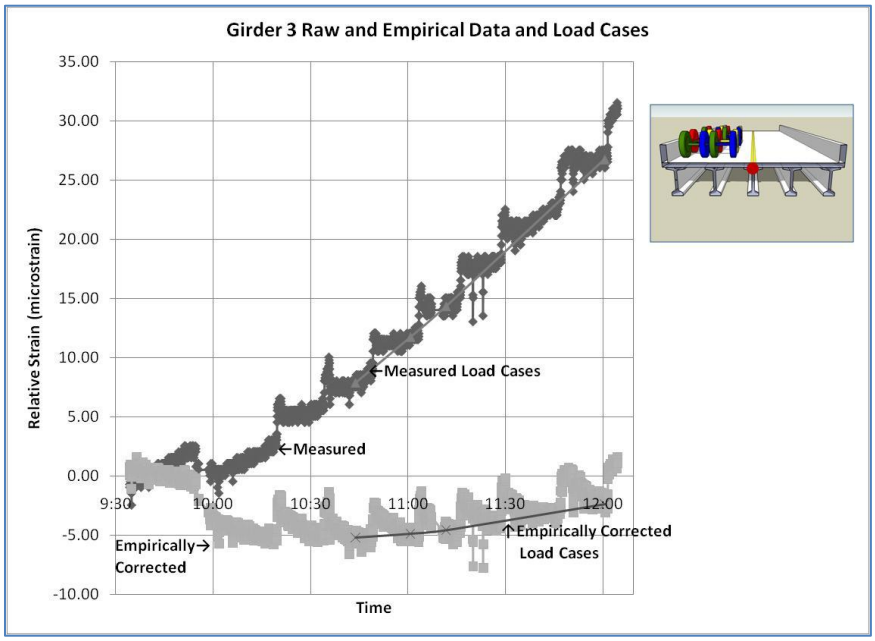

Figure 46: Girder 3 raw and empirical data with manual model updating load cases

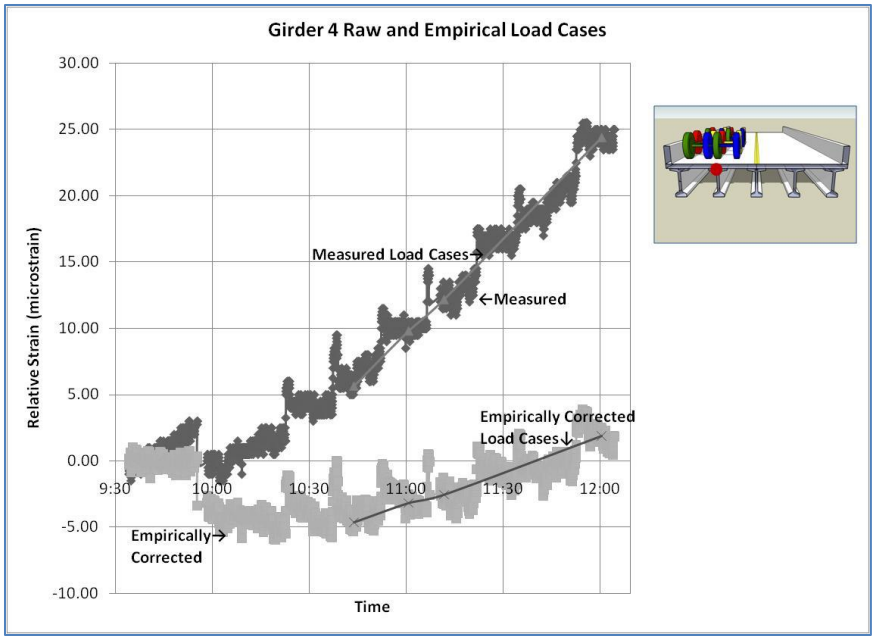

Figure 47: Girder 4 raw and empirical data with manual model updating load cases

The same correction methodology that was applied to the Girder 3 and Girder 4 top sensors was also applied to the Girder 5 top and middle sensors. Figure 48 and Figure 49 show the raw, theoretical, and empirical data for Girder 5 top and Girder 5 middle sensors respectively.

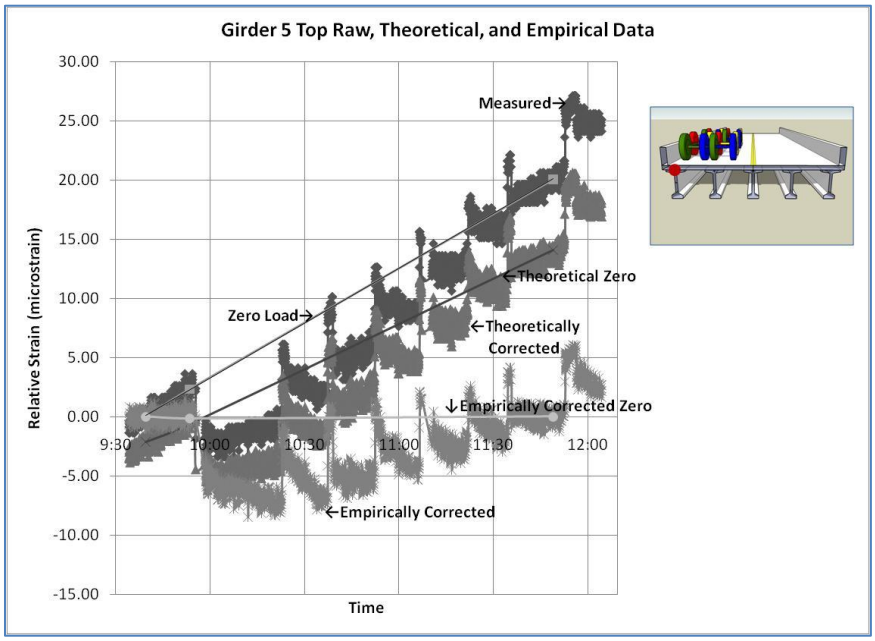

Figure 48: Girder 5 top raw, theoretical and empirical Data from April 2008 load test, with three zero-load data points and trend lines included

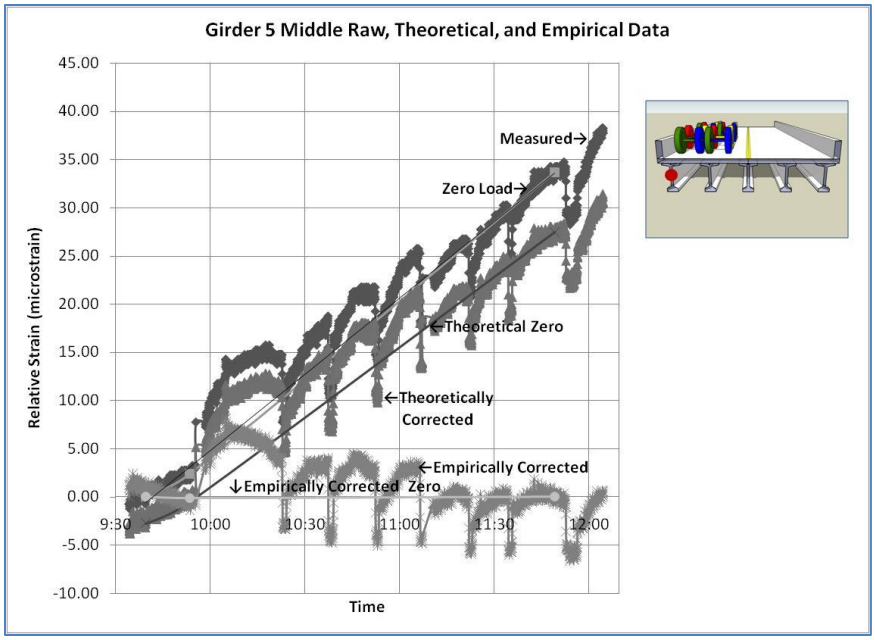

Figure 49: Girder 5 middle raw, theoretical and empirical data from April 2008 load test, with three zero-load data points and trend lines included

Similar to the load cases used from the Girder 3 and Girder 4 empirically corrected data, four load cases simultaneously were created from the Girder 5 top and middle empirically corrected data, see Figure 50 and Figure 51.

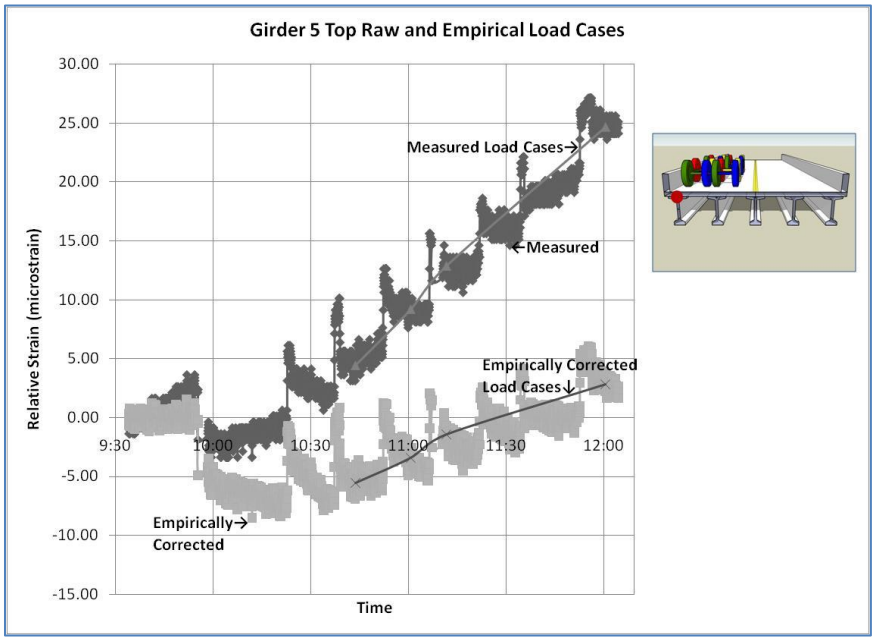

Figure 50: Girder 5 top raw and empirical data with manual model updating load cases

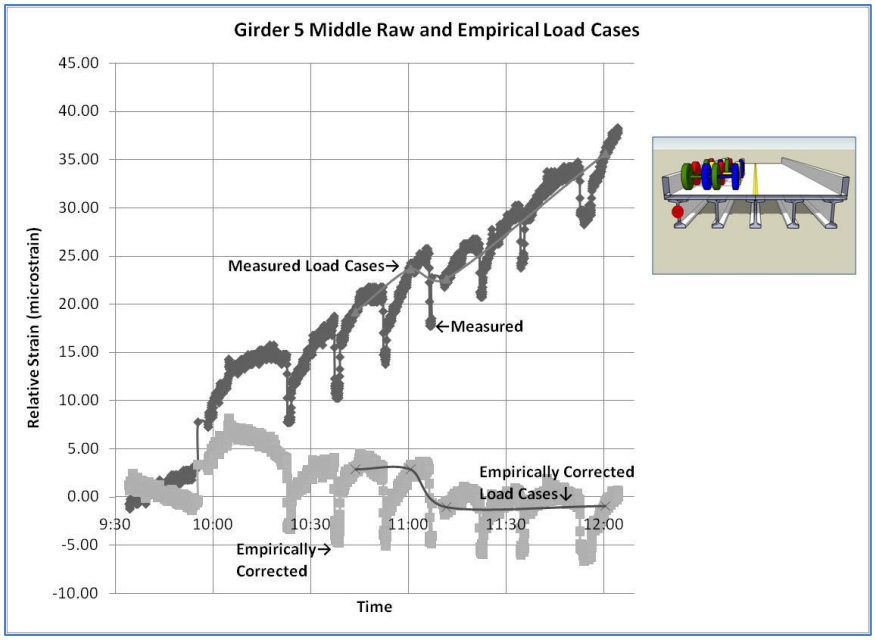

Figure 51: Girder 5 middle raw and empirical data with manual model updating load cases

4.3.5 – Interpretation of Results

In all of the measured data, it can be seen that there is a general positive slope in the collected data, with variation that corresponds to the truck's position on the bridge. The strain values return to the zero-load line when the truck drives off of the bridge to turn around and prepare for the next run. Figure 52 shows the empirically corrected data from Girder 3, which includes spikes due to traffic being allowed to pass between runs, strain values obtained from SAP2000® at the seven stop locations, and empirically-corrected strain values at those same seven stop locations. Refer to Figure 17 for the stop locations on the bridge plan.

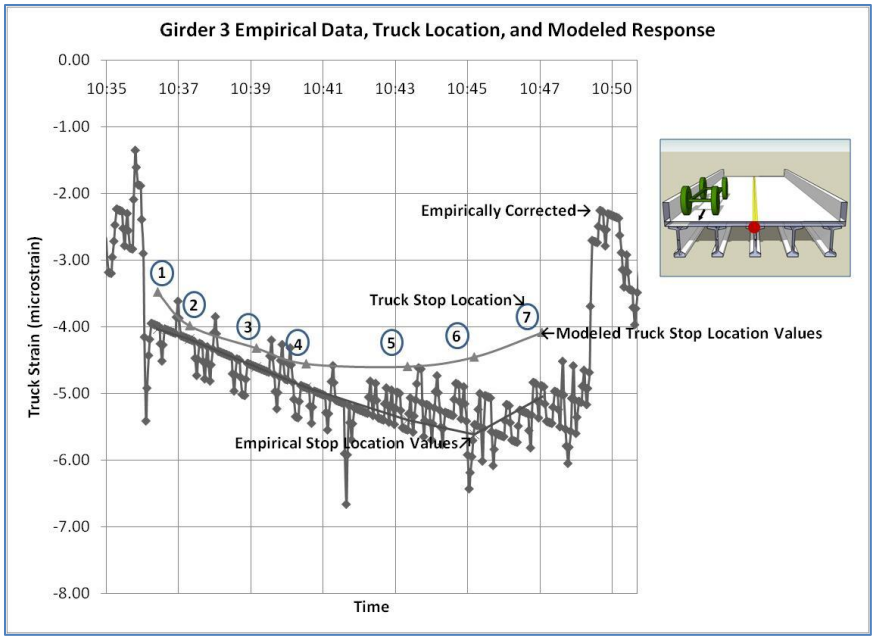

Figure 52: Truck run #3 snapshot for girder 3 with empirical data including traffic, modeled values at stop locations, and empirical values at stop locations

Between each stop location, traffic was allowed to pass on the opposite side of the load test truck, which accounts for the data spikes between truck stop locations. The linear trend for points two through four can be related back to the linear correction performed on the measured response data. The modeled strain values from stop 5 to stop 7 reverse slope and increase. This increase makes sense since the center of gravity of the truck has passed the centerline of the bridge and this measurement is collected at the centerline. Additional zero-load readings would permit a polynomial fit and therefore the environmental correction would more accurately account for environmental effects.

CHAPTER V

MODELING PROTOCOL FOR ROLLINS ROAD BRIDGE

A goal of the Rollins Road Bridge Research Project is to create an analytical predictive monitoring based model to accurately capture the behavior of the bridge. While creating the model, researchers ensured usability was maintained and that tools available for the creation and use of the model were incorporated. Two different programs were looked at for modeling, GT Strudl® and SAP2000®. Specific structural properties such as carbon fiber reinforced polymers in the concrete deck, the New England Bulb Tee Girder, prestressing pattern, and the steel reinforced elastomeric bearing pad were included in the model. Five special topic studies were also done to verify results and ensure that the desired results were being achieved.

5.1 - Program Selection

Modeling is an important part of a value-added SHM program. A project goal was to pass a model along to the NHDOT for use in developing their internal SHM program. It was important to use a modeling program that the personnel at the NHDOT were already familiar with. The NHDOT currently owns both GT Strudl® and SAP2000®. Both programs can be used in conjunction with AutoCAD for importing model geometry and Excel for importing material and section properties. Due to the user interface of SAP2000® and its ability to export both the stiffness and the mass matrix, SAP2000® was chosen from this research.

SAP2000® contains an advanced programming interface (API) which would allow for a seamless integration between SAP2000® and a MATLAB® based parameter estimation program, MUSTANG (Model Updating STructural ANalysis proGram), currently under development at UNH. GT Strudl® does not have these API capabilities. MATLAB® and SAP2000® are also industry partners, which also makes programming MUSTANG much easier. Another huge benefit of SAP2000® is that it contains the Bridge Information Modeler (BrIM™) which is a GUI, step-by-step wizard that allows the user to construct a bridge model.

The BrIM™, as seen in Figure 53, allows for an easy graphical creation of the bridge model. Users can decide whether to create a basic or complex bridge model using the BrIM™. The BrIM™ also offers the NHDOT a friendly module that can be used for model creation of different bridge types. SAP2000® has the ability to view the model as a stick model or extruded, where the actual appearance and thickness of different elements are seen. This makes the model more visually appealing, adding value to the use of SAP2000®.

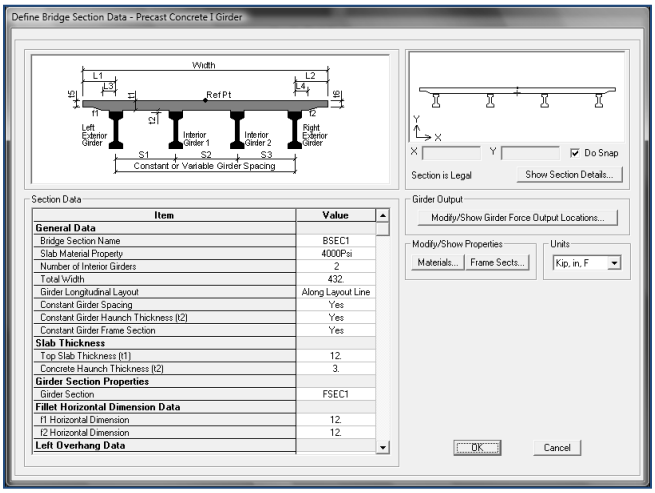

Figure 53: SAP2000® Bridge Modeler (SAP2000, 2007)

In the model creation portion of the BrIM™, the amount of discretization for size of shells in deck and the amount of discretization in the beam element in the girders are user defined variables. Once the base model is created using the BrIM™, the model can be modified

through property and material definitions to transform the model from a design model to a monitoring model. Benefits to using SAP2000® include usability, appearance, linkability between SAP2000® and MATLAB®, ease of creation, and a more advanced user interface.

5.2 - Initial Modeling

The first analytical model of RRB was created in GT Strudl®, modeling the NEBT as frame elements and the deck as shell elements, as seen in Figure 54. The original plan was to put a considerable amount of time into node creation and load position correlating to the load tests so that the weight of the truck can easily be transferred to the modeled deck through nodes. Nodes were specifically created at the point of truck load application. The material properties in the GT Strudl® model were user defined, but not applied easily. The need for several calculations to get the correct elements modeled correctly made it tedious, and then the element did not show up as a visual representation.

In order to model the NEBT section properly in GT Strudl®, wide flange section properties had to be modified to match that of the NEBT. There was also difficulty in trying to get the bridge deck and NEBT frame members to act in composite action. The use of "master" and "slave" joints was attempted, however that was not successful because the joints on the edges of the deck were not associated with a girder underneath, so they did not deform with the rest of this structure. During the time when the problem was being investigated, the decision to use SAP2000® was made. The time to create a comparable model using the SAP2000® BrIM™ took significantly less than the hours devoted to the creation the first GT Strudl® model.

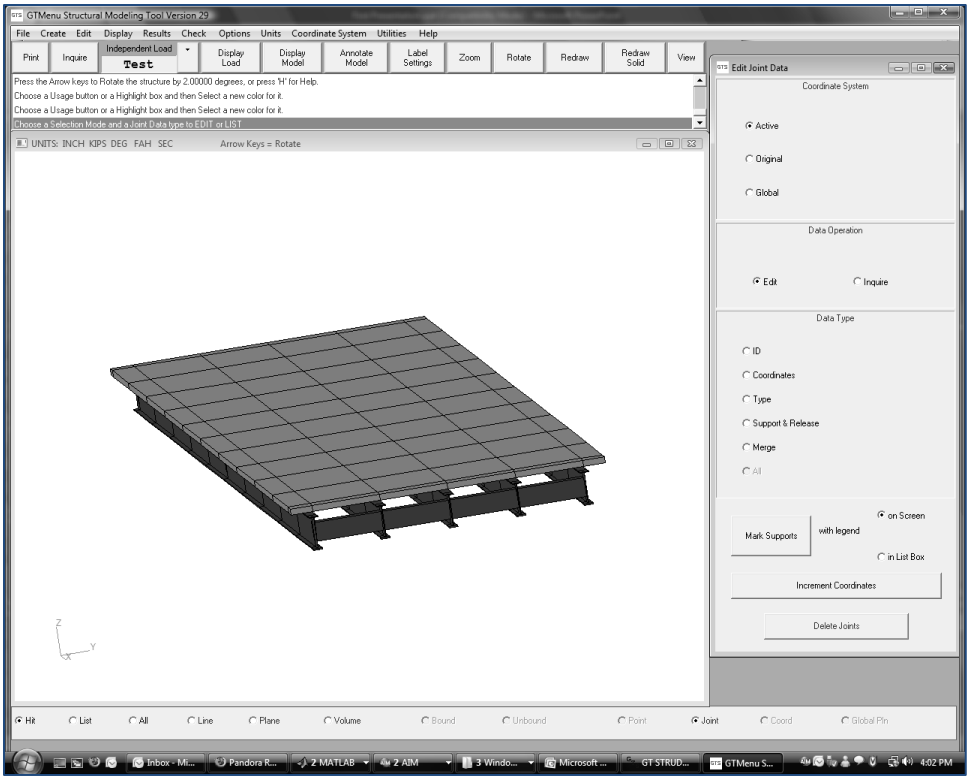

Figure 54: GT Strudl® bridge model (GT Strudl, 2007)

Using SAP2000® and the BrIM™, the end model was visually appealing, relatively easy to create, and the results were accurately and easily obtained. The original plan for modeling was to create three models; model 1 having the girder as frame elements and the deck as shell elements, model 2 having the girder as frame elements and the deck as brick elements, and model 3 having the girder and the deck modeled as brick elements.

5.3 - Modified Modeling Plan

Once the research project was underway, the initial model plan was refocused to include specific elements and environmental impacts. The goal of creating a usable model for the NHDOT SHM program was still maintained, however the focus of that model was slightly modified. The first model, GT Strudl® model, was used for comparison between the software programs. The second model was created using the BrIM™ in SAP2000®.

Once the design based model was created and verified using the BrIM™, the bridge modeler was disabled to allow the modeler to fully control the model creation. The use of the BrIM™ takes full advantage of all the research done by Computer & Structures, Inc. (CSI) for the creation of the base bridge structural model and then allows modelers to adjust that model to fit the goals of each particular project. Structural components included in this monitoring model were (1) prestressing tendons in the girder, (2) CFRP reinforcement in the deck, (3) the bridge rail, and (3) boundary conditions modeled as linear springs with prescribed stiffness.

5.3.1 – Modeling the CFRP Reinforce Concrete Deck

The deck was modeled using design plans for the RRB and measured distances (Bowman M. M., 2002). The CFRP reinforcement in the deck was included once the bridge modeler was disabled and the finite elements used for the bridge deck were changed from shell elements to layered shell elements. The deck of the RRB contains two layers of CFRP reinforcement, one above and one below the centroid of the deck section.

In order to correctly model the CFRP material, the material specifications, the modulus of elasticity and the density were obtained from previous work (Bowman M. M., 2002) and (Trunfio, 2001). The thickness of the CFRP throughout the entire width of the deck was maintained to keep the correct moment of inertia in the transformed section. Since the layered shell material was throughout the entire thickness, not just present every 6-inches, the modulus of elasticity was transformed to capture the same behavior as it is placed in the bridge, see Figure 55. The modification was achieved by calculating the ratio between the actual area of CFRP in the cross section and the modeled area of the CFRP. This ratio was used to reduce the modulus of elasticity for the CFRP layer. The associated calculations are contained in Appendix B –

CFRP Reinforcement Calculations. Figure 56 shows the SAP2000® shell section layer definition window and how the material properties, distance, and thickness were specified.

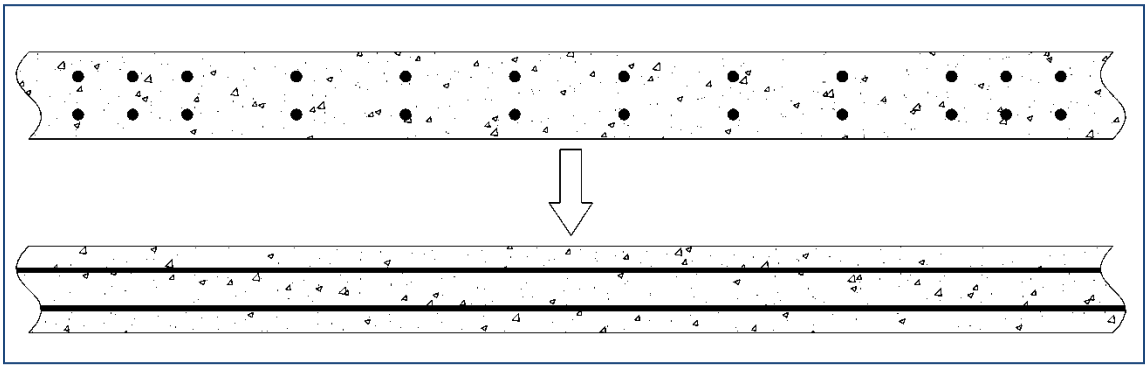

Figure 55: Graphical representation of how CFRP is modeled as layered shell element

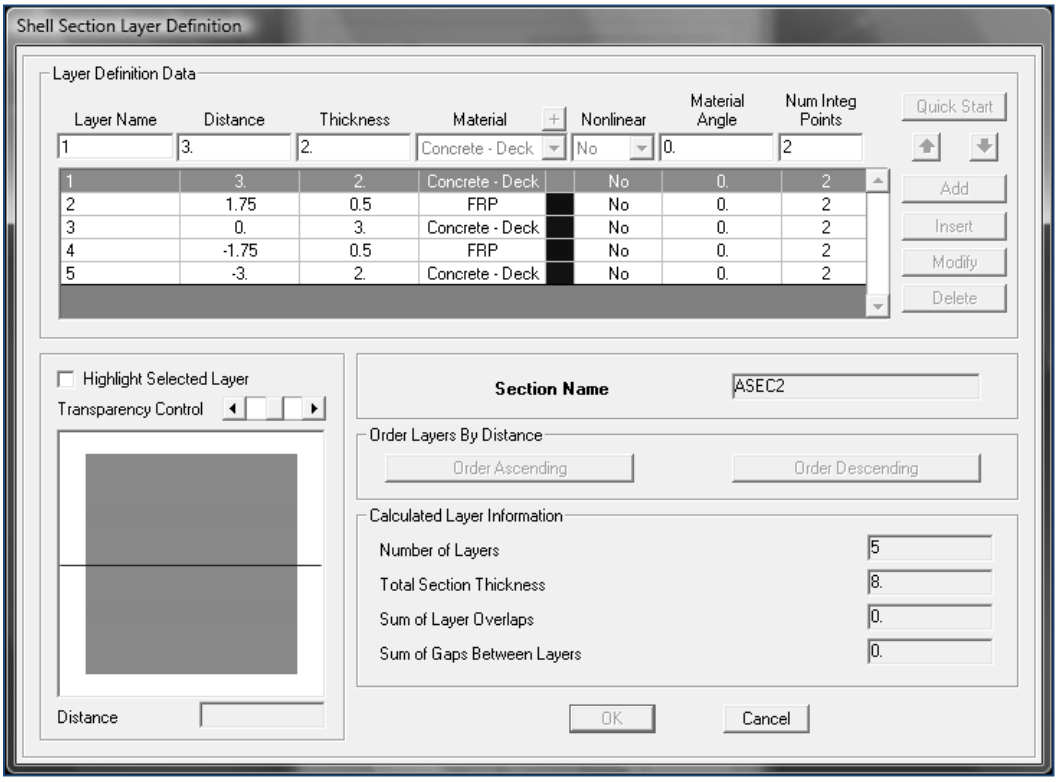

Figure 56: Layered shell properties for RRB deck (SAP2000, 2007)

5.3.2 – Modeling the Prestressed/Precast/HPC NEBT Girders

The SAP2000® BrIM™ contains preloaded concrete girder sections. Those sections can be used or modified depending on the properties of the girder located at the bridge. BrIM™ was a significant benefit to using SAP2000®. BrIM™ contains several options, such as NEBT

elements that make model creation easy for all bridges, not only the RRB. Figure 57 shows the preloaded AASHTO PCI bulb tee included in the BrIM™ with the modified dimensions to match that of the properties of the NEBT.

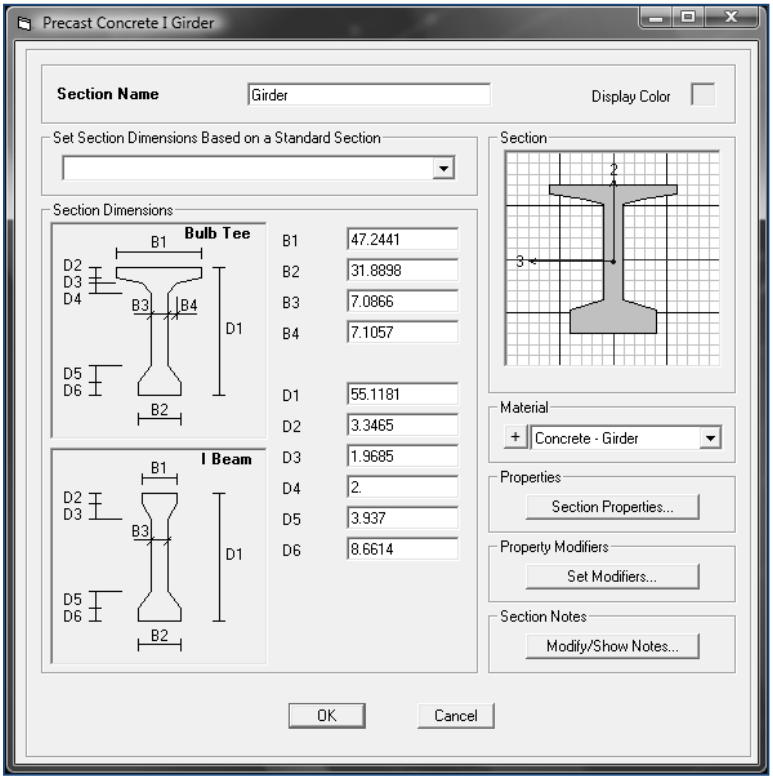

Figure 57: Preloaded NEBT section in SAP2000®

Prestressing tendons were included in the RRB model to accurately capture the bending behavior of the girders. SAP2000® has the ability to add strand patterns, as shown in Figure 58. The two deflection point pattern used at RRB was one of the many options in the BrIM™. The design plans were used for all of the stressing, arrangement, and steel specification information. Losses were calculated using the AASHTO Bridge Code (AASHTO, 2004). The use of these values was validated through *NCHRP Report 496* which looked at the actual prestressing losses at the RRB and compared them with prestressing losses calculations using AASHTO (Tadros & Al-Omaishi, 2003). During fabrication, the strand pattern was laid out, as prescribed in the plans,

and researchers were present at time of prestressing and pouring of the precast girders to ensure compliance.

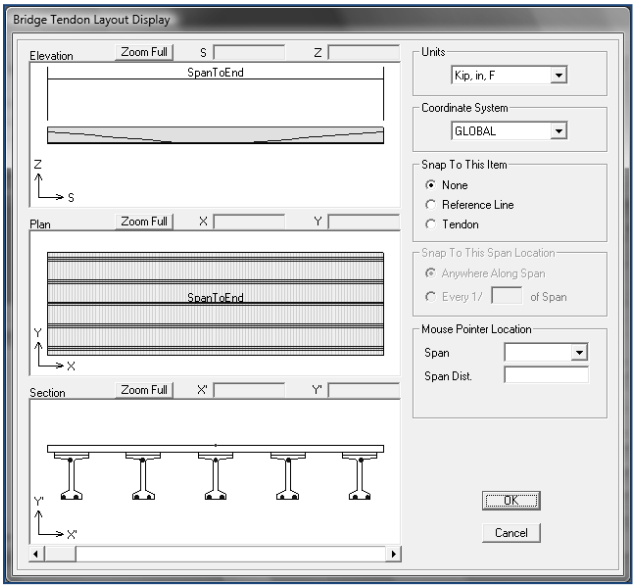

Figure 58: SAP2000® bridge tendon layout (SAP2000, 2007)

5.3.3 – Modeling the Steel Reinforced Elastomeric Bearing Pad

Steel reinforced elastomeric bearing pads support the RRB on the abutments, which transfer all loads into the ground. The bearing pads have three different possible directions of motion, as seen in Figure 59, caused by axial load, shear forces, and rotation.

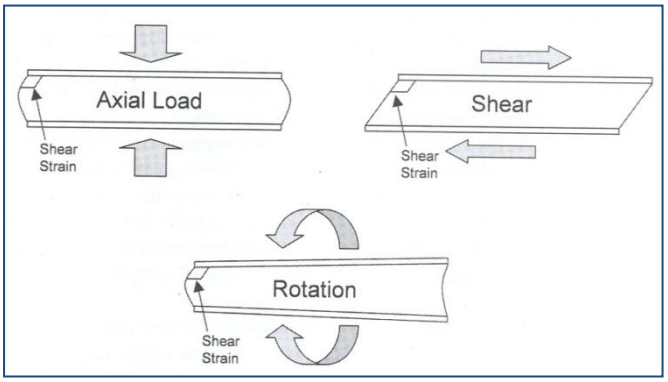

Figure 59: Deformations of a laminated elastomeric bearing pad (Stanton, Roeder, Mackenzie-Helnwein, White, Kuester, & Craig, 2008)

The steel reinforced elastomeric bearing pads were a focus of this research, because there is not a conventional equation to calculate the horizontal stiffness, which will be discussed in

detail in this section. Visual inspection showed no cracking or deterioration in the deck or girders. Representatives from D.S. Brown, Inc. have stated that the elastomeric bearing pads have a service life of up to 75-years. Research has been conducted beyond the initial research performed by AASHTO, on both the axial and rotational stiffness of steel reinforced elastomeric bearing pads in order to develop bearing pad stiffness (Stanton, Roeder, Mackenzie-Helnwein, White, Kuester, & Craig, 2008). This research and physical testing, has resulted in two equations, seen in Equation 4 that can be used to calculate axial and rotational stiffness for one layer of the elastomer. Combining the layers of elastomer and steel together, results in an overall stiffness for the bearing pad (Stanton, Roeder, & Mackenzie-Helnwein, 2004). Calculations of the bearing pad stiffness can be seen in Appendix d – Calculation of Reinforced Elastomeric Bearing Pad Stiffness.

Equation 4: Axial and rotational stiffness of one layer of elastomer (Stanton, Roeder, & Mackenzie-Helnwein, 2004)

$$K_a = \frac{P}{\Delta_a} = \frac{EA(A_a + B_a S^2)}{t}$$

$$K_r = \frac{M}{\theta_r} = \frac{EI}{t} \; A_r + B_r S^2$$

A total of ten, 16-inch diameter, steel reinforced elastomeric bearing pads are installed at RRB, one at each end of each girder. The bearing pads allow slight vertical compression while allowing the beam to rotate. Modeling spring boundary conditions, via links, in SAP2000® is also fairly simple. The BrIM™ allows for several different types of boundary conditions to be used, from traditional fixed or pinned connections, to user defined links. When links are used, the user is allowed to specify stiffness in all directions, as seen in Figure 60. Links are used because they can be updated in the model updating process and more accurately capture the behavior of the actual bearing as opposed to a pinned or fixed condition. In the U2 directions

(translation parallel to the abutment) a stiffness of $1.000E^{+09}$ kip/in is used to show translational fixity in those directions and in the R1 and R3 directions (rotation about a line normal to the abutment and about a vertical line) a stiffness of $1.000E^{-09}$ kip/rad is used when rotational stiffness is not included. These values are specified instead of using the traditional boundary condition option to be fixed or free in SAP2000®. Using values that accurately represent fixed and free did not cause the numerical instability but essentially gave the same response.

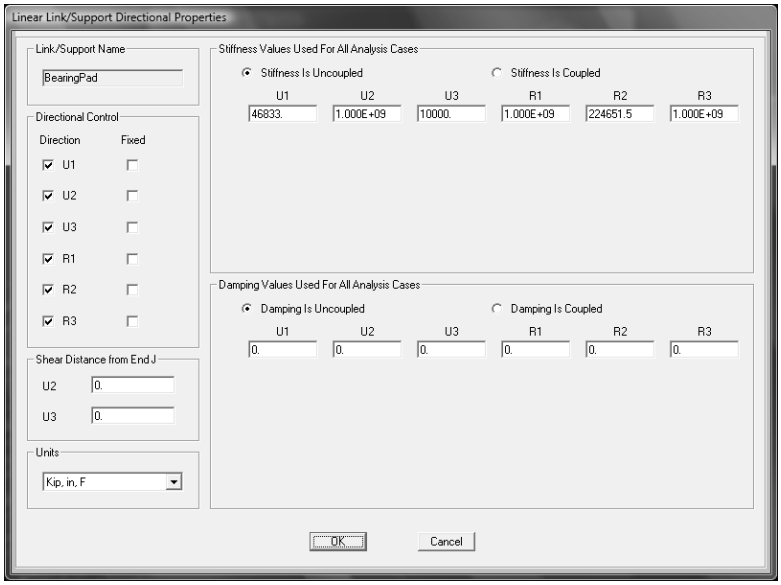

Figure 60: Stiffness parameters for modeled reinforced elastomeric bearing pad (SAP2000, 2007)

Stanton et al. (2008) has equations to calculate axial and rotational stiffness of the elastomeric bearing pads, however, it does not provide equations for the calculation of horizontal stiffness caused by shear effects. That value is what was used in the manual parameter estimation exercise for this research.

5.3.4 – Modeling the Bridge Rail

The bridge rail at Rollins Road Bridge is a cast-in-place concrete rail. The rail will be modeled as a frame element and connected to the bridge deck through links since, as seen in Figure 61, it is connected to the bridge deck using stainless steel reinforcement.

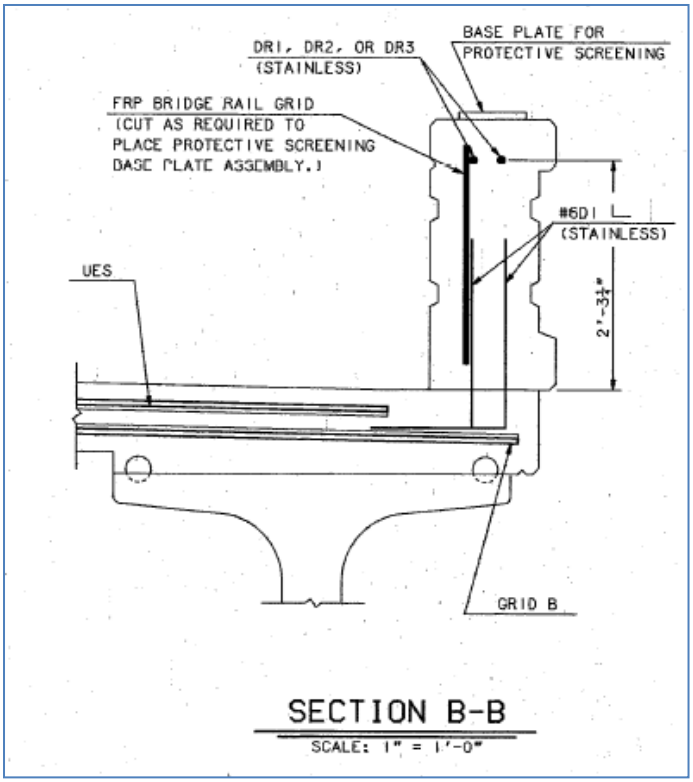

Figure 61: Section view of bridge rail connection to bridge deck (NHDOT Bureau of Bridge Design, 1999)

5.4 - Special Topic Studies

Five special topic studies were conducted during this research project. Special studies are meant to examine specific, smaller issues that affect modeling. These studies try to ensure that the structural behavior is being properly captured by the structural model. They also assist in the development of a universal protocol for correlation between collected and predicted structural response. Special studies tie into the goal of maintaining model usability while enhancing capabilities. The five studies include hand calculations to verify the SAP2000® model, hand calculations to verify strain obtained from the SAP2000® model, looking at the stiffness matrix export from SAP2000®, looking at an easier way for load application, and looking at the different ways to apply thermal load in the model.

5.4.1 – Hand Calculation Verification of SAP2000® Model

The structural properties included in the model are known to a high degree. However, including these structural properties without any verification would make that data blindly valid. Several steps were taken to verify that the bridge was being properly modeled, and that the desired results were being extracted from the analysis. To do this verification, hand calculations were performed using structural analysis and bridge design techniques to obtain numerical results and compare to the SAP2000® output. The model that was used in these hand calculations and modeled separately from the RRB model in SAP2000® was a reduced model. The model was reduced for ease of hand calculation, and because this is a verification. The hand calculations would be tedious to verify the entire bridge model, however if individual components are verified, it can be assumed that the model as a whole is performing as desired.

This reduced model maintained the geometry of the RRB, was simply supported, and did not have the prestressing forces. The prestressing loads and strand pattern were known with a high degree of certainty. In hand calculations, as assumed with the NDT load test, the bridge remains in the linear elastic range, which also simplifies calculations. The CFRP remained in the model for hand calculations to ensure that it was modeled properly using transformed sections. The base material for the transformed section was the girder concrete. The material properties of the deck and the CFRP were transformed, accordingly. In the hand calculations, a point load of 100-kips was placed at the midspan of the transformed section. A similar load was placed in the SAP2000® model, discretizing the point load along the width of the bridge deck to total the 100-kips put in the hand calculations. All of the hand calculations can be seen in Appendix e - Calculations for Model Verification. Both deflection and strain measurements were calculated

and compared to the SAP2000® model. The results of the hand calculation versus SAP2000® can be seen in Table 11.

Table 11: Hand calculations and SAP2000® model comparison for deflection and strain

	Hand Calculated	SAP2000® Model	% Difference
Deflection *inches*	0.253	0.243	1.94%
Strain *microstrain*	24.9	25.7	3.21%

With this information, as well as all of the details included in the model listed above, researcher had a high confidence in the accuracy of the model of RRB.

5.4.2 – Obtaining Strain from SAP2000® Model

In order to compare the data from the SAP2000® model to the measured response, an important calculation had to be performed. The output from the beam elements that represent the girders, in SAP2000® is limited to displacements, rotations, axial force, bending moment, and shear. These outputs values must then be translated into strain. Initially, axial force and bending moment predicted in the girder along with the girder geometry, are transformed into axial and bending strain. After a close examination of these values, it was determined that they did not accurately capture the composite action between slab and girder occurring at the bridge.

Several other methods to get strain were considered, including re-modeling the entire bridge using solid elements, in which strains can be taken directly. However, that method would require remodeling the bridge and reducing the usability of the model. It was finally determined that the displacement of the deck and girder could be manipulated to find strain values. Since the behavior exhibited by the bridge is within the linear elastic range of the material, it can be assumed that the strain is linearly varying throughout the depth of the bridge. Using this principle, the deflection values, in both the x- and y-direction, from SAP2000® can be extruded

for the nodes that comprise the deck above the sensor location, as well as the nodes that comprise the girder at sensor location. Once these values are obtained, and the initial values are known, strain at the deck level and girder center line can be calculated, and then linear interpolation allows finding the exact strain value at the depth of the strain gauge. Figure 62 shows a basic diagram on how strain is calculated. Knowing the new and original length of both elements, the difference between new and original length divided by the original length equals the strain value at the deck and girder levels. This can then be transformed to any depth in the bridge cross section. Sample calculations to obtain actual strain values can be seen in Appendix f – Strain Calculations.

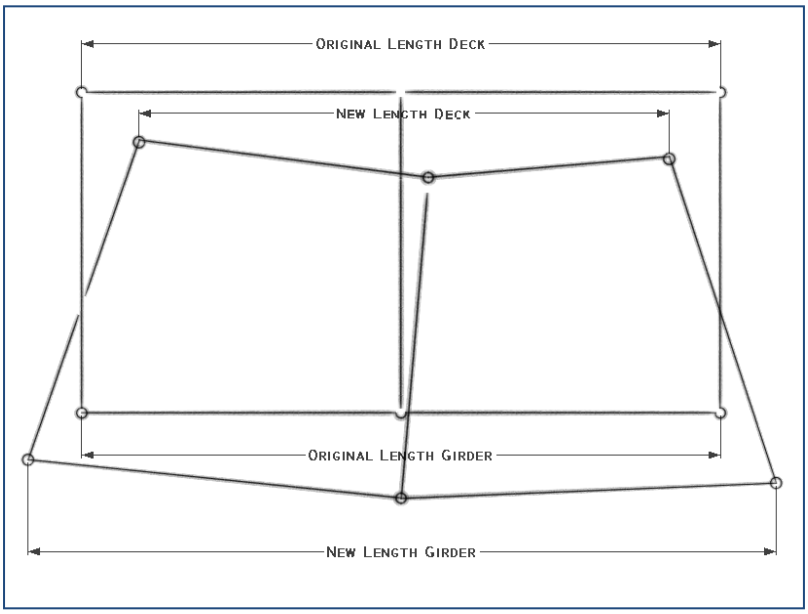

Figure 62: Strain calculation diagram

5.4.3 – Stiffness Matrix Export

The capability for SAP2000® to export the stiffness matrix of models was an important characteristic for choosing SAP2000®. This special topics study was done to verify the output from SAP2000® compared with conventional stiffness calculations. This was done by comparing the SAP2000® output to hand calculations using matrix structural analysis

techniques. A simple cantilever beam model was created in SAP2000®. The same cantilever beam was analyzed using matrix structural analysis, and the results were compared. An illustration of the cantilever beam and both hand (MATLAB®) and SAP2000® outputs can be seen in Figure 63.

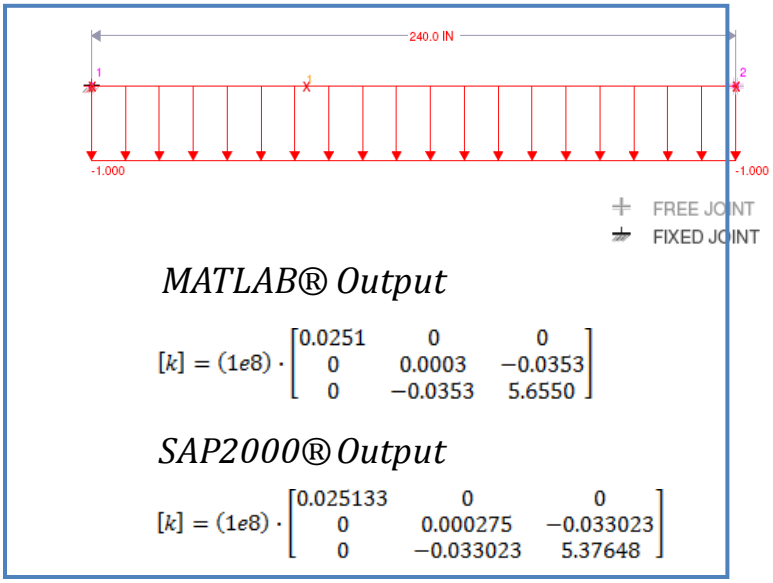

Figure 63: Modeled cantilever beam with MATLAB® and SAP2000® stiffness matrix output

The output from both methods correlated within an acceptable degree of accuracy. This matching of stiffness matrices will allow for the programmers of MUSTANG to take full advantage of the exported stiffness matrix from SAP2000®. This link eliminates the need for a parameter estimation program to develop its own stiffness matrix by exploiting the modeling capabilities of SAP2000®.

5.4.4 – Load Application

Typical load application is achieved by applying a load to a node in the model. The BrIM™ has a predetermined pattern for creating joint locations in the bridge model, which did

not correspond to the location of the truck tires. There could be an infinite number of locations for load application during a load test that may not necessarily already be a joint. Typical truck load application is achieved by applying the wheel loads over an area. Accurately modeling these loading points on the shell elements nodes proved to be a challenge.

If a tight finite element mesh was created and the area loads were applied to this separate mesh, resultant forces could be calculated at points of actual node locations on the bridge. A fine mesh, using 3-inch spacing, was created to obtain the force resultants. Once this mesh was created, it could be moved to any location on the bridge to find resultant forces. This universal method proved to be useful during the analysis portion of this research project, allowing loads to be applied in different locations on the bridge, depending on the specific load case. Once the mesh was moved to the area of load application, the equivalent area loads were applied to the mesh model, and the two existing nodes on the deck were selected as boundary conditions in the mesh model. This was done for all areas of load application and the mesh model was run. The resulting reaction forces from the mesh model were then applied to the deck nodes, as seen in Figure 64.

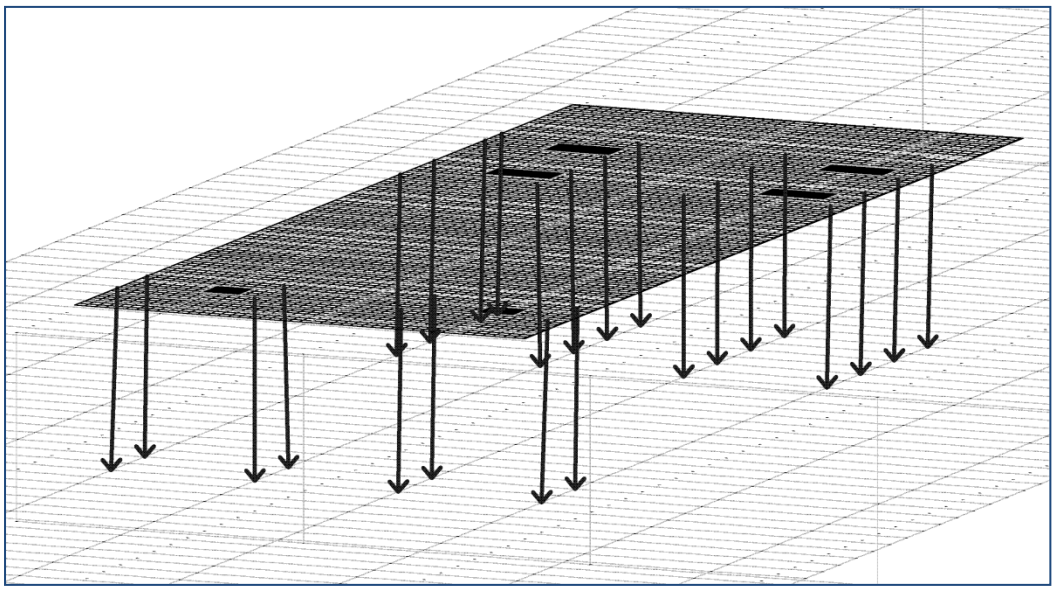

Figure 64: Truck load mesh to bridge deck graphic

The use of force resultants is appropriate for this research because the purpose of the load tests was to look at the overall effect on the bridge. The sensors used in the analysis were in the girders, so local effects from the truck wheels were not of concern. It also takes full advantage of using the BrIM™, while still being universal enough to apply loads to existing nodes at any location on the bridge. Future analysis and load tests at UNH will use this method.

5.4.5 – Thermal Load Application

A special topics study was performed by an undergraduate research assistant, Jacob Carmody, to validate the behavior of a beam under thermal loading in SAP2000® as influenced by element selection. First, using the assumption of beam behavior, hand calculations determine the displacement of a beam due to a uniform thermal loading. These calculations were then compared to two SAP2000® models, a shell element model and a solid element model. The displacement calculated from by hand calculations was 0.0264-inches, the shell element beam had a displacement of 0.0277-inches, and the solid element beam had a displacement of 0.0265-inches. All are well within a 5% difference, which is acceptable for these types of calculations. Figure 65 shows an example SAP2000® output for the analysis done during the temperature special study.

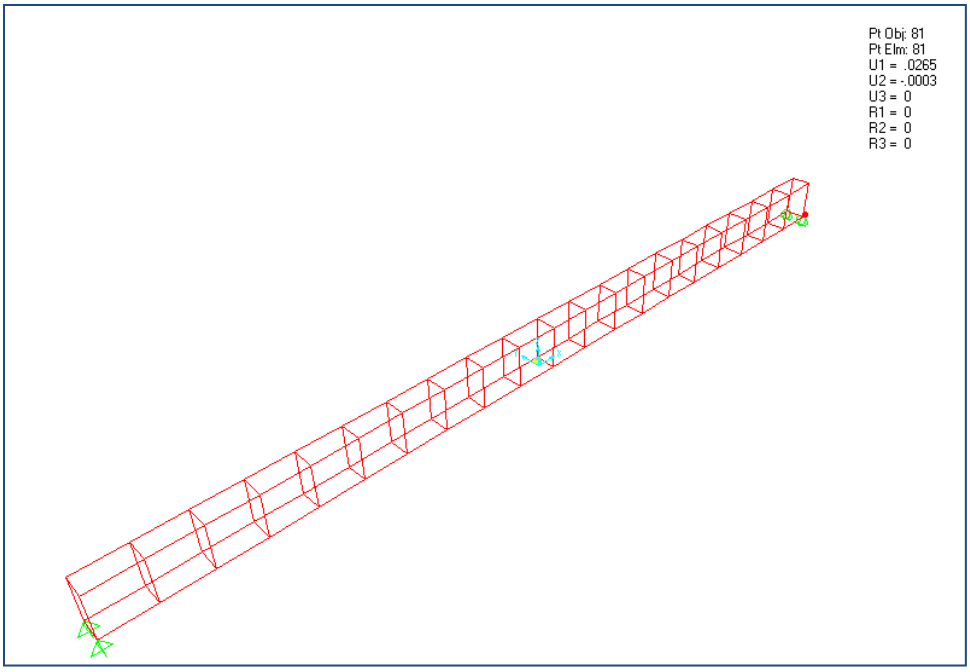

Figure 65: Sample output from SAP2000® for temperature special study

5.5 - Use of Rollins Road Bridge Load Test Data

The Rollins Road Bridge provides an invaluable field lab and research facility to collect structural response data. The original 2000 testing and instrumentation programs for the RRB did not include long-term SHM. For this reason, there was difficulty using the previous load test data since initial strain values were not known. Since initial strain values were unknown, it was hard to determine the change in behavior from an "initial" condition to the 2008 condition. The definition of initial is also an arbitrary choice. There really is no time in the bridge's life that can be used as an initial state because it is not created in a vacuum. If strain readings were collected prior to the bridge commissioning, these initial readings could serve as a baseline, provided that all environmental factors were also recorded. Since the 2008 load test was created for the purpose of structural health monitoring, researchers included three zero-load points which allowed the temperature data and all other environmental effects to be removed from the load

test data, which made the comparison between load test data and model analysis results data possible.

5.6 – Three-Year Analysis of Rollins Road Bridge Load Test Data

Analysis was attempted using all three years of data to capture the global response. However, the results showed that environmental factors, such as temperature and humidity, had a large effect and the lack of initial readings for the strain gauges made a proper comparison of the data to the analytical model difficult. The results from this attempt can be seen in Appendix g – First Analysis of Rollins Road Bridge Load Test Data for All Three Years. Researchers determined that using all three years of data was not practical due to lack of critical information. However, the correction of the 2008 load test data would provide that critical information.

5.7 – 2008 Analysis of Rollins Road Bridge Load Test Data

The analysis of the condition of Rollins Road Bridge through model updating was performed using the corrected 2008 load test data and the SAP2000® model to perform condition assessment on the steel reinforced elastomeric bearing pads. Correcting the data allowed researchers to see structural response caused solely by applied truck load and removed ambiguity caused by environmental factors, as seen in Figure 66. The 2008 load test data was corrected for temperature effects, as seen in Section 5.4 - Special Topic Studies. With this correction, a change in strain due to applied load became the focus. In order to properly compare this with the analytical model, a procedure had to be developed in order to look at the same thing in the model that was now being observed in the data.

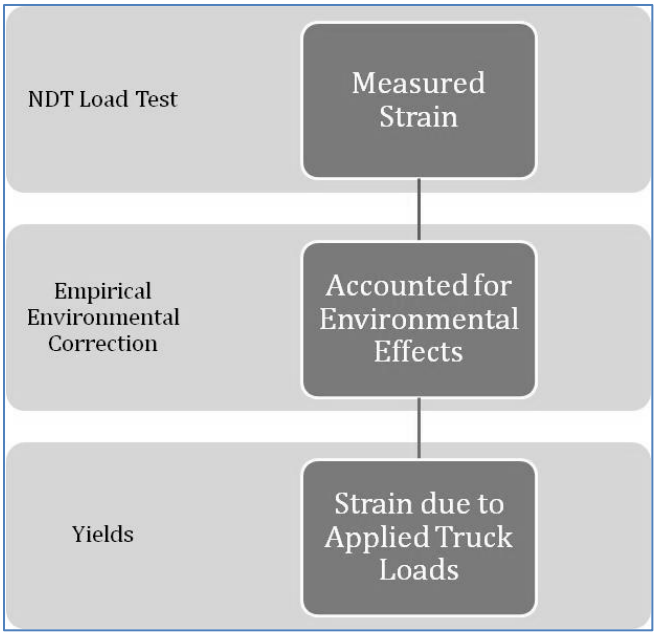

Figure 66: Measured strain to strain due to applied truck load diagram

5.7.1 – Establishing a Running Benchmark for SAP2000® 2008 Model

Since temperature and environmental effects were removed from the measured data set, the remaining measured strain values are only due to the applied truck load. In order to have the SAP2000® model reflect this same condition, two models were created. The reason for creating these two models is that the prestressing forces in SAP2000® are modeled as a force that needs to be an active load case in the analysis, not as a behavior. The CFRP is modeled as a component or structural element. The prestressing strands must be included in the analysis as a load case in order to capture the behavior of the prestressing forces. Due to this, prestress and dead load cases were active for one model, while prestressing force, dead, and applied truck load cases were active for the other model. Figure 67 shows how the two structural models were created and the difference between those resulted in strain due to applied truck load, matching the output from the measured data.

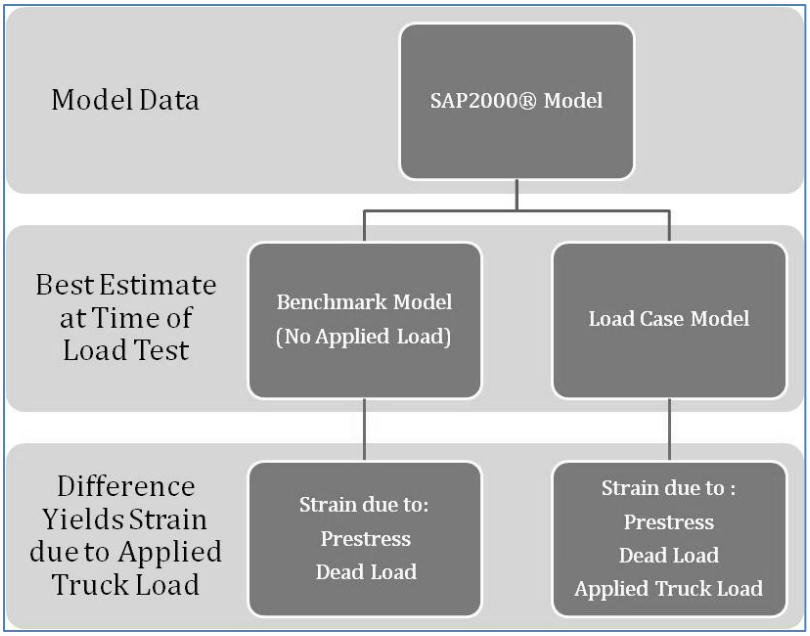

Figure 67: SAP2000® modeled strain data to strain due to applied truck load

This benchmark model included all structural components modeled as the best estimate at current bridge conditions. Calculations of bearing pad stiffness were maintained, and since the bridge is in such good structural condition, researchers have a high degree of confidence in modeled structural parameters such as area, modulus of elasticity, and moment of inertia. The strain values from the model are determined through techniques described in Section 5.4 - Special Topic Studies.

Since the condition assessment was performed on the elastomeric bearing pads, the stiffness values were modified in the model to match the measured behavior. Since researchers wanted to examine the change in behavior from a zero-load state to an applied load state, the modeled response had to be compared to a zero-load state, benchmark model with the same bearing pad stiffness as the applied load model. For each set of bearing pad stiffness case, a benchmark model was created and benchmark strain values were obtained.

5.7.2 – Established Model Loads

The applied truck load cases are simple to establish in the model. The wheel weights are known, as they were weighed at the RRB test site, and the location of the truck is dependent on the load case being analyzed. Using the truck mesh, the loads are applied to the nodes of the model. Using the measured wheel weights and truck load mesh, node loads are calculated and applied to the SAP2000® model in four different load cases, depending on the location of the truck.

5.7.3 – Established Measured Response Values

Once the measured data was corrected for temperature, as mentioned in Section 4.3.3 – Empirical Environmental Correction, a small bit of analysis had to be performed to get the strain readings into compared strain data. The times at which the load case occurred were noted and pulled from the corrected data set. This resulted in about 25 data points per sensor for the time the truck was at that position. A 95% confidence interval was then performed on the mean of those numbers, to determine if the data was within acceptable limits. The strain gauge tolerance was set to ±0.40-microstrain (Bowman M. M., 2002). All variations in the data were within a 0.25-microstrain range during the one to five minute period of recording, which was determined to be acceptable by researchers. Table 12 shows the resulting measured strain values for the load test data with environmental factors removed.

Table 12: 2008 measured strain values corrected for environmental effects

	Channel 32 Girder 3 Top	*Channel 3 Girder 4 Top*	*Channel 5 Girder 5 Middle*	*Channel 6 Girder 5 Top*
2008 LC1	-5.21	-4.67	2.85	-5.59
2008 LC2	-4.88	-3.21	2.82	-3.44
2008 LC3	-4.58	-2.59	-1.11	-1.46
2008 LC4	-2.39	1.85	-0.99	2.81

5.8 – Load Test Data to SAP2000® Comparison

With corrected data from the field measurements, data from the SAP2000® model, and a running benchmark SAP2000® model, the change in strain reading between the SAP2000® model and the running benchmark was calculated. This change is compared with the empirically corrected strain value in the manual model updating process seen in Chapter VI: Manual Model Updating. This data will also be used for full scale parameter estimation and model updating exercise, once MUSTANG is fully developed by fellow graduate student researcher, John Welch at UNH.

CHAPTER VI

MANUAL MODEL UPDATING

There are open source parameter estimation programs, such as PARameter Identification System Software (PARIS©) from Tufts University and Damage Identification and MOdal aNalysis for Dummies (DIAMOND) from Los Alamos Labs (Sanayei, 1997) (Los Alamos National Laboratories, 1997). This research specifically looked at PARIS©. MUSTANG (Model Updating STructural ANalysis proGram) is currently under development at UNH and will be able to handle the shell and solid elements, along with being tied to SAP2000®. The objective for the RRB required shell elements for accurately modeling the bridge span. The exported stiffness matrix from SAP2000® for the RRB model was a 7704 square matrix, resulting in 59 million values. With a matrix this size, it is not possible to do successful parameter estimation without an automated program. Another graduate student research assistant will use the model and data with MUSTANG. For the focus of this research project, manual parameter estimation will be performed to show how the process works on a local level, which will then be taken to the global level when MUSTANG is fully operational.

6.1 – Three Data/Model Comparisons

There were a total of three comparisons done using the data obtained from the RRB. The first analysis, which did not provide the desired results, can be seen in Appendix g – First Analysis of Rollins Road Bridge Load Test Data for All Three Years. The second and third

analysis were done on the 2008 load test data that had been corrected for environmental factors, as described in Section 4.3 - Environmental Effects on Bridge Response. The second analysis looks at the effects of modifying the horizontal stiffness of the bearing pads to obtain a correlation with measured structural response. In the second analysis the vertical and rotational stiffness values of the elastomeric pads were also modified to see the effect on the model response. Once the data SAP2000® model matched the measured response, the third analysis shows the importance of included specific structural properties in the RRB SAP2000® model. This is achieved by removing those structural parameters that were included to show what the response would be if they were not included in the analysis. The MUSTANG Research Project will examine the values of structural parameters such as area, moment of inertia, and modulus of elasticity using the data obtained from this research project.

For the second analysis of the 2008 model all structural components including CFRP, prestressing, and bridge rail, were kept in the model. Manual parameter estimation is performed on the RRB model, specifically on the bearing pads, by modifying the stiffness in three directions; vertical stiffness (z-direction, compression), horizontal stiffness (x-direction, shear), and rotation about the abutment (ry-direction, rotation). All bearing pad stiffness values were kept consistent for all 10 bearing pads in the model, which can be referred to as grouping (Sanayei, Imbaro, McClain, & Brown, 1997). The axial and rotation stiffness values that were calculated in Section 5.3.3 – Modeling the Steel Reinforced Elastomeric Bearing Pad, were kept constant for the final case when the horizontal stiffness values were changed to correlate the change in model response and change in measured data. Separately modifying stiffness values will be a focus of the runs in MUSTANG as part of future work. Parameters such as modulus of elasticity and moment of inertia for specific elements will also be included in the parameter

estimation. However, for the scope of this research project those properties were not examined in the manual parameter estimation.

6.1.1 – Analysis of Modifying Bearing Pad Stiffness

Table 13 shows the five different support conditions (SC) used in second manual model updating analysis. The vertical stiffness values are modified in the first four cases, and the fifth case shows that modification of the horizontal stiffness value must be done in order to get the change in model strain to correlate with the measured change in strain. The error of ±0.40-microstrain shown in the error bars for the measured strain corresponds to the accuracy of the gauges as set when installed. The manual model updating results can be seen in Figure 68, Figure 69, Figure 70, and Figure 71.

Table 13: Manual model updating cases and corresponding bearing pad stiffness values for second analysis

	Vertical Stiffness *(kips/in)*	**Rotational Stiffness** *(kips/rad)*	**Horizontal Stiffness** *(kips/in)*
Support Condition 1	46833	224651.5	fixed
Support Condition 2	46833	free	fixed
Support Condition 3	fixed	free	fixed
Support Condition 4	46833	fixed	fixed
Support Condition 5	46833	224651.5	10000

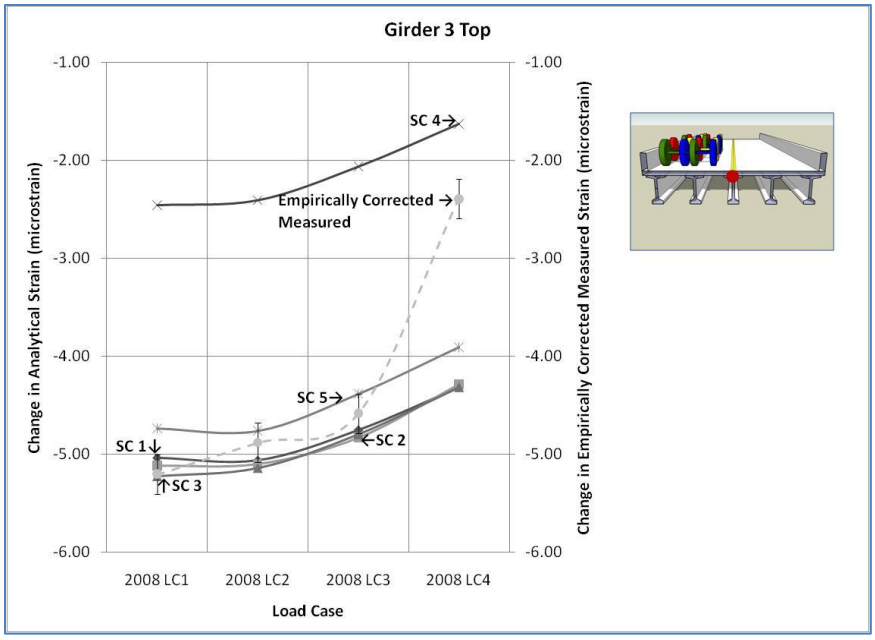

Figure 68: Manual model updating using girder 3 top strain sensor

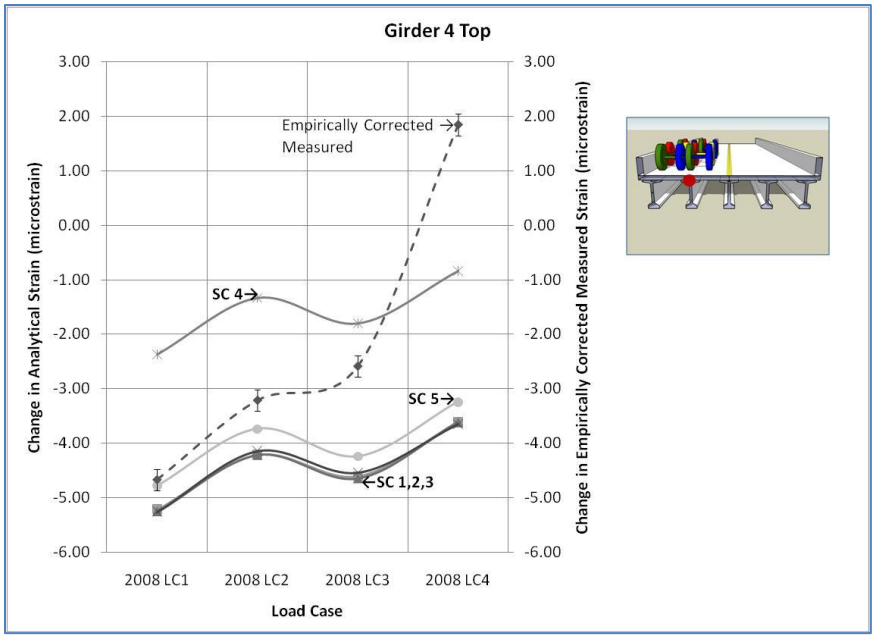

Figure 69: Manual model updating using girder 4 top strain sensor

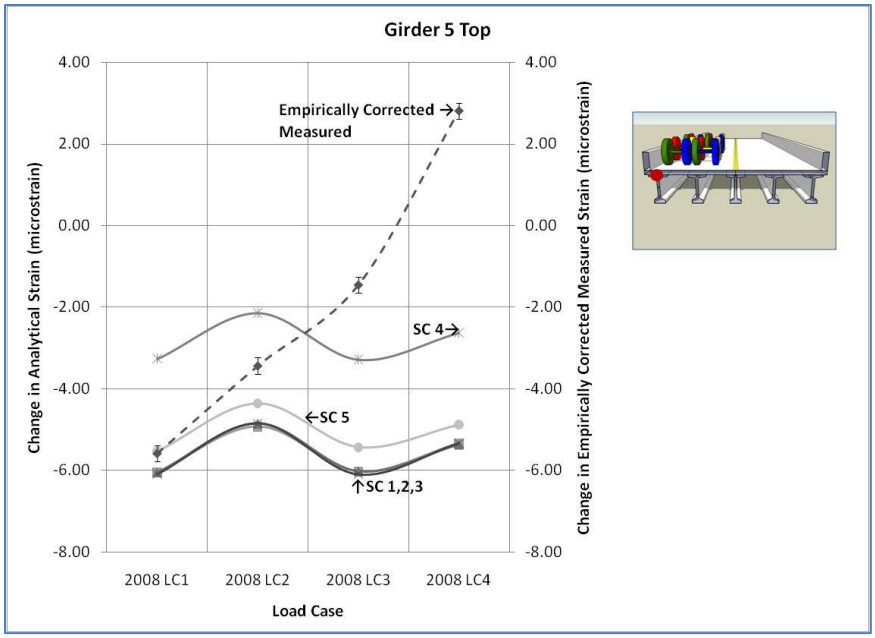

Figure 70: Manual model updating using girder 5 top strain sensor

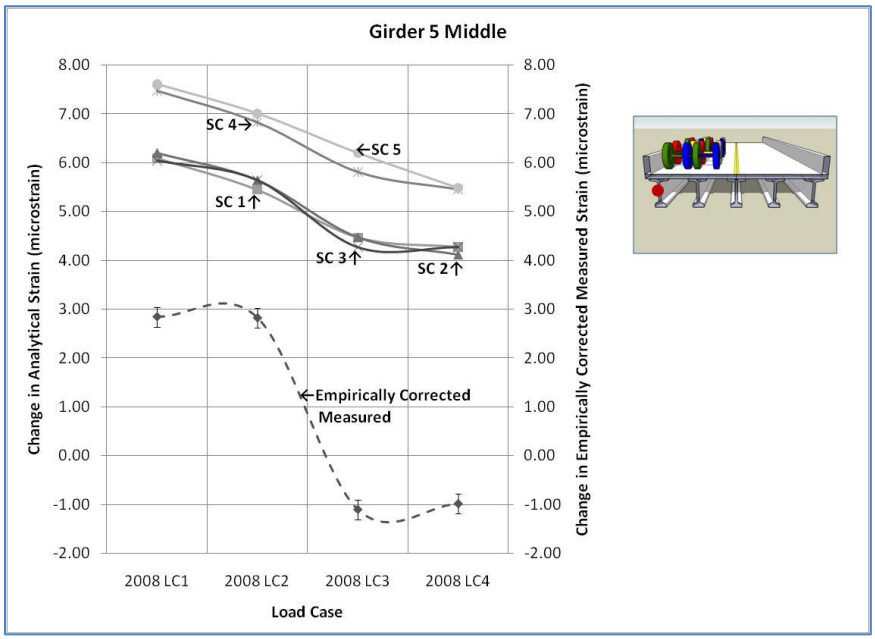

Figure 71: Manual model updating using girder 5 middle strain sensor

Figure 68 through 71 show the impact of varying the bearing pad stiffness values on the modal updating protocol. The predicted model responses correlate with the measured responses fairly well for support condition five (SC-5) when the horizontal bearing pad stiffness value is modified from the fixed condition. Further analysis using a parameter estimation and model

updating program will be able to get a more precise value by varying each component independently as part of an algorithm to obtain the optimal conditions. There is a shift in Girder 5 middle which could suggest a change in the location of the neutral axis. For Girder 3, Girder 4, and Girder 5 top, the change in the model trends follow the change in measured strain trends.

Examining strain is viewed to be a more accurate method for manual parameter estimation when compared to deflection measurements, since there is a larger opportunity for human error and the reference dependent nature of deflection measurements. Considering the value of deflection, the deflection measurements collected during the 2008 load test were also used as a way to validate the strain response seen in Figures 68-71. Figure 72, Figure 73, and Figure 74 show the modeled deflection compared with the measured deflection. The deflections typically fall within the error bars for the measured response which gives researchers more confidence in the results obtained from the strain comparisons for manual model updating. The outliers could be associated with the variability in the survey measurements due to non-optimal conditions as previously discussed.

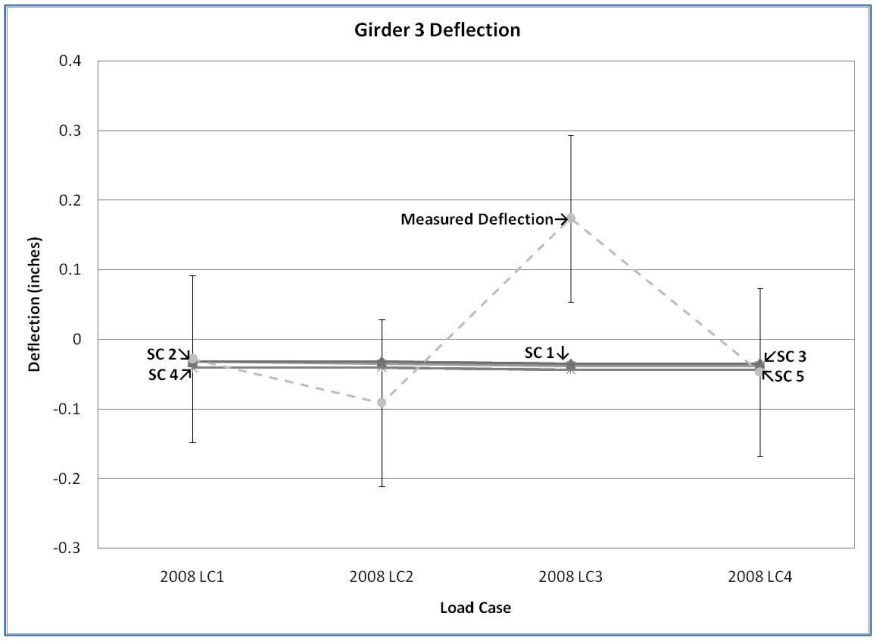

Figure 72: Manual model updating verification using girder 3 deflection measurements

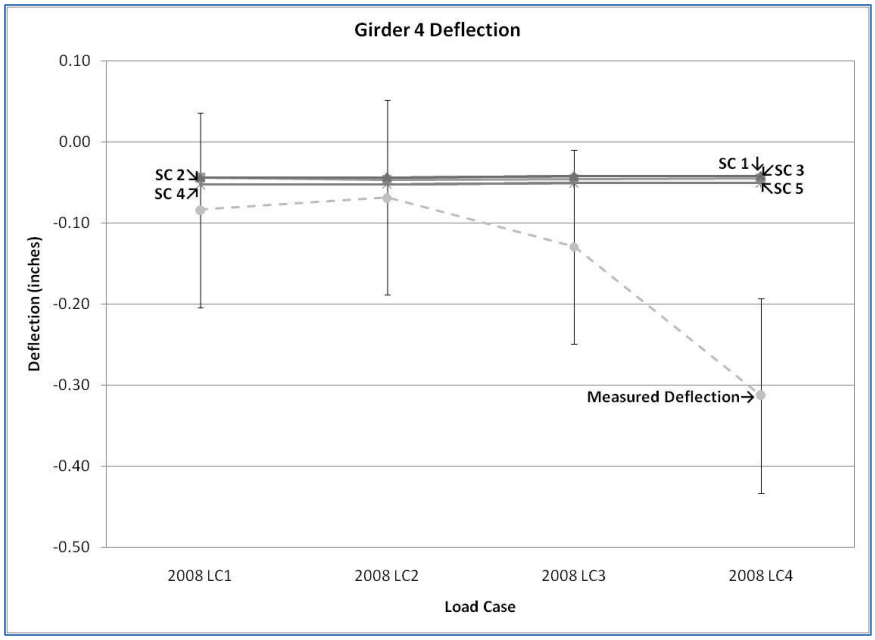

Figure 73: Manual model updating verification using girder 4 deflection measurements

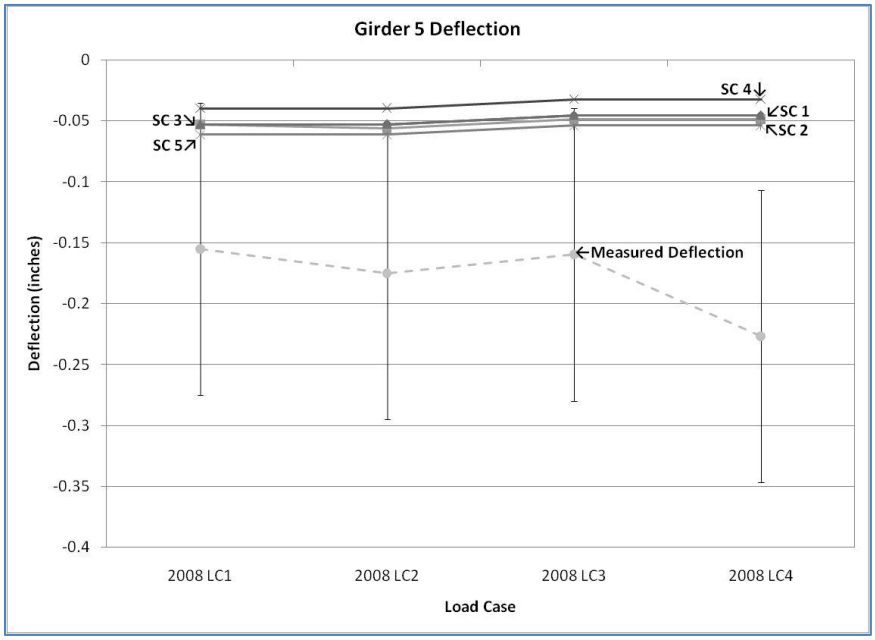

Figure 74: Manual model updating verification using girder 5 deflection measurements

6.1.2 – Analysis of Removing Specific Structural Elements

The bearing pad stiffness obtained from the above analysis, support configuration 5, was included the benchmark model and will be kept constant for the next phase of predicted model responses. Table 14 shows the four cases that will be used to show the effect of specific

parameters in the model. Structural parameters such as CFRP, prestressing, and bridge rail will be removed from the SAP2000® model, and the response will be seen in Figure 75, Figure 76, Figure 77 and Figure 78.

Table 14: Manual model updating cases and corresponding bearing pad stiffness values for third analysis

	Vertical Stiffness *(kips/in)*	**Rotational Stiffness** *(kips/rad)*	**Horizontal Stiffness** *(kips/in)*
Benchmark	46833	224651.5	10000
No CFRP	46833	224651.5	10000
No Prestress	46833	224651.5	10000
No Bridge Rail	46833	224651.5	10000

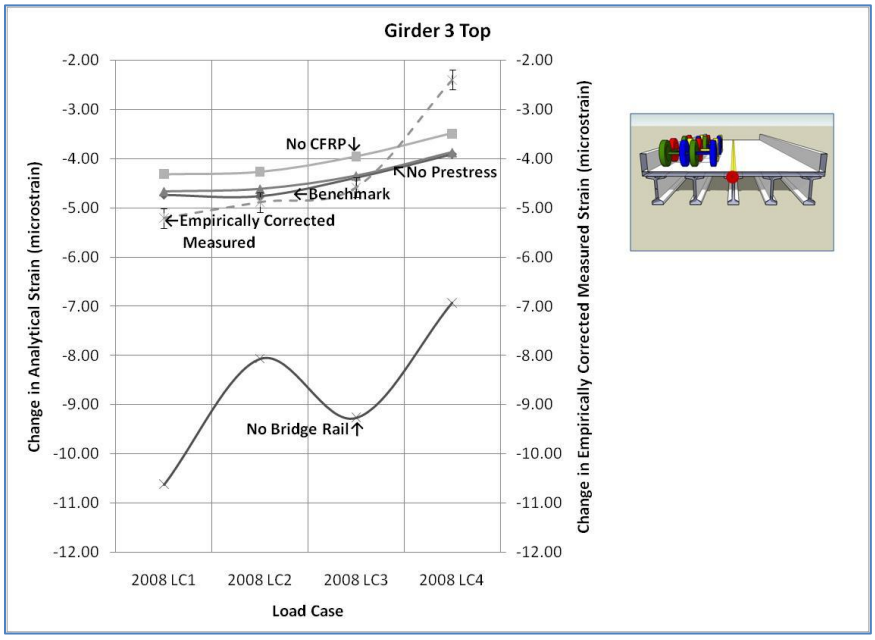

Figure 75: Manual model updating using girder 3 top strain sensor

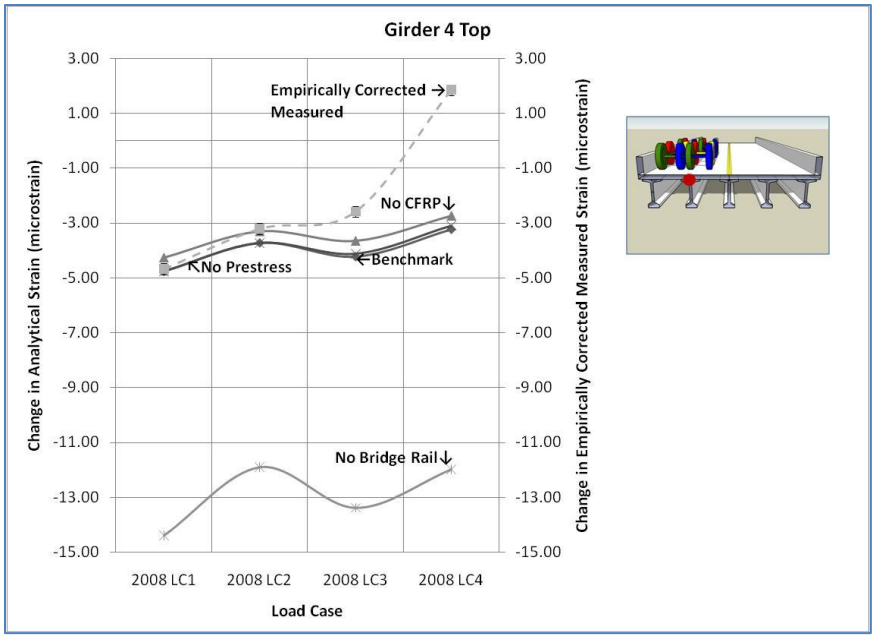

Figure 76: Manual model updating using girder 4 top strain sensor

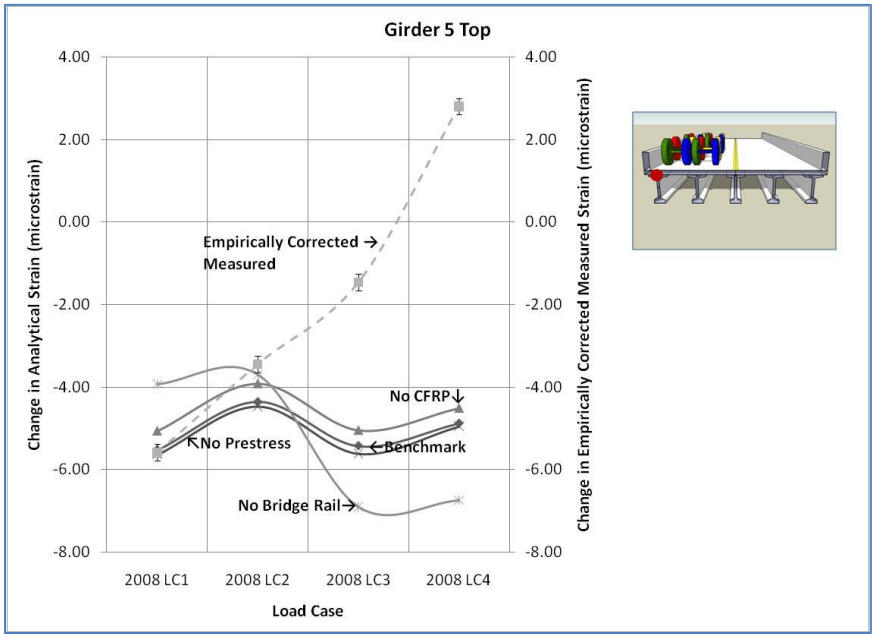

Figure 77: Manual model updating using girder 5 top strain sensor

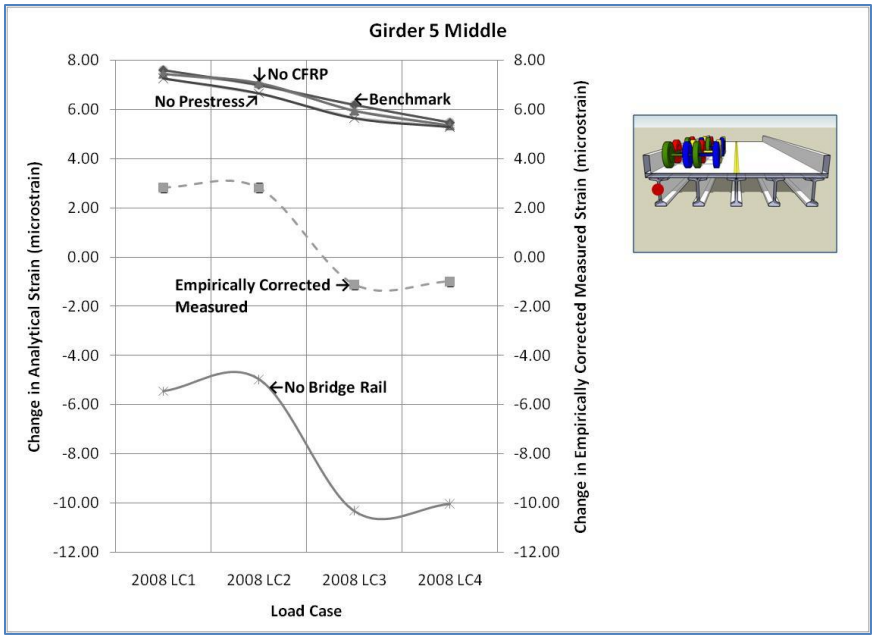

Figure 78: Manual model updating using girder 5 middle strain sensor

Figures 75 through 78 show that not including the bridge rail in the structural model significantly impacts the predicted response of the bridge model. Removing the prestressing tendons and/or CFRP has a smaller effect in change of strain but it must also be remembered that this is a change in strain, so the benchmark model for the base also has no CFRP or prestressed tendons, which explains why the values appear to be similar.

As with the second analysis case, deflection measurements were also shown for a second comparison and validation. Figure 79, Figure 80 and Figure 81 show the deflection comparison done for the third analysis case.

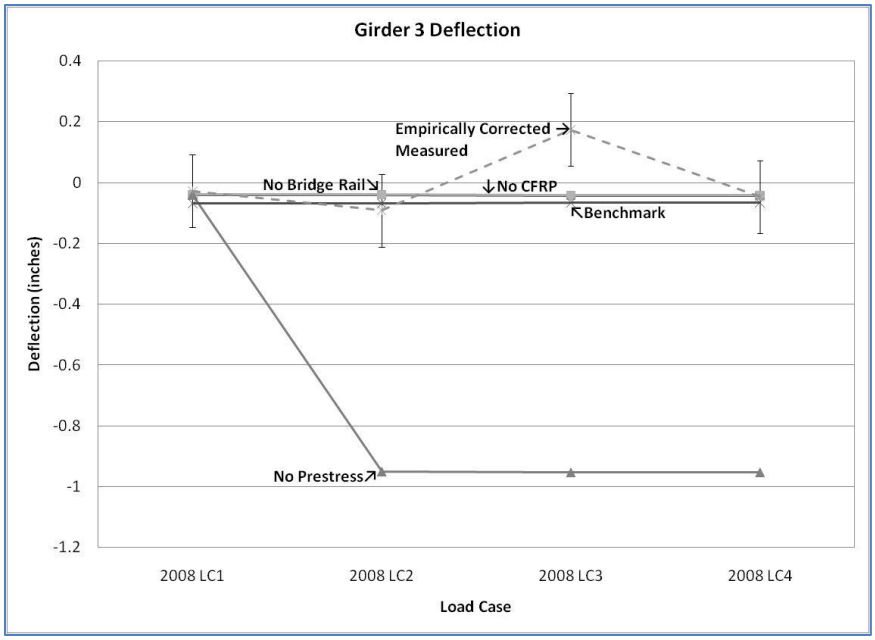

Figure 79: Manual model updating comparison using girder 3 deflection measurements

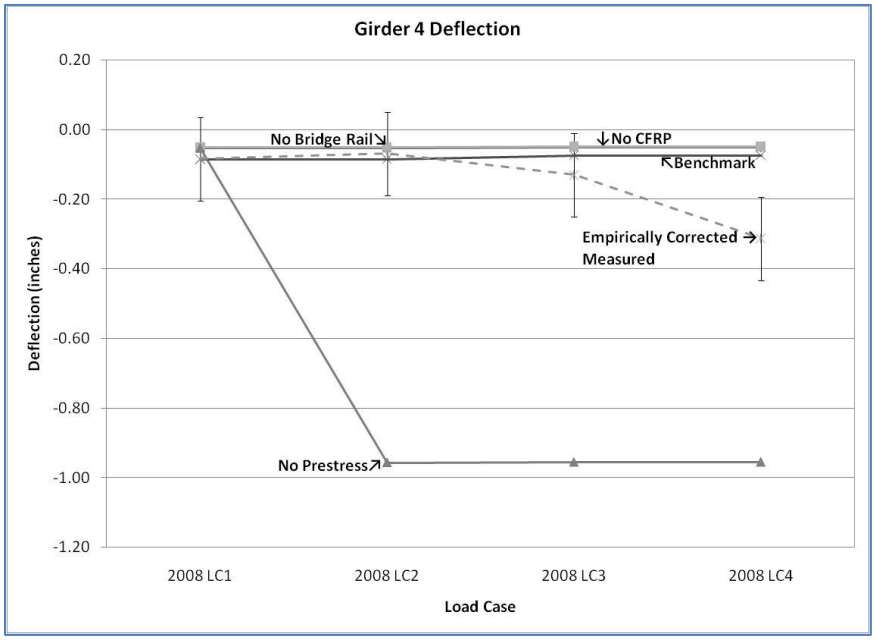

Figure 80: Manual model updating comparison using girder 4 deflection measurements

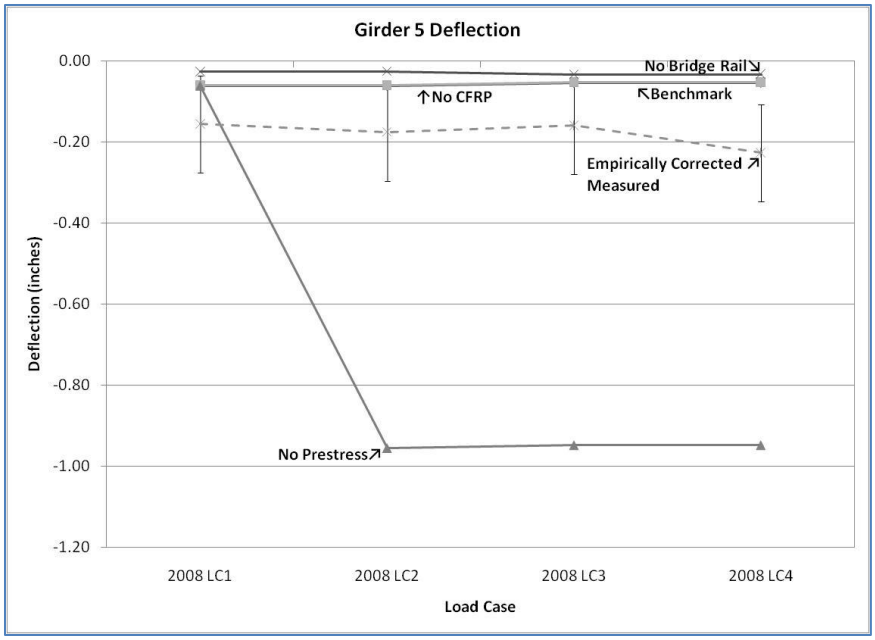

Figure 81: Manual model updating comparison using girder 5 deflection measurements

In the deflection comparison, it can be seen that not having the prestress produced the biggest change when compared to measured response. Removing CFRP and the bridge rail had less of an effect; however it should still be noted.

6.2 – Discussion of Manual Parameter Estimation Results

To reiterate, the only gauges used in the SHM program for RRB were the gauges embedded in the HPC girders. These gauges are oriented in the longitudinal direction and capture the global structural response of the bridge given the loadings. Using only the girder gauges also limits the computations to a reasonable limit for the scope of the Rollins Road Bridge Research Project. The 2000 and 2001 load test were not geared towards SHM and proved to be not as useful as the 2008 load test, which was specifically designed for SHM purposes. Including three zero-load points allowed researchers to remove strain due to change in environmental factors and perform manual model updating on the structural model to match the measured response.

6.3 – Conclusions on Manual Parameter Estimating Results

The results from the manual parameter estimation show that the change in measured structural response could match the change in modeled response by modifying the horizontal stiffness of the elastomeric bearing pad. The final bearing pad stiffness ended up being 46,833-kip/in in the axial direction (k_a), 10,000-kip/in in the horizontal direction (k_h), and 224,651-kips/rad for rotation (k_r). Figure 82 and Figure 83 show a quantification of the bearing pad stiffness values used as compared to a roller, pinned, and fixed connection. This is only to show the effects of the spring on an example 40-foot beam with a 10-kip point load, not the actual bridge configuration. The axial and horizontal stiffness remained as calculated since there was nothing to suggest otherwise, and the horizontal direction was modified to get the structural response to match. According to Stanton et al. (2008), there are no standard calculations for the horizontal stiffness value.

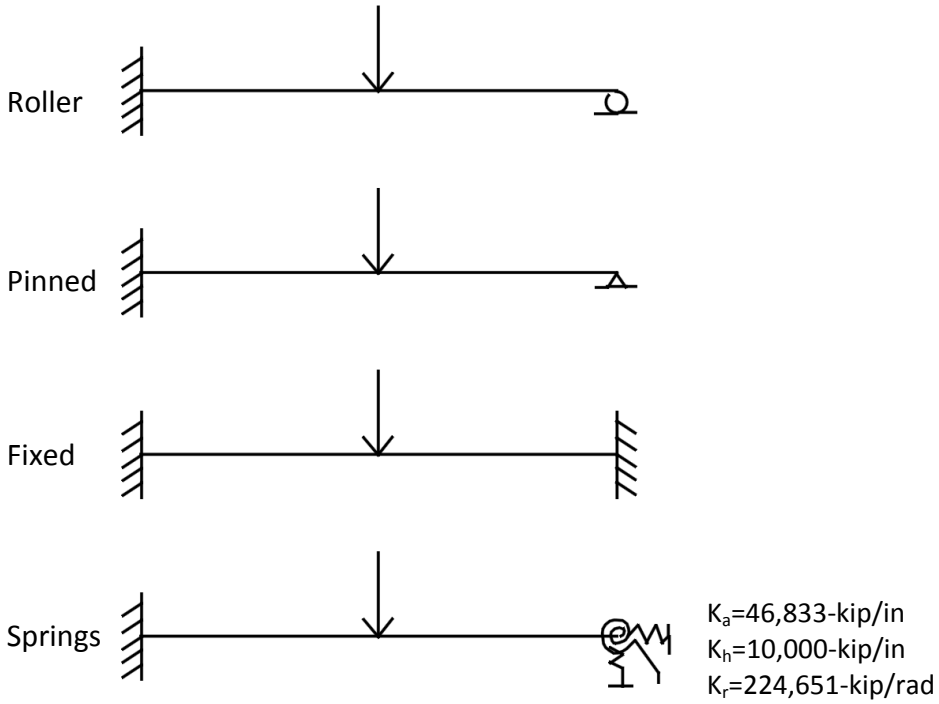

Figure 82: Quantification of bearing pad stiffness examples

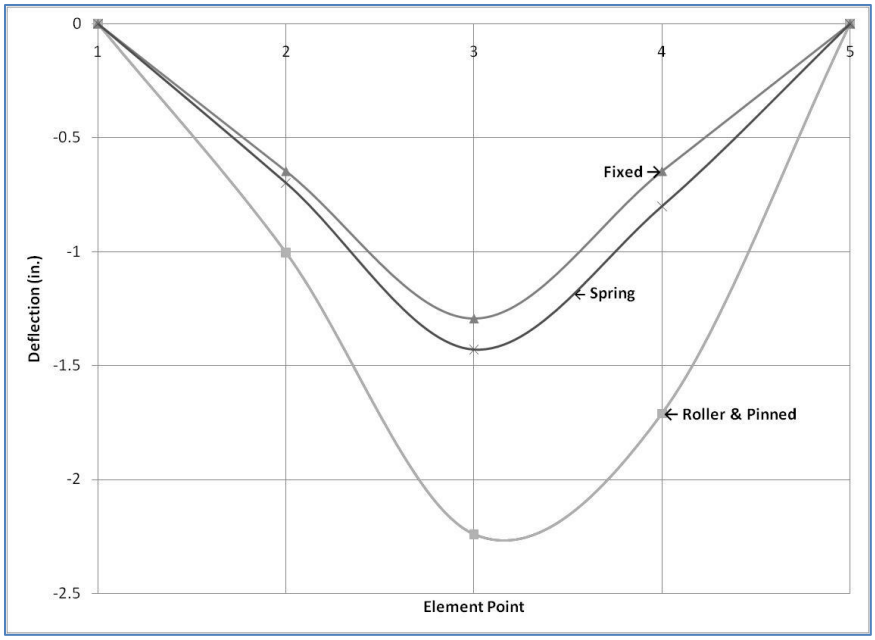

Figure 83: Quantification of bearing pad stiffness results

When this model is run through MUSTANG, structural parameters such as moment of inertia, modulus of elasticity, and individual bearing pad stiffness properties can be modified to see the effect on the modeled response. Including the abutment and ground conditions into the model and then running parameter estimation could also give insight into the structural response exhibited by the bridge in the field. A good way to see if the abutments are affecting the structural response would be to take survey measurements during the load test and throughout the year to see how the abutments are moving. This could then be correlated to changes in structural response of the bridge.

6.4 – Variations in Data

Several observations may be noted in the results for both strain and deflection comparison. In the strain comparisons for Girder 3 top, Girder 4 top, and Girder 5 top, there seems to be a large variation between the third and fourth load case. This variation could be due to the fact that the linear environmental correction was based on three data points that were not

evenly distributed throughout the load test program. This is because it was a linear correction based on only three data points, two recorded towards the beginning of the load test and only one recorded towards the end.

In the strain comparisons for the second analysis, the structural response for support conditions one through three are grouped very close together in most cases. This can be due to the fact that if the stiffness conditions are examined closely, the ones that would have the greatest effect on the bridge response are either not changed at all or only changed by a small amount while keeping the horizontal stiffness fixed.

The deflection comparison shows the variation inherent with the type of survey measurements and survey conditions that were present during the load test, i.e. having the measuring rod in a lift bucket. It would be optimal to collect more measurements and be able to perform statistical operations to eliminate outliers and assess the statistical relevance of the collected data.

In the third analysis the strains from the benchmark, no CFRP and no prestressed tendons, are also grouped in the same range. This is because the numbers in the graph are changing in response, with respect to a benchmark that has the same conditions as the truck load model. The biggest change with not including the bridge rail, in both the truck load model and the benchmark model for that situation, can be attributed to a change in the load and configuration of the bridge. The third analysis deflection readings follow a similar group with the benchmark, no CFRP, and no bridge rail being grouped together while the no prestressing tendons model shows significant deviation. This is obviously due to the effects of camber on the dead and applied load not being included in the deflection measurements.

6.5 - Optimal Conditions

As seen with the parameter estimation, and the not so successful initial parameter estimation run as seen in Appendix g – First Analysis of Rollins Road Bridge Load Test Data for All Three Years, it is important when doing a load test for SHM to design the load test with that in mind. Also, if a better initial value was known for the strain readings on the bridge it might have been possible to perform successful parameter estimation in the initial analysis. However, not knowing the initial values of strain, exact environmental factors, and not being able to properly model all of those environmental factors, made the initial analysis challenging. As seen in the second analysis, being able to remove environmental effects from the measured response data and not having to worry about the initial gauge value, proved to be useful in the model updating of the RRB SAP2000® model.

CHAPTER VII

STRUCTURAL HEALTH MONITORING, PARAMETER ESTIMATION, AND MODEL UPDATING

The Rollins Road Bridge Research Project has created a model that captures the behavior of the RRB. This model has undergone minor manual model updating to calibrate the model to the observed structural behavior. Some trends in the behavior of the model can be observed, however the values are still not exactly where they should be. This was to be expected since only minor model updating was done. MUSTANG will be used to do a full-scale parameter estimation using the model created and the post-processed data analyzed in this research project.

7.1 - Parameter Estimation

The parameter estimation that will be performed on the RRB SAP2000® model includes investigating boundary conditions as well as other structural parameters that affect the stiffness of the structure, such as moment of inertia, area, and modulus of elasticity. Parameter estimation uses measured data and a comparative, predictive model to give validity to both the model and the data. Once the parameters are updated and behaviors match, the difference between the design parameters and estimated parameters can be used to show the change in state of the structure.

When a structure is designed, several things are assumed to be known, such as modulus of elasticity (E), moment of inertia (I), boundary conditions, torsional rigidity (GJ) and area (A). In the design phase, if finite element models are used, the assumed EA, EI, GJ, and design loads are applied to that model. Finally displacements and rotations are calculated. Parameter estimation is, in some senses, the inverse to direct structural analysis. The existing structure is known, with initially assumed EA, EI, and GJ. Experimental loads are applied, through nondestructive test techniques, and the response of several degrees of freedom are measured. Through the use of a model, the response data, and parameter estimation software, the information is combined and actual EA, EI, and GJ of the structure are determined. Figure 84 shows a graphical representation of the process of parameter estimation.

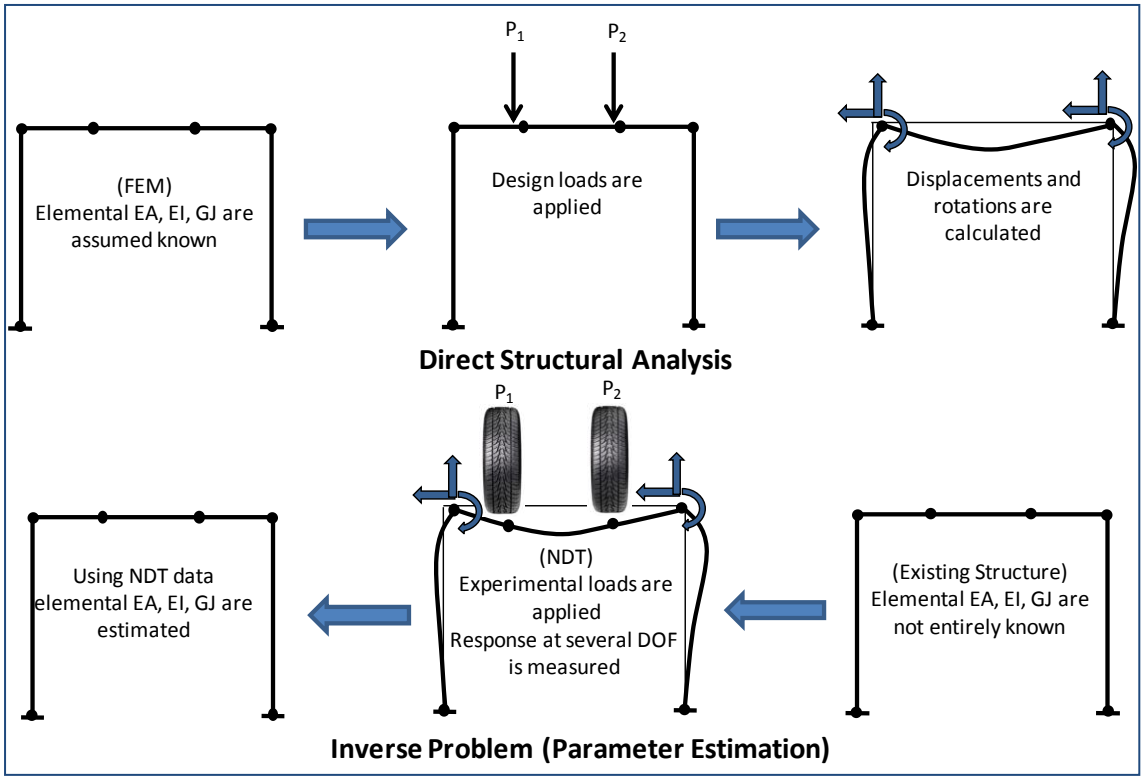

Figure 84: Graphical representation of parameter estimation (Sipple, 2008)

Once this parameter estimation has been performed on the RRB model, researchers and the NHDOT will have an up-to-date model of actual conditions at the RRB. This model could easily be used for special permitting.

During a special permitting operation that took place in Norco, Louisiana on the Bonnet Carré Spillway Bridge, Bridge Diagnostics, Inc. (BDI) used a calibrated model to match the measured structural response induced by a superload passing over the bridge. This model successfully predicted the response and the results showed that the approach of using a model was the same as the typical load rating procedure. An added benefit of using the model was being able to see the global structural response instead of analyzing beams with distribution factors (Grimson, Commander, & Ziehl, 2008).

7.2 - Current Ongoing Research at UNH – MUSTANG

During the permitted process of the Bonnet Carré Spillway Bridge, it took 3,276 strain comparisons from 28 strain gauges and 117 load cases, three truck paths with 39 stop positions to calibrate the model before it was used to match response caused by the superload (Grimson, Commander, & Ziehl, 2008). This entire process, instead of being done by hand or manual model updating, could be done using an automated program such as MUSTANG.

MUSTANG uses the modeling power and capabilities of SAP2000® to get all of the connectivity tables, joint locations, boundary conditions, element types, material properties and stiffness matrices used for parameter estimation. MUSTANG will take full advantage of the SAP2000® Advanced Programming Interface (API) to make linking MUSTANG with SAP2000® easier. The program and research into linking the two programs is being performed at the University of New Hampshire by John Welch.

7.3 - Structural Health Monitoring Program

An efficient SHM takes full advantage of the modeling done by designers through upgrading the design model to a monitoring model. Visual inspection information can be incorporated into the model as well as load test programs. This can allow structural response data from nondestructive testing to provide an invaluable resource for bridge owners. This data satisfies needs of bridge owners including determining serviceability and load capacity, investigating the reliability of the structure, and giving a record, through models, of the progression of the health of the bridge. This information may also be able to provide insight into how long the bridge will operate at current capacities.

Ensuring all new bridge construction projects have a SHM component in the design of the bridge, whether that included sensors embedded in girders or tilt meters installed after construction, will provide invaluable insight into the health of bridges well into the future. There is interest at the NHDOT to include a SHM layer in their current GIS system, allowing officials to know, at a glance, which bridges are instrumented and have the capabilities of performing SHM. This GIS layer could go even a step further when linking up to the data acquisition and processing systems to alert the NHDOT if there is an abnormal structural response at one of their bridges. This will allow for a more efficient allocation of time and money, which is already spread fairly thin for DOTs throughout the country.

Retrofitting existing bridges, or even just troubled bridges, may be able to offer the same benefits as installing instrumentation during new construction, if not more. Instrumentation of aging bridges could allow bridge owners to see which bridge is most in need of structural repairs. With existing bridges, instrumentation incorporated into a GIS layer may also serve to provide an early warning for changes that could affect public safety.

The RRB was instrumented for the IBRC program to look at prestress losses and performance of the CFRP reinforcement in the deck. This research project successfully took that instrumentation plan and used it to find the global structural response for SHM. This same process can easily be repeated on other instrumented bridges in the state of New Hampshire and throughout the Northeast to examine structural behavior and can eventually be included on a GIS layer linking the data acquisition and processing systems.

CHAPTER VIII

CONCLUSIONS, FUTURE WORK, AND RECOMMENDATIONS

8.1 – Key Observations

During the course of this research project there were several key observations made. Some of those observations include the large effect that temperature has on the relatively short span Rollins Road Bridge. The technical papers and presentations related to this project as listed in APPENDIX H – Papers/presentations Related to this Research. Change in environmental conditions and the resulting change in bridge response must either be included in the modeled aspect or accounted for in the measured structural response data. The stiffness of the bearing pads was updated solely for the reason of experimentally determining the horizontal stiffness of the elastomeric reinforced bearing pad, the one stiffness value not given through experimentally verified equations. The linear correction can be seen when closely examining the measured response; however this does not capture all of the data, specifically towards the end of each run. Using more zero-load points and a parabolic correction could more accurately correct the data for environmental effect, which increased the accuracy of the structural response due solely to the applied truck load. The effects of including the bridge rail can be seen when that element is removed during the third analysis. Another option to deal with the bridge rail would be to break

up the element that models the bridge so it is not modeled as a continuous bridge rail, which would more accurately reflect how it is cast on the bridge.

8.2 – Conclusions

The RRB load test data shows that the structural performance of the CFRP grid, concrete deck, and concrete girders matches the excellent rating from visual inspections. The strain values are either bounded by, or shown to be less than, the two prior tests performed in December 2000 and August 2001. It is difficult to do an exact data-to-data comparison since testing conditions, including truck weight and location and environmental factors, varied from all three load tests. The difference between 2000/2001 and 2008 load tests included stopping locations and gross weight of the truck. The reason for the differences in stop locations was because the goal of the 2008 load test was to observe global response while the 2000/2001 load tests examined local response in the CFRP and deck. The performance of the CFRP was an important aspect of the 2008 RRB project, however not the ultimate goal.

A monitoring model, with added specific structural components, was created to capture the behavior of the bridge. The effects of removing those components can be seen in the third analysis of the data. This model and the data from the load test is currently in a phase where it can be used by fellow researcher, John Welch, for automated parameter estimation via the parameter estimation program being developed at UNH called MUSTANG (Model Updating StrucTural ANalysis proGram).

As noted in the current bridge inspection report, there are no visible signs of deterioration or cracking, which caused the main focus of the parameter estimation to be the horizontal stiffness of the elastomeric bearing pads. Visual inspections will continue to be performed at the RRB, and once there is noted deterioration, the model will be easily updated to model that

change in behavior. The modeling of structural deterioration will also allow that deterioration to be quantified as a reduction in area, moment of inertia, or modulus of elasticity instead of a note on an inspection report.

Environmental effects, including temperature changes, had a much larger effect on load test data than originally expected. The change in temperature over the three hour load tests overshadowed the effect of the 19-ton truck. Environmental effects can be easily removed if zero-load data points are collected at several different times in the load test program. Removing environmental effects through empirical methods allowed a normalization of the data without relying on theoretical calculations. All information used to remove temperature using the empirical method was determined by the bridge and current structural conditions at the exact time of the load test. The two previous load tests did not include zero-load data points, which is why the manual parameter estimation was not performed on those sets of data. Subsequent tests should include enough of those points to be able to properly correct for environmental effects potentially using a parabolic or quadratic fit functions.

The empirical temperature correction proved to be beneficial. Performing the empirical temperature correction allowed for manual model updating to be successfully performed on the 2008 RRB SAP2000® model. The SAP2000® data converged with the measured structural response after only a few iterations, and will be more precisely determined using MUSTANG. This manual model updating has shown that by changing structural properties of a monitoring based model, that analytical model can be matched to measured structural response.

8.3 – Future Work

The performance of the CFRP, bridge deck, and NEBT girders will continue to be monitored by collecting long-term SHM data and the occasional load test. These load tests will

be performed with all the knowledge gained from this load test and will add a significant amount of new knowledge to the testing program for the RRB and SHM programs for the bridges of the state of New Hampshire. Parameter estimation and model updating will be performed on the RRB SAP2000® model in the summer of 2010 in MUSTANG. This model will be maintained at UNH so that information collected in future visual inspections and load test can be integrated into the model. This analysis will ensure that the behavior experienced by the bridge is captured in the model. Also, the post processing structural model output will be refined, possibly using the SAP2000® API and the strain transformation matrix, [B], to obtain strain values without having to perform radius of curvature calculations.

This project has also raised questions on the modeling techniques and how results are obtained from the model. The abutment was not modeled in this project because it was decided that modeling would only be done to the bearing pads. It would be beneficial to see the results of manual or automated parameter estimation if the abutments and ground conditions were modeled. The structural model, including the abutments, could then be compared to the structural model for this research project to determine the cost benefit of modeling the abutments.

A goal for future SHM projects is to eliminate looking for the change in response due to truck loading to correlate the collected response with the predicted response. By evaluating the collected response, the long-term performance of the bridge can be assessed. This will require significant research related to each structural element included in the model in addition to information relating to the initial value and shift in the collected data. Environmental effects will also have to be measured. There is also the possibility of using weigh-in-motion sensors or

closed-circuit video monitoring at the bridge to use everyday traffic as a load and then measure the structural response from traffic loading.

There are now three different sets of load test data. Continuous temperature and strain data collected specifically for the CFRP and bridge deck can be closely analyzed to determine an assess changes in the behavior of the CFRP and bridge deck. The data collection will continue as most of the problems associated with data collection have been resolved during this research project.

8.4 – Recommendations

Lessons learned in this project can be applied to an upcoming research partnership including UNH, NHDOT, Tufts University, Fay, Spofford, and Thorndike, Inc. (FST), and Geocomp Corporation. This project involves the development and deployment of an instrumentation plan, monitoring model, and testing plan for a new bridge with FST and NHDOT. This project is sponsored by the Project for Innovation (PFI) through the National Science Foundation (NSF). The original target bridge was the Black Brook Bridge crossing over I-293 in Manchester, New Hampshire. Due to scheduling conflicts, the Vernon Avenue Bridge in Barre, Massachusetts was selected at the target bridge for this project. The structural behavior of the bridge was more accurately captured since the instrumentation plan will designed around SHM. The instrumentation plan for the Vernon Ave Bridge includes 100 strain gauges, 16 tiltmeters, 24 accelerometers and 48 temperature sensors, both on the girders and in the concrete deck. The temperature sensors are installed throughout the cross section to be able to apply the temperature as a gradient throughout the bridge, rather than just a thermal load applied to the surface.

During the initial load test that was performed on September 3, 2009, prior to the bridge commissioning, zero-load or ambient points are collected were collected providing the opportunity to establish a baseline for the behavior of the bridge (Santini et al, 2010). The temperature and strain values recorded at commissioning create a snapshot of the first moments in the service life of the bridge. All following data will then be compared to this snapshot in order to assess current conditions at the bridge, whether that is two years or 30 years down the road. Pressure plates are installed in the approach slab of the bridge, which enabling ambient conditions to be recorded remotely allowing for the evaluation of the diurnal and seasonal changes in bridge structural response.

For future tests at RRB, more zero-load readings can be taken to create a better trend line for temperature removal. There were logistical issues with taking the deflection reading with the leveling rod, having a small lift bucket and having to make several different moves to get to each point. Having a larger bucket that can remain up under the bridge allowing the surveyor to walk down the length of the bucket to reach each survey point would make gathering deflection data easier. Also, recent advancement in digital image correlation has facilitated the use of digital photography to accurately capture bridge deflection in a non-contact protocol. Any future test of the RRB would include digital imaging.

The Rollins Road Research Project proved valuable for the amount of information obtained from doing one load test on an instrumented bridge. Most importantly, it showed that manual model updating can be performed on a monitoring based model to calibrate the analytical results to the measured response. Doing the data analysis for the load test and having a comparative model to make the data analysis accountable to the model and vice-versa gives an aspect of accountability through a predictive model. The original research plans adapted to the

needs of the project as components, such as element number, discretization, became less important and other components, such as thermal effects, modeling of specific structural characteristics became the focus of the research. Research projects involving SHM for bridges will take all the lessons learned from this project to further advance SHM programs.

WORKS CITED

AASHTO. (2008). *AASHTOWare Catalog July 1, 2008 - June 30, 2009.* American Association of State Highway and Transportation Officials.

AASHTO. (2008). *Bridging the Gap - Restoring and Rebuilding the Nation's Bridges.*

AASHTO. (2004). LRFD Bridge Design Specifications Third Edition. *14.5 Bridge Joints* , pp. 14-8.

Aktan, A. E., Farhey, D. N., Helmicki, A. J., Brown, D. L., Hunt, H. J., & Lee, K. L. (1997). Structural Identification for Condition Assessment: Experiment Arts. *Journal of Structural Engineering, ASCE , 123* (12), 1674-1684.

Bailey, J., & Murphy, K. (2008). The Effectiveness of Fiber Reinforced Polymers in Modern Day Bridge Building. *Eigth Annual Freshman Conference* (p. 5). Pittsburgh, PA: University of Pittsburgh.

Bardow, A. K., Seraderian, R. L., & Culmo, M. P. (1997). Design, Fabrication and Construction of the New England Bulb-Tee Girder. *PCI (Precast/Prestressed Concrete Institute) Journal* , 29-40.

Beal, D. (2008, September 9). Retrieved September 23, 2008, from Transportation Research Board of the National Academies: http://www.trb.org/TRBNet/ProjectDispaly.asp?ProjectID=2507

Bell, E. S., Sanayei, M., Javdekar, C. N., & Slavsky, E. (2007). Multiresponse Parameter Estimation for Finite-Element Model Updating Using Nondestructive Test Data. *Journal of Structural Engineering - ASCE* , 1067-1079.

Benmokrane, B., El-Salakawy, E., El-Ragaby, A., & Lackey, T. (2006). Designing and Testing of Concrete Bridge Decks Reinforced with Glass FRP Bars. *ASCE Journal of Bridge Engineering* , 217-229.

Bowman, M. M. (2002). *Load Testing of the Carbon FRP Grid Reinforced Concrete Bridge Deck on the Rollins Road Bridge, Rollinsford, New Hampshire.* Durham, NH: University of New Hampshire.

Bowman, M. M., Yost, J. R., Steffen, R. E., & Goodspeed, C. H. (2003). Diagnostic Testing and In-Service Performance Monitoring of a CFRP Reinforced HPC Bridge Deck. *Second New York City Bridge Conference - Recent Developments in Bridge Engineering* (pp. 361-371). New York, NY: Bridge Engineering Association.

Branco, F. A., & Mendes, P. A. (1993). Thermal Actions for Concrete Bridge Design. *Journal of Structural Engineering , 119* (8), 2313 -2331.

Brownjohn, J. M., Moyo, P., Omenzetter, P., & Chakraborty, S. (2005). Lessons from monitoring the performance of highway bridges. *Structural Control and Health Monitoring* , 12:227-244.

Choquet, P., Juneau, F., & Bessette, J. (2000). New generation of Fabry-Perot fiber optic sensors for monitoring of structures. *SPIE's 7th Annual International Symposium on Smart Structures and Materials.* Newport Beach, CA.

Computer Structures, Inc. (2007, October). CSI Analysis Reference Manual for SAP2000®, ETABS®, and SAFE™. Berkeley, California, USA.

El-Salakawy, E., Benmokrane, B., & Desgagne, G. (2003). Fibre-reinforced polymer composite bars for the concrete deck slab of Wooton Bridge. *Canadian Journal of Civil Engineering , 30*.

Farhey, D. N. (2005). Bridge Instrumentation and Monitoring for Structural Diagnostics. *Structural Health Monitoring* , 301-318.

Farhey, D. N. (2007). Quantitative Assessment and Forecast for Structurally Deficient Bridge Diagnostics. *Structural Health Monitoring* , 39-48.
FISO. (2008). *EFO Strain Sensor Product Data Sheet*. Retrieved August 18, 2008, from http://www.fiso.com/modules/AxialRealisation/img_repository/files/documents/2007/MC-00086%20R6_PDS_EFO.pdf
Fu, G., Feng, J., & Dekelbab, W. (2003). *NCHRP Report 495 - Effect of Truck Weight on Bridge Network Costs.* Washington, D.C.: Transportation Research Board.
Grimson, J. L., Commander, B. C., & Ziehl, P. H. (2008). Superload Evaluation of the Bonnet Carre Spillway Bridge. *Journal of Performance of Constructed Facilities - ASCE , 22* (4), 253-263.
GT Strudl. (2007). *Version 29* . Georgia Tech - CASE Center.
Guan, H., Karbhari, V. M., & Sikorsky, S. C. (2007, August). Long-term Structural Health Monitoring System for a FRP Composite Highway Bridge Structure. *Journal of Intelligent Material Systems and Structures, Vol. 18* , 809-823.
Haenni. (2008). Retrieved November 2008, from HAENNI Wheel Load Scales, a division of Baumer Borudon Haenni AG: http://www.haenni-scales.com/e/
Hearn, G. (2007). *NCHRP Synthesis 375 - Bridge Inspection Practices.* Washington, D.C.: Transportation Research Board.
Hibbler, R. C. (2005). 4.6 Thermal Stress. In *Mechanics of Materials - Sixth Edition* (pp. 154-158). Upper Saddle River, New Jersey: Prentice Hall.
Howell, D. A., & Shenton III, H. W. (2006). System for In-Service Strain Monitoring of Ordinary Bridges. *Journal of Bridge Engineering - Vol. 16, No. 6* , 673-680.
Karbhari, V. M., Chin, J. W., Hunston, D., Benmokrane, B., Juska, T., Morgan, R., et al. (2003). Durabilitiy Gap Analysis for Fiber-Reinforced Polymer Composites in Civil Infrastructure. *Journal of composites for construction , 7* (3), 238-247.
Los Alamos National Laboratories. (1997). DIAMOND. Los Alamos, New Mexico.
Moorty, S., & Roeder, C. W. (1992). Temperature-Dependent Bridge Movements. *Journal of Structural Engineering , 118* (4), 1090-1105.
National Climatic Data Center. (n.d.). *Snowfall - Average Total in Inches*. Retrieved August 18, 2008, from http://lwf.ncdc.noaa.gov/oa/climate/online/ccd/snowfall.html
NHASCE. (2006). *2006 Report Card for New Hampshire's Infrastructure.* NHASCE.
NHDOT Bureau of Bridge Design. (2007). *Bridge Inspection Report - Rollinsford 091/085.* NHDOT.
NHDOT Bureau of Bridge Design. (1999, July). Rollins Road Bridge Over B&M Railroad and Main Street Plans.
NHDOT . (2008, August 5-6). *New Hampshire bridges and related maintenance issues.* Northeast Bridge Preservation Partnership Meeting, Worcester, Massachusetts.
Nystrom, H. E., Watkins, S. E., Antonio, N., & Murray, S. (2003). Financial Viability of Fiber-Reinforced Polymer (FRP) Bridges. *Jounral of managment in engineering , 19* (1), 2-8.
Office of Bridge Technology. (2008, August 18). *IBRC - Bridge*. Retrieved from FHWA: http://www.fhwa.dot.gov/bridge/ibrc/
Peeters, B., & De Roeck, G. (2001). One-year monitoring of the Z24-Bridge: environmental effects versus damage events. *Earthquake Engineering and Structural Dynamics , 30* (2), 149-171.
Petroski, H. (2007, August 4). Learning from bridge failure. *Los Angeles Times* .

Phares, B. M., Rolander, D. D., Graybeal, B. A., & Washer, G. A. (2000). Studying the Reliability of Bridge Inspection. *Public Roads , 64* (3).
Robert-Nicoud, Y., Raphael, B., Burdet, O., & Smith, I. F. (2005). Model Identification of Bridges Using Measurement Data. *Computer-Aided Civil and Infrastructure Engineering* (20), 118-131.
Sanayei, M. (1997). PARIS - PARameter Identification System©. Medford, MA: Tufts University.
Sanayei, M., Bell, E. S., Javdekar, C. N., Edelmann, J. L., & Slavsky, E. (2006). Damage Localization and Finite-Element Model Updating Using Multiresponse NDT Data. *ASCE Journal of Bridge Eingineering , 11* (6), 688-689.
Sanayei, M., Imbaro, G. R., McClain, J. A., & Brown, L. C. (1997). Structural Model Updating Using Experimental Static Measurements. *Journal of Structural Engineering* , 792-798.
Santini-Bell, E., Sanayei, M., Brenner, B., Sipple, J., & Blanchard, A. (2008). Nondestructive testing for design verification of Boston's Central Artery underpinning frames and connections. *Bridge Structures - Assessment, Design and Construction , 4* (2), 87-98.
SAP2000. (2007). Verision Advanced 11.0.7. Berkely, California, USA: Computer and Structures, Inc.
Sipple, J. (2008, April 26). *2008 Structures Congress Presentation.* Vancouver, BC.
Sohn, H., Dzwonczyk, M., Straser, E. G., Kiremidjian, A. S., Law, K. H., & Meng, T. (1999). An Experimental Study of Temperature Effect on Modal Parameters of the Alamosa Canyon Bridge. *Earthquake Engineering and Structural Dynamics* , 879-798.
Stanton, J. F., Roeder, C. W., & Mackenzie-Helnwein, P. (2004). *Rotational Limits for Elastomeric Bearings Appendix F.* Washington: Transportation Research Board.
Stanton, J. F., Roeder, C. W., Mackenzie-Helnwein, P., White, C., Kuester, C., & Craig, B. (2008). *NCHRP Report 596 - Rotational Limits for Elastomeric Bearings.* Washington, D.C.: Transportation Research Board.
Tadros, M. K., & Al-Omaishi, N. (2003). *NCHRP Report 496 - Prestress Loss in Pretensioned High-Strength Concrete Bridge Girders.* Washington, D.C.: TRB.
Taly, N. (1998). *Design of Modern Highway Bridges.* New York: McGraw-Hill.
The D.S. Brown Company. (2008, October 09). *The D.S. Brown Company Corporate Website*. Retrieved from http://www.dsbrown.com/
Trunfio, J. P. (2001). *Experimental Testing for the use of Carbon FRP Grids in the Rollins Rd. Bridge, Rollinsford, NH.* Durham, NH: University of New Hampshire.
U.S. Department of Transportation. (2006). *2006 Status of the Nation's Highways, Bridges, and Transit - Conditions and Performance.*
Wipf, T. (1991). Use of tilt sensing equiptment for monitoring long-term bridge movement. *Canadian Jounral of Civil Engineering* , 1033-1046.

APPENDICES

APPENDIX A –DETAILED LITERATURE SURVEY OF INSTURMENTATION AND STRUCTURAL HEALTH MONITORING PROJECT

The study and deployment of SHM techniques is a multidisciplinary research area which uses nondestructive testing (NDT) techniques and instrumentation plans to examine the global response or specific structural components. To date, beneficial developments have been seen through instrumentation of short-span bridges, as short-span bridges are easier to instrument for full-scale tests and have a more sensitive global response (Brownjohn, Moyo, Omenzetter, & Chakraborty, 2005). SHM systems include, but are not limited to, the use of strain gauges, temperature sensors, tilt meters, accelerometers, and data acquisition systems. SHM systems with post-processing protocol allow for real time evaluation of current bridge conditions, having the ability to provide early warning of deteriorating or unsafe conditions. SHM systems can also provide long term structural health information. This information can help bridge owners decide when and how to repair or replace bridges by optimizing maintenance budgets, while improving the safety of the general public (Guan, Karbhari, & Sikorsky, 2007).

Technically and economically feasible, practical, and rapid solutions created through administrative and engineering solutions are necessary for modern bridge management programs (Farhey, 2005). The data collection from bridges is only one part of SHM. A major component of SHM is the art of reconciling the collected data with an analytical model. Another large part of SHM is identifying characteristics of the bridge and possible means of failure, by using finite element modeling and analysis, along with field tests to provide an accurate model of the structural behavior at the bridge (Farhey, 2007). Creating a structural model which aids in the design process is common practice for bridge designers. Modifying that design model into a

monitoring based model to be used with the goal of performing parameter estimation and model updating makes the SHM process a very useful tool in bridge management (Bell, Sanayei, Javdekar, & Slavsky, 2007). "The best 'model' of the bridge is the bridge itself," (Howell & Shenton III, 2006) which makes conducting a load test the best way to obtain information on the bridge behavior. Information obtained from the NDT can be correlated to the behavior seen in the bridge model. A SHM program that compares data to data without providing accountability and a predictive model, gives little quantification of the data, and is, therefore, of little use to bridge owners (Guan, Karbhari, & Sikorsky, 2007).

Data can be collected on all types of structures in different ways, but what makes the information beneficial for decision making is how it is used to obtain value added information. Several SHM research projects have been performed using different SHM techniques. A popular method in SHM and damage detection is the use of vibration data and modal parameters (Brownjohn, Moyo, Omenzetter, & Chakraborty, 2005). This is popular because it does not require measuring displacement, strain, and rotations, which are subject to load application and environmental effects. Modal/vibration testing can be done fairly easily and often, using traffic as the excitation, to obtain results that aid in damage detection, parameter estimation, and model updating. Continuous monitoring with vibration testing allows observing seasonal changes, detecting damage, and observing gradual changes to the bridge. However, due to recent advancements in technology, static measurements such as strain, tilt, and displacement are easier to obtain and are viewed as being more reliable than in past generations (Robert-Nicoud, Raphael, Burdet, & Smith, 2005).

Static experimental data has been used in parameter estimation and model updating, and in certain situations has proven to be more economical than dynamic loading (Sanayei, Imbaro,

McClain, & Brown, 1997). Adding the parameter estimation and model updating component of SHM provides a decision making and predictive aspect to the program. Static measurement data is more practical when compared to dynamic measurements, due to lower computational cost and better insight into actual parameters (Sanayei, Imbaro, McClain, & Brown, 1997). Parameter estimation techniques, through the use of a finite element model and model updating, allow direct variation of structural parameters such as area, moment of inertia, and modulus of elasticity. Multi-response, using strain, displacement, and rotation, parameter estimation has been shown as a robust method for flexibility-based parameter estimation and model updating using the University of Cincinnati Infrastructure Institute bridge deck laboratory model (Sanayei, Bell, Javdekar, Edelmann, & Slavsky, 2006).

Table 15: Structural health monitoring measurement comparison (Sanayei, Imbaro, McClain, & Brown, 1997) (Aktan, Farhey, Helmicki, Brown, Hunt, & Lee, 1997)

	Pros	**Cons**
Displacement	• Typical measured response • Easy to rapidly deploy • Global, overall measurement	• Reference dependent • Difficult to measure
Strain	• Typical measured response • Not reference dependent • Direct structural behavior due to gauges being installed on surface of structural element	• Need baseline reading • Expense associated with strain gauges and data collection
Rotation	• Typical measured response • Not reference dependent	• Needs to settle out before readings

Parameter estimation on an in-service bridge was performed for calibrating a model for special permitting for an overloaded vehicle pass by Bridge Diagnostics, Inc. in 2000 (Grimson, Commander, & Ziehl, 2008). Three superloads were scheduled to cross the Bonnet Carré Bridge near Norco, Louisiana with the first weighing 2,460-kips and the second and third weighing

1,000-kips. The permitting and rating process for allowing the superloads to pass was done before any decision was made about integrating a load test into the process. The bridge was instrumented with quarter bridge electronic resistance strain gauges. A model was created based on material properties, containing elastic supports for boundary conditions, and initial observations from the bridge. The model was then calibrated using snooper truck weighing 66-kips passing along the length of the bridge. The calibration included modifying certain properties and boundary conditions and performing parameter estimation and model updating in order to match the results from the field test data. Calibration of the model involved 3,276 strain comparisons obtained from 28 locations, with 117 analysis load cases. The load cases and locations consisted of three truck paths with 39 truck positions along each pass.

Once the tedious calibration process was completed to an acceptable level of accuracy, the superloads were applied to the model. The results showed that the model was fairly accurate with modeled peak strains being within 10% of predicted peak strains. There was a discrepancy between model and measured data where the peak strains were experienced. That problem was fixed by adjusting the percentage of load carried by each dolly. A benefit from this process, as opposed to traditional load rating procedures, was the response of the entire structure was investigated as opposed to the conventional method of load distribution factors and beam analysis. Researchers found that the field-verified model process is identical to the typical process of load rating (Grimson, Commander, & Ziehl, 2008).

APPENDIX B - CFRP REINFORCEMENT CALCULATIONS

Actual Area of CFRP through cross-section

$$A_{actual} = 10.86in^2$$

If CFRP was in a layer throughout entire cross-section

$$A_{desired} = 202.5in^2$$

Transform moment of inertia to maintain thickness of material

$$E_{equivalent} = \frac{E_{actual}}{\eta}$$

$$\eta = \frac{A_{desired}}{A_{Aactual}} = \frac{202.5in^2}{10.86in^2} = 18.646$$

$$E_{equivalent} = \frac{104000ksi}{18.646} = 557.75ksi$$

APPENDIX C – LOAD CASES FOR ALL YEARS

2000 Load Cases

Load Case 1

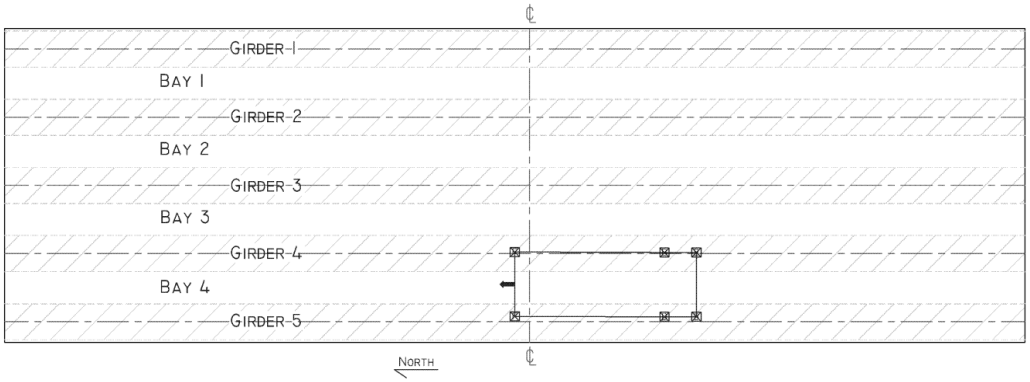

Load Case 2

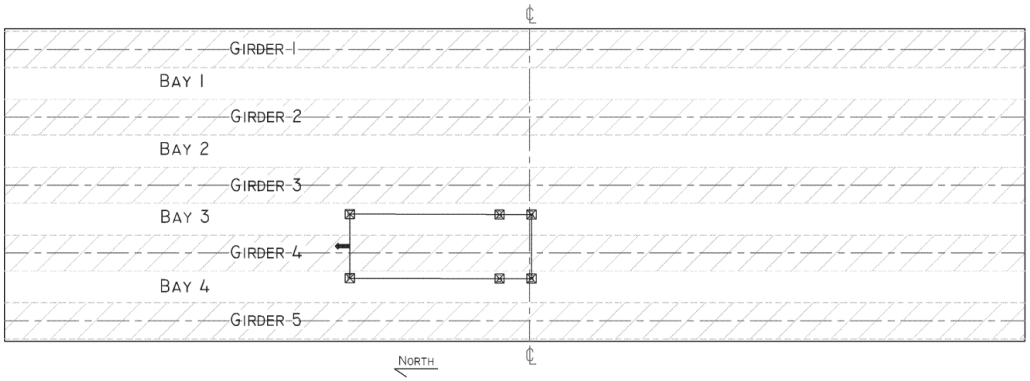

Load Case 3

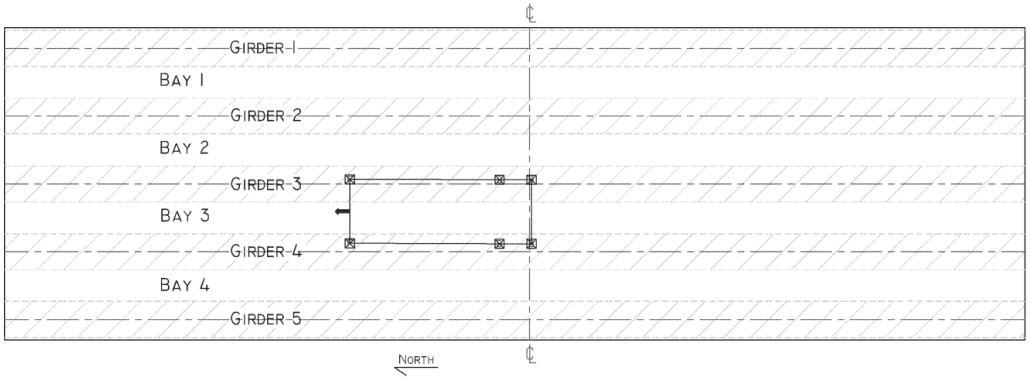

Load Case 4

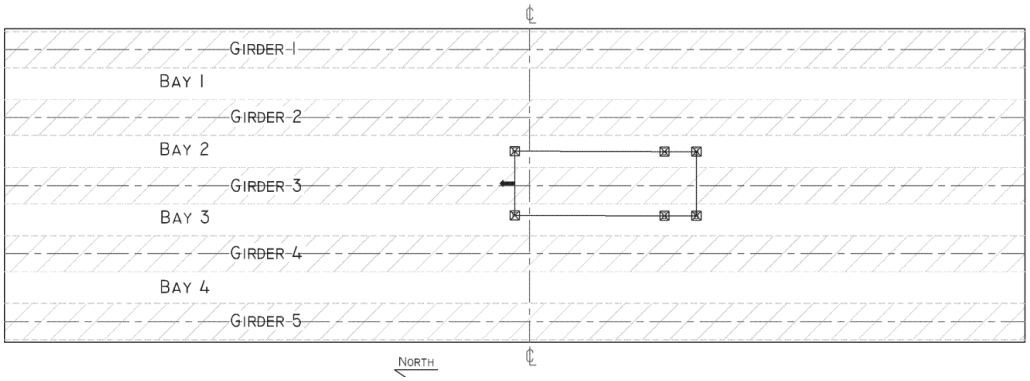

2001 Load Cases

Load Case 1

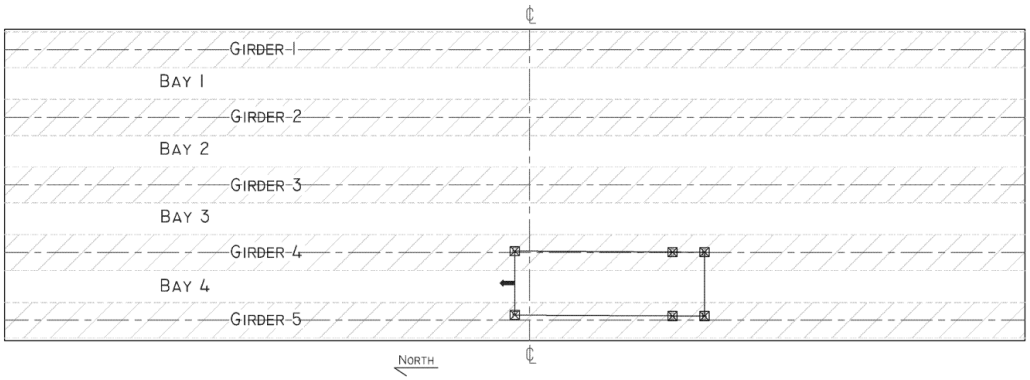

Load Case 2

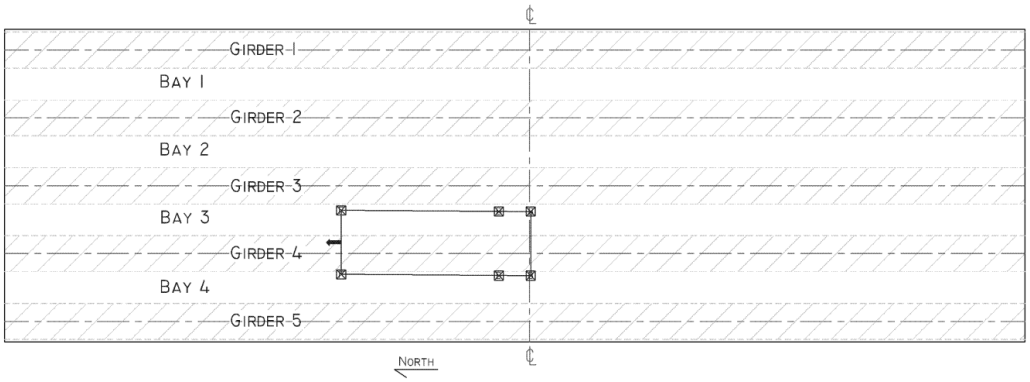

Load Case 3

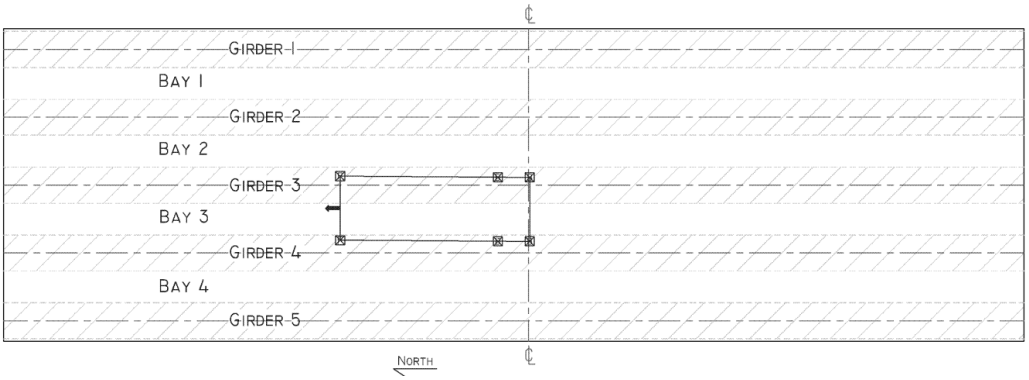

Load Case 4

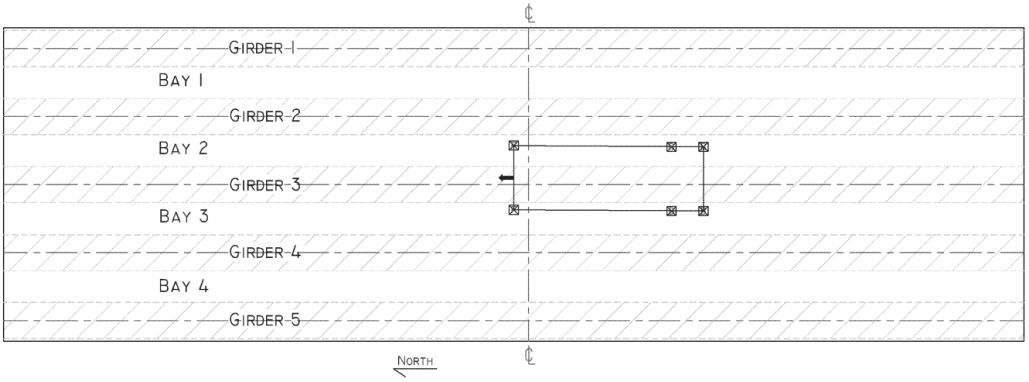

2008 Load Cases

Load Case 1

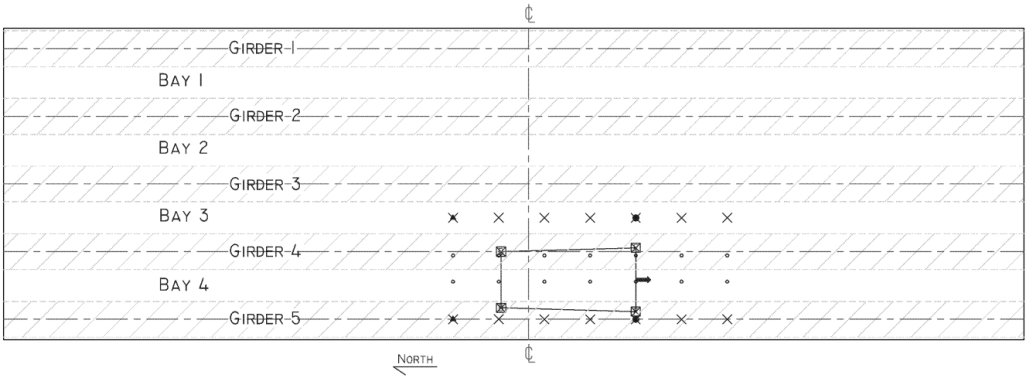

Load Case 2

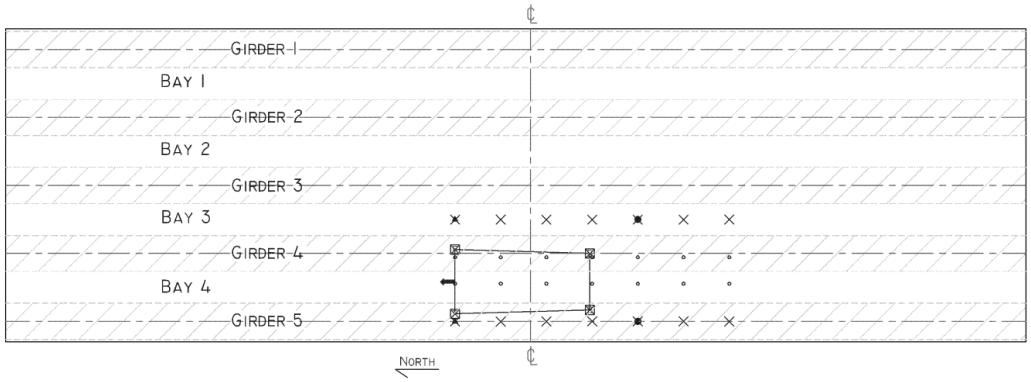

Load Case 3

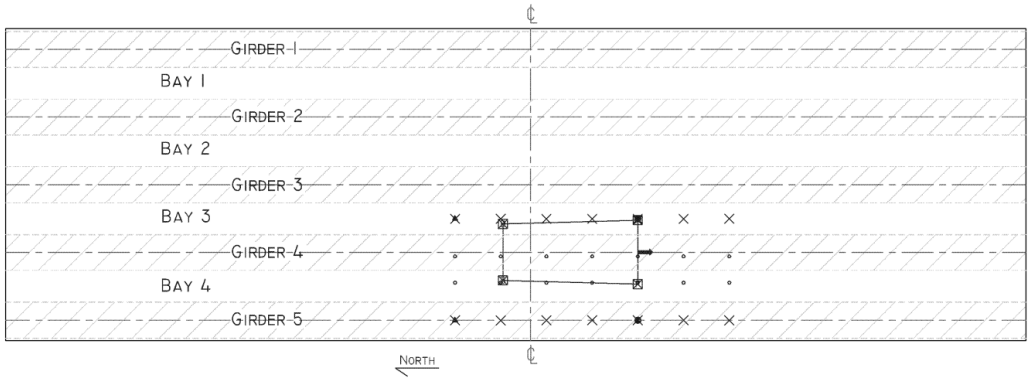

Load Case 4

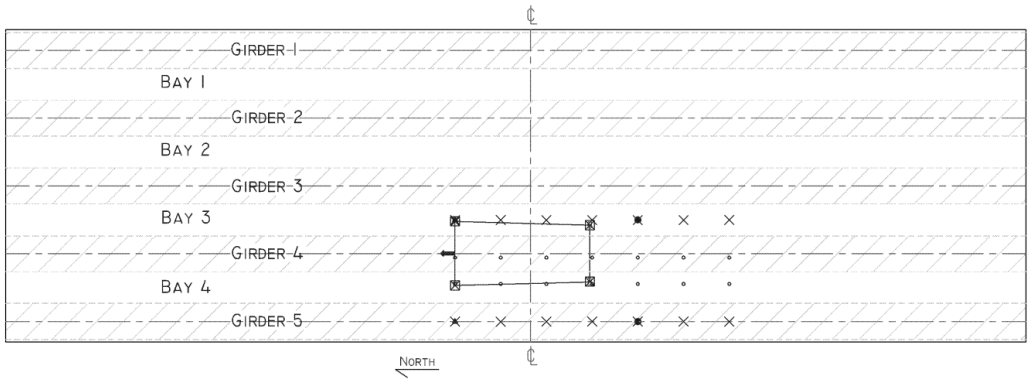

APPENDIX D – CALCULATION OF REINFORCED ELASTOMERIC BEARING PAD STIFFNESS

All calculations in this equations and table values taken from Stanton, Roeder, & Mackenzie-Helnwein, NCHRP Report 596 - Rotational Limits for Elastomeric Bearings

$$S = Shape\ Factor = \frac{Loaded\ Plan\ Area}{Perimeter\ Area\ Free\ to\ Bulge}$$

$$Loaded\ Plan\ Area = \left(\frac{16in}{2}\right)^2 * \pi = 201in^2$$

$$Perimeter = 16in * \pi = 50.3in$$

$$\therefore S = 4.00$$

$$\lambda = S\ \sqrt{\frac{3G}{K}}$$

$$G = Shear\ Modulus$$
$$K = Bulk\ Modulus$$

$G = 0.1300ksi$	$G = 0.200ksi$	$G = 0.1300ksi$	$G = 0.200ksi$
$K = 363ksi$	$K = 464ksi$	$K = 464ksi$	$K = 363ksi$
$\therefore \lambda$ =0.1312	$\therefore \lambda = 0.1438$	$\therefore \lambda = 0.1160$	$\therefore \lambda = 0.1627$

$$\lambda_{average} = 0.1384$$

$B_a = 2.1$ (from graph)

$B_r = 0.7$ (from graph)

$$K_a = \frac{EA\ A_a + B_a S^2}{t}$$

$$A_a = 1$$

$$E = 3 * G = 3 * 0.1300ksi = 0.390ksi$$

$$t = \frac{5}{8}in$$

$$K_a = 4341 \frac{kips}{in}$$

$$t = \frac{1}{2} in$$

$$K_a = 5426 \frac{kips}{in}$$

$$Total = 36{,}899 \frac{kip}{in}$$

$$E = 3 * G = 3 * 0.200ksi = 0.600ksi$$

$$t = \frac{5}{8} in$$

$$K_a = 6678 \frac{kips}{in}$$

$$t = \frac{1}{2} in$$

$$K_a = 8348 \frac{kips}{in}$$

$$Total = 56{,}767 \frac{kip}{in}$$

$$Total_{average} = 46{,}832$$

$$K_a = \frac{EI}{t} \ A_r + B_r S^2$$

$$I = \frac{1}{4} \pi \ \left(\frac{16in}{2} \right)^4 = 3217in^4$$

$$E = 3 * G = 3 * 0.1300ksi = 0.390ksi$$

$$t = \frac{5}{8} in$$

$$K_r = 24490 \frac{kips}{rad}$$

$$t = \frac{1}{2} in$$

$$K_r = 30613 \frac{kips}{rad}$$

$$Total = 208{,}168 \frac{kip}{rad}$$

$$E = 3 * G = 3 * 0.200 ksi = 0.600 ksi$$

$$t = \frac{5}{8} in$$

$$K_r = 24490 \frac{kips}{rad}$$

$$t = \frac{1}{2} in$$

$$K_r = 47097 \frac{kips}{rad}$$

$$Total = 241{,}135 \frac{kip}{rad}$$

$$Total_{average} = 224{,}652 \frac{kip}{rad}$$

APPENDIX E - CALCULATIONS FOR MODEL VERIFICATION

Hand verification of SAP2000® Rollins Road Bridge Bridge Model

Assumptions:

No dead load

No prestressing force

No temperature effects

Simply supported

No bridge rail in stiffness

Bridge cross section:

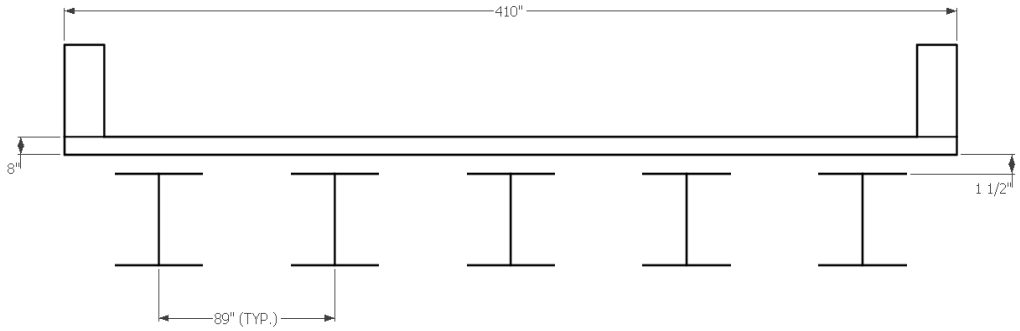

Material Properties:

Nominal Strength were used for the calculation of the Material Properties

Bridge Deck

$$f_c^{'} = 6000psi$$

$$E = 57 \ \overline{f_c^{'}} = 57 \ \overline{6000psi} = 4415ksi$$

Girder

$$f_c^{'} = 8000psi$$

$$E = 57 \ \overline{f_c^{'}} = 57 \ \overline{8000psi} = 5098ksi$$

$$I = 146.5 * 10^9 mm^4 \quad \frac{1in^{\ 4}}{25.4mm^{\ 4}} \quad = 351968in^4$$

$$A = 553 * 10^3 mm^2 \quad \frac{1in^{\ 2}}{25.4mm^{\ 2}} \quad = 857in^2$$

CFRP

$$E = 10400ksi$$

$$Area\ in\ 111in\ section = 2.976\ in^2$$

$$Total\ length\ of\ reinforced\ area = 410in - (2 * 2.5in) = 405in$$

$$\frac{405in}{111in} = 3.65$$

$$3.65 * 2.976in^2 = 10.86in^2$$

Transform Section

Base material is concrete in girder

$$n_{deck} = \frac{E_{girder}}{E_{deck}} = \frac{5090ksi}{10400ksi} = 1.155$$

$$Equivalent\ width\ of deck = \frac{Actual}{n} = \frac{410in}{1.155}$$

If CFRP was solid across cross section – for ease of transforming section and using SAP2000® layered shell elements

$$A = 10.86in^2$$

$$\frac{10.86in^2}{0.5} = 21.7in \Leftarrow Width$$

$$n_{CFRP} = \frac{E_{girder}}{E_{CFRP}} = \frac{5090ksi}{10400ksi} = 0.489$$

$$Equivalent\ width = \frac{21.7in}{0.489} = 44.3in$$

Moment of inertia for section

$$I = \Sigma\ I_o + Ad^2$$

$$I_{deck} = \frac{1}{12}\ 355in\quad 8in\ ^3 = 15150in^4$$

$$I_{CFRP_1} = I_{CFRP_2} = \frac{1}{12}\ 44.3in\quad 0.5in\ ^3 = 0.462in^4$$

$$I_{girder} = 351968in^4$$

$$A_{deck} =\ 355in\quad 8in\ = 2841in^4$$

$$A_{CFRP_1} = A_{CFRP_2} =\ 44.3in\quad 0.5in\ = 22.15in^2$$

$$A_{girder} = 857in^2$$

Centroid for area:

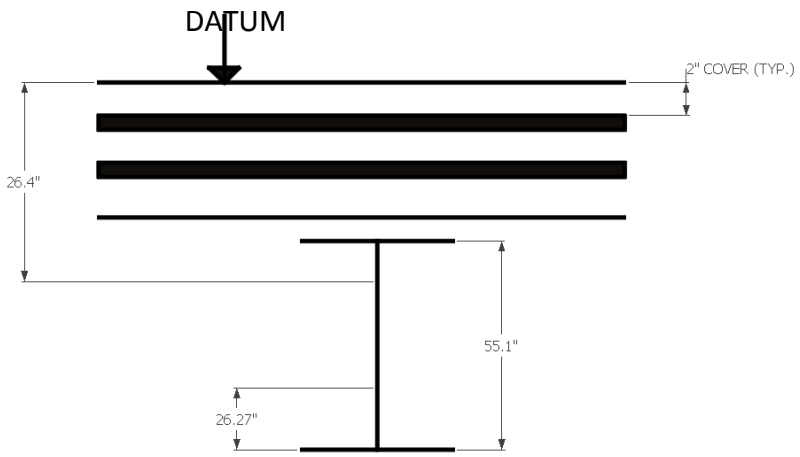

$$y = \frac{\Sigma A_i y_i}{\Sigma A_i}$$

$$y_{deck} = 4in$$

$$y_{CFRP_1} = 2.25in$$

$$y_{CFRP_2} = 5.75in$$

$$y_{girder} = 8in + 1.5in +\ 55.1in - 26.27in\ = 38.33in$$

$$y = \frac{(2841in^2 + 4in) + (22.15in^2 + 2.25in) + (22.15in^2 + 5.75in) + 5 * (857in^2 + 38.33in)}{2841in^2 + (2 * 22.15in^2) + (5 * 857in^2)}$$

$$= \frac{175785}{7170} = 24.52in$$

$$I = 15150in^4 + 2841in^2 * 24.5in - 4in^2$$

$$+ 0.462in^4 + 22.15in^2 * 24.5in - 2.25in^2$$

$$+ 0.462in^4 + 22.15in^2 * 24.5in - 5.75in^2$$

$$+ 5\ 351968in^4 + 857in^2 * 24.5in - 38.33in^2$$

$$= 1210887in^4 + 10975in^4 + 7796in^4 + 2577404in^4 = 3807062in^4$$

$$P = 100kips\ at\ center\ of\ bridge$$

$$\Delta = \frac{PL^3}{48EI} = \frac{100kips\ 1340in^3}{48 * 5098ksi * 3807062in^4} = 0.258in$$

From SAP2000®

$$\Delta = 0.253in$$

Find moment at center

$$M_{max} = \frac{PL}{4} = \frac{100kips * 1340in}{4} = 33500in * kips$$

$$\frac{33500in * kips}{5} = 6700in * kips = 558ft * kips$$

Calculating Strain Values

Assuming still within linear elastic range

$$\sigma = \frac{My}{I}$$

$$\sigma = E\varepsilon$$

Look at top gauge, down 2.5in from top of girder

$$y = distance\ from\ centriod\ to\ depth\ of\ gauge$$

$$Depth\ to\ center = 26.4in$$

$$Depth\ to\ gauge = 8in + 1.5in + 2.5in$$

$$26.4in - 12in = 14.4in$$

$$\sigma = \frac{33500in * kips\ \ 14.4in}{3807062in^4} = 0.1267ksi$$

$$\varepsilon = \frac{\sigma}{E} = \frac{0.1267ksi}{5098ksi} = 24.9\mu\varepsilon$$

From SAP2000®

$$strain = 25.7\mu\varepsilon$$

APPENDIX F – STRAIN CALCULATIONS

Sample calculation for one strain sensor, girder 5

x,y Notation	Point	Undeformed X-Coordinate	Undeformed Y-Coordinate
1	*g5-d1*	658.074	-176
2	*g5-g1*	658.074	-176
1	*g5-d2*	670	-176
2	*g5-g2*	670	-176
1	*g5-d3*	681.926	-176
2	*g5-g3*	681.926	-176

x,y Notation	Point	Deformed X-Coordinate	Deformed Y-Coordinate
1	*g5-d1*	658.0762350	-4.8103190
2	*g5-g1*	658.0757090	-12.3103190
1	*g5-d2*	669.9999410	-4.8108300
2	*g5-g2*	669.9998850	-12.3108300
1	*g5-d3*	681.9236500	-4.8104460
2	*g5-g3*	681.9240630	-12.3104460

$$Azimuth = \arctan \frac{g5-g1\ _{xcord} - \ g5-d1\ _{xcord}}{g5-g1\ _{ycord} - \ g5-d1\ _{ycord}}$$

$$Gauge\ Point_x = Deformed\ X\ Coordinate + \ Depth\ to\ Gauge * \sin \ Azimuth$$

$$Gauge\ Point_y = Deformed\ Y\ Coordinate + \ Depth\ to\ Gauge * \cos \ Azimuth$$

Point	Depth to Gauge	Azimuth	Gauge Point Coordinates	
			x	y
g5-t1	-13.5	7.0133E-05	658.075288	-18.310319
g5-t2	-36.118	7.0133E-05	658.073702	-40.928319
g5-t3	-13.5	7.4667E-06	669.999840	-18.310830
g5-m1	-36.118	7.4667E-06	669.999671	-40.928830
g5-m2	-13.5	-5.5067E-05	681.924393	-18.310446
g5-m3	-36.118	-5.5067E-05	681.925639	-40.928446

$$Strain = \frac{New\ Length - Original\ Length}{Original\ Length}$$

APPENDIX G – FIRST ANALYSIS OF ROLLINS ROAD BRIDGE LOAD TEST DATA FOR ALL THREE YEARS

Modeling Temperature Effects

Special care was taken to include the coefficient of thermal expansion into the material properties for all materials used the model. Experimental coefficients of thermal expansion were obtained from Martha Bowman who performed tests on concrete samples.

Benchmark Data for Data Set and SAP2000 Model

To go from 120,000 data points to a more manageable data set, some data reduction was required. The four load cases previously discussed were created for all three years, resulting in a total of 12 load cases run throughout the analysis. At every predetermined truck stop, the truck sat at the location for approximately one minute. These one minute time intervals corresponding to load cases were removed from the large data set. From this reduced data, material temperatures were separated and transformed to thermal loads. This transformation of temperature measurements to thermal loads involved comparing the data to the benchmark data set, and finding the difference and therefore thermal load. The strain values for the load cases were also grouped together and will be examined and included in Chapter 6: Manual Model Updating.

Establishing the Benchmark Data Set

The earliest recorded data, with no loading, was recording at the start of the December 2000 load test. At that time, the strains in the bridge were caused by self weight, environmental effects, and prestressing loads only. During this period there was no load applied, it was used as

a benchmark for all the data sets. All strain values were compared to this zero-load reading, to show either a positive or negative change in strain values. The bridge elevations, which were taken at this time through surveying techniques, will serve as the benchmark for all displacement measurements. A similar method was performed to the model, to have cohesion between measured data and modeled response.

Table G-1 shows the benchmark data set used for the strain values on the Rollins Road Bridge Research Project. Table G-2 shows the benchmark elevation values used for data analysis. All changes in elevation will be a positive or negative displacement.

Benchmark Data Set														
	Channel 32 3gc 1002965 *Girder 3* *Middle/Top*	Channel 27 gg6 4421663 *Girder 3* *Temp*	Channel 3 gg1 1003038 *Girder 4* *Top*	Channel 28 gg7 4615676 *Girder 4* *Temp*	Channel 5 gg3 1002992 *Girder 5* *Middle*	Channel 6 gg4 1003137 *Girder 5* *Top*	Channel 30 gg9 4617690 *Girder 5* *Temp*	Channel 1 TS1G3 4517683 *Girder 3* *Bottom*	Channel 21 T1M3B 4498646 *Midspan 3* *Bottom*	Channel 23 T1G4B 4501635 *Girder 4* *Bottom*	Channel 22 T1G4T 4620728 *Girder 4* *Top*	Channel 2 TS1M4 4458658 *Midspan 4* *Top*	Channel 25 T1G5B 4498644 *Girder 5* *Bottom*	Channel 24 T1G5T 4536689 *Girder 5* *Top*
12/11/2000 10:35:10	3792.6	25.15	4273.4	28.6	4674.8	4369.6	451.55	28.95	34.6	38.85	26.85	36.45	26.35	27.95
12/11/2000 10:35:20	3792.2	25.1	4273.2	28.65	4674.4	4369.2	451.4	28.95	34.65	38.9	26.9	36.45	26.3	27.95
12/11/2000 10:35:30	3792.2	25.15	4273.2	28.6	4674.4	4369	451.4	28.95	34.65	38.85	26.9	36.45	26.35	27.95
12/11/2000 10:35:40	3792.6	25.2	4273.4	28.7	4674.8	4368.4	451.4	29	34.6	38.95	26.9	36.45	26.25	27.9
12/11/2000 10:35:50	3792.6	24.95	4273.2	28.65	4674.6	4369.4	451.55	28.95	34.6	38.95	26.9	36.45	26.35	28
12/11/2000 10:36:00	3792.6	25.15	4273	28.65	4674.6	4369.4	451.6	28.95	34.65	38.95	26.9	36.45	26.3	28
12/11/2000 10:36:10	3792.2	25.1	4273.4	28.65	4674.8	4369.6	451.55	29	34.65	39	26.85	36.5	26.25	27.95
12/11/2000 10:36:20	3792.4	25.2	4273.2	28.65	4675	4369.6	451.5	28.95	34.65	38.95	26.9	36.5	26.3	28
12/11/2000 10:36:30	3792.2	25.05	4273.4	28.65	4674.8	4370	451.4	29	34.65	38.95	26.95	36.45	26.4	27.85
12/11/2000 10:36:40	3792.6	25	4273.2	28.7	4674.6	4369.2	451.5	29	34.65	38.95	26.9	36.45	26.3	28.05
12/11/2000 10:36:50	3792.6	25.2	4273.4	28.65	4674.6	4369.2	451.55	29	34.7	38.95	26.9	36.55	26.3	27.95
Average	3792.44	25.11	4273.27	28.65	4674.67	4369.33	451.49	28.97	34.64	38.93	26.90	36.47	26.31	27.96
Standard Deviation	0.20	0.08	0.13	0.03	0.18	0.41	0.08	0.03	0.03	0.05	0.03	0.03	0.05	0.05
95% Confidence	0.12	0.05	0.08	0.02	0.11	0.24	0.05	0.02	0.02	0.03	0.02	0.02	0.03	0.03
CI Low	3792.32	25.06	4273.19	28.63	4674.56	4369.08	451.45	28.96	34.62	38.90	26.88	36.45	26.29	27.93
CI High	3792.55	25.16	4273.35	28.67	4674.78	4369.57	451.54	28.99	34.66	38.96	26.91	36.49	26.34	27.99

Table G-1: Benchmark Data Set

Table G-2: Benchmark Elevations

Benchmark Elevations (ft.)		
December 2000 No Load	*Girder 3*	151.7338
	Bay 3	156.6243
	Girder 4	151.6632
	Bay 4	156.4805
	Girder 5	151.5077

Again, 95% confidence intervals (CI) on the mean were used and examined to determine if the values where within acceptable limits for this project. The data did not follow a normal distribution, so standard deviation techniques were not used, even though they are still displayed on the table. All 95% CIs were less than 0.25-microstrain, which was deemed an acceptable CI for the measured strain values.

Establishing Benchmark SAP2000 Model

From this data, the material temperatures for the SAP2000® benchmark model were established. The material temperatures, as recorded during the December 2000 zero-load reading were applied as material temperatures for the bridge model. This allows for the thermal load derived from the benchmark data set to be accurately applied to the model. Table G-3 and Table G-4 show the temperature values used for initial material temperatures for the SAP2000® benchmark model. Since the bridge is only instrumented on one side, symmetry was used and assumed acceptable to get material temperatures for the entire bridge.

Table G-3: Deck Temperatures used for SAP2000 Benchmark Model

Deck Temperature (°F)								
Girder 1	*Bay 1*	*Girder 2*	*Bay 2*	Girder 3	Midspan 3	Girder 4	Midspan 4	Girder 5
27.14	*36*	*32.91*	*35*	29	35	32.91	36	27.14

Table G-4: Girder Temperature used for SAP2000 Benchmark Model

Girder Temperature (°F)				
Girder 1	*Girder 2*	Girder 3	Girder 4	Girder 5
23.06	*28.65*	25.11	28.65	23.06

An analysis was performed having the applied loads being self weight, material temperature, and prestressing loads. The properties for that benchmark model are as close to the initial design

conditions as possible. The optimal condition would be to know the initial zero-set values for the strain gauges and then run a calibration on the model to get it to match those initial zero-set values; however, that was not the case with the RRB. The strain values at girder locations were calculated and will be used as benchmark strain values. Displacements were also calculated and will be used as benchmark displacement values. The benchmark model strain and displacement values can be seen in Table G-5 and Table G-6. All changes in strain or displacement will be referenced to these benchmark values.

Table G-5: SAP2000 Benchmark Model Strain Values

SAP Benchmark Strains		
Middle	*Top*	
	-48.471	*Girder 3*
	-47.792	*Girder 4*
-16.019	-46.389	*Girder 5*

Table G-6: SAP2000 Benchmark Model Displacements

SAP Benchmark Displacements		
		Displacement
Benchmark	**Girder 3**	-0.4055
	Girder 4	-0.4060
	Girder 5	-0.4084

SAP2000 Output

In SAP2000®, load cases were created for each applied vehicle load and corresponding thermal load case. These results, in a total of 24 load cases, four per year for vehicle load and four per year for thermal loading. A load combination is created for each load case in order to include dead, prestress, applied vehicle load, and applied thermal loading. As a result, there are 12 load combinations, four per year. The load combinations are titled 2000LC1ALL, 2001LC2ALL, 2008LC4ALL and so on. Those titles specify the year that the data is being analyzed, the load case, and that it includes all loads. Once the analysis cases are successfully run, the output data from SAP2000® needs to be post-processed. SAP2000®, as most structural

analysis packages, only exports forces and moments for beam elements. From axial force and moment, stresses and resulting strains in the member at the location of the strain gauge is calculated. Figure 84 shows the process used to calculate strain at gauge locations from the SAP2000® output tables. Further calculations for each load case can be seen in Figure G-1.

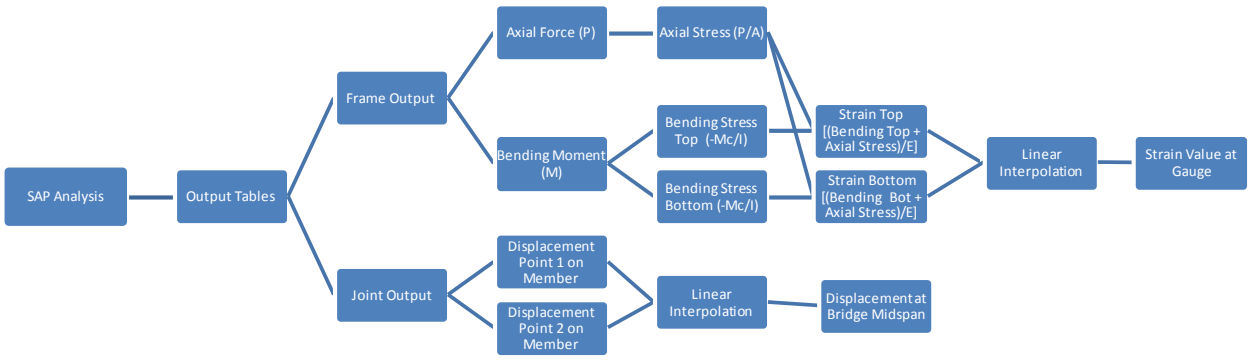

Figure G-1: SAP Output to Bending Strain at Gauge Location Flowchart

In summary, axial forces are used to calculate axial stresses, while bending moments are used to calculate bending stress in the top and bottom of the beam section. These stresses are combined to form strain throughout the depth of the beam. Using linear interpolation, the strain value at the depth of gauge is calculated. For displacement measurements, the displacements at the end nodes of the element are output from SAP2000®, and then linear interpolation is used to get the displacement at the location where the surveyors took the measurement.

Load Test Data to SAP2000 Comparison

There is post-processed data from the field measurements, post-processed data from the SAP2000® model, benchmark readings from the field measurements, and a benchmark SAP2000® model. To get the comparison used in this research, the delta comparisons, several simple steps must be done once the data is post-processed and the benchmarks are determined.

The delta comparison is done for both the recorded data and model response data. It is achieved by comparing measured data versus benchmark data. Once the delta is established for recorded and model response data, conclusions may be made. The theory behind this process is that a change in the behavior of the bridge will be accurately captured and will be shown as a similar change in behavior in the SAP2000® model if all conditions are properly modeled, since the expected behavior will be within the linear elastic range.

The purpose of comparing measured structural response data to an analytical model is for the purpose of parameter estimation and model updating. MUSTANG is currently in the design phase by other researchers at UNH. Upon completion of manual parameter estimation and model updating, the predicted structural response was reflective of the 2008 status of the bridge as captured during the April 2008 Load Test.

Levels of Different Models

In order to simplify to assessment of the three different load tests, three separate models were created. All models were originally based on the initial benchmark model, only differing in the load cases that were applied to the model. Using the load test data, the structural properties of these models are updated to track the progress of the bridge.

For the 2000 model, the bearing pad stiffness was left as calculated because the benchmark model was also created using the first recorded 2000 load test data. The selected structural properties that were changed from the 2000 model included the removal of specific structural components, such as the CFRP reinforcement, prestressing tendons, and thermal loads. By removing these elements from the model, the difference between design and monitoring based models can be seen.

For the 2001 and 2008 models, all structural components were kept in the models. The parameter that was changed during the manual parameter estimation was the stiffness of the elastomeric bearing pads. This will also be the focus of the runs in MUSTANG as part of future work. Also, looking at the most recent bridge inspection report, there are no noted changes to the deck, girders or abutment since the opening in 2000. The rotational and axial stiffness values of the elastomeric bearing pad will be altered independently to gages the effect of each on the performance of the bridge. When the models are run through MUSTANG, aspects such as modulus of elasticity and moment of inertia, for specific elements, will also be included in the parameter estimation, however for the scope of this research project, those properties will not be examined in the manual parameter estimation.

Discussion of Manual Parameter Estimation Results

To reiterate, the only gauges used in the SHM program for the RRB were the gauges embedded in the HPC girders. These gauges are oriented in the longitudinal direction and capture the global structural response of the bridge given the loadings. Using only the girder gauges also limits the computations to a reasonable limit for the scope of the Rollins Road Bridge Research Project. A variety of results were seen after running the manual parameter estimation, which was expected, and will prove to be a good base when it comes time to run the bridge model in MUSTANG. For the post-processing, the tables entitled "SAP Relative Strain" and "Measured Relative Strain" are the sets of values that are compared when the table "2000 Runs" is created and follows the same method for all three years.

Table G-8 shows the results from the 2000 bridge model run through manual parameter estimating techniques. The first run shows the differences between the benchmark model and this model; the only change between those two is temperature and load application location. In

the two contributing tables, the changes in trends can be easily seen. These results are fairly promising, showing only slight changes in the data. A larger difference in values was noticed as the test progressed, suggesting temperature might have an even greater effect on the bridge than originally assumed.

The abutments could also be affected by the change in temperature, therefore changing the global response. Not including thermal loads in the model does not have much effect in the beginning, since that is very close to the time of the benchmark model. As time progresses the difference increases because thermal loads start to have a large effect. When the prestressing tendons are removed from the analysis, there is a strong difference between measured and modeled strain response, however, this effect will lessen over time. Omitting the CFRP reinforcement from the model, follows a similar trend with the initial model; however the differences are a little larger. The deflection measurements, when temperature is not included are very similar to the initial model with only slight variations. When the structural model does not include prestressing tendons, the predicted deflection measurements have a larger difference overall as when compared to the first model. When the structural model does not include the CFRP gird, the predicted deflection measurements are similar to the initial model with a slightly larger difference. When temperature is modeled as a gradient there is a slight difference seen as well.

SAP Relative Strain				
	Girder 3 Top	*Girder 4 Top*	*Girder 5 Middle*	*Girder 5 Top*
u3 46833		***u2 224651.5***		
2000LC1ALL	-5.14	-3.54	8.68	-3.56
2000LC2ALL	-4.05	-3.06	9.65	-3.97
2000LC3ALL	-2.42	-3.31	8.32	-1.60
2000LC4ALL	-1.50	-3.39	6.78	0.77
u3 46833		***u2 224651.5***		***No Temperature***
2000LC1ALL	-4.97	-3.66	8.49	-3.83
2000LC2ALL	-4.30	-3.41	8.19	-6.11
2000LC3ALL	-3.26	-3.72	5.28	-6.06
2000LC4ALL	-2.64	-3.73	2.73	-5.19
u3 46833		***u2 224651.5***		***No prestress***
2000LC1ALL	8.19	10.23	40.87	10.37
2000LC2ALL	9.28	10.71	41.84	9.96
2000LC3ALL	10.91	10.46	40.51	12.33
2000LC4ALL	11.83	10.38	38.97	14.70
u3 46833		***u2 224651.5***		***No FRP***
2000LC1ALL	-7.54	-5.83	6.51	-5.75
2000LC2ALL	-6.48	-5.44	7.30	-6.40
2000LC3ALL	-4.85	-5.77	5.90	-4.01
2000LC4ALL	-3.83	-5.81	4.40	-1.55
u3 46833		***u2 224651.5***		***Temp as gradient***
2000LC1ALL	-5.29	-3.73	8.60	-3.44
2000LC2ALL	-5.47	-4.41	9.08	-3.08
2000LC3ALL	-5.03	-6.21	7.11	0.18
2000LC4ALL	-4.69	-7.32	5.16	3.08

Measured Relative Strain				
	Channel 32 3gc 1002965 Girder 3 Top	*Channel 3 gg1 1003038 Girder 4 Top*	*Channel 5 gg3 1002992 Girder 5 Middle*	*Channel 6 gg4 1003137 Girder 5 Top*
2000LC1ALL	-5.44	-7.07	17.38	-9.16
2000LC2ALL	-1.09	-3.64	18.13	-6.10
2000LC3ALL	4.74	3.27	20.27	1.47
2000LC4ALL	7.85	7.84	22.58	7.67

2000 Runs

Stiffness Value	u3	46833	0				
	r2	224651.5					
		Strain				Deflection	
		Girder 3 Top	Girder 4 Top	Girder 5 Middle	Girder 5 Top	Girder 3	Girder 4	Girder 5
	2000LC1ALL	-0.30	-3.53	8.71	-5.60	-0.17	-0.23	-0.37
	2000LC2ALL	2.95	-0.58	8.48	-2.13	-0.20	-0.31	-0.28
	2000LC3ALL	7.16	6.58	11.95	3.07	-0.14	-0.31	-0.31
	2000LC4ALL	9.34	11.23	15.81	6.90	-0.15	-0.02	-0.05

Stiffness Value	u3	46833	No Temperature				
	r2	224651.5					
		Strain				Deflection	
		Girder 3 Top	Girder 4 Top	Girder 5 Middle	Girder 5 Top	Girder 3	Girder 4	Girder 5
	2000LC1ALL	-0.46	-3.41	8.89	-5.33	-0.17	-0.23	-0.37
	2000LC2ALL	3.20	-0.24	9.94	0.01	-0.21	-0.33	-0.30
	2000LC3ALL	7.99	6.99	14.99	7.54	-0.17	-0.34	-0.35
	2000LC4ALL	10.49	11.57	19.86	12.86	-0.19	-0.06	-0.09

Stiffness Value	u3	46833	No prestress				
	r2	224651.5					
		Strain				Deflection	
		Girder 3 Top	Girder 4 Top	Girder 5 Middle	Girder 5 Top	Girder 3	Girder 4	Girder 5
	2000LC1ALL	-13.63	-17.30	-23.49	-19.53	-0.37	-0.43	-0.56
	2000LC2ALL	-10.38	-14.35	-23.72	-16.05	-0.39	-0.51	-0.47
	2000LC3ALL	-6.17	-7.19	-20.24	-10.86	-0.33	-0.51	-0.50
	2000LC4ALL	-3.98	-2.54	-16.39	-7.03	-0.35	-0.21	-0.24

Stiffness Value	u3	46833	No FRP				
	r2	224651.5					
		Strain				Deflection	
		Girder 3 Top	Girder 4 Top	Girder 5 Middle	Girder 5 Top	Girder 3	Girder 4	Girder 5
	2000LC1ALL	2.10	-1.24	10.87	-3.41	-0.18	-0.24	-0.38
	2000LC2ALL	5.39	1.79	10.83	0.30	-0.20	-0.32	-0.29
	2000LC3ALL	9.58	9.04	14.37	5.49	-0.14	-0.32	-0.32
	2000LC4ALL	11.67	13.66	18.18	9.23	-0.16	-0.02	-0.05

Stiffness Value	u3	46833	Temp as gradient				
	r2	224651.5					
		Strain				Deflection	
		Girder 3 Top	Girder 4 Top	Girder 5 Middle	Girder 5 Top	Girder 3	Girder 4	Girder 5
	2000LC1ALL	-0.14	-3.34	8.78	-5.71	-0.17	-0.23	-0.37
	2000LC2ALL	4.37	0.76	9.05	-3.02	-0.19	-0.31	-0.29
	2000LC3ALL	9.76	9.48	13.16	1.30	-0.13	-0.31	-0.33
	2000LC4ALL	12.54	15.17	17.43	4.59	-0.14	-0.01	-0.06

Table G-8: 2000 Manual Parameter Estimation Results

Table G-9 shows the results from the August 2001 bridge model, after manual parameter estimation. The first run uses the load cases from the August 2001 load test while keeping the

same model used in the beginning of the 2000 analysis. This shows that there is a definite difference in the behavior between 2000 and 2001. An initial thought was that this could be due to stiffening of the bearing pads, so that was modeled as fixed in the axial direction and allowing complete rotation. The results from that change were a slight improvement to the first results, however, an additional characteristic was not captured accurately. Both the rotational stiffness and axial stiffness were increased in the third run, which did not differ much from the first run. As seen in the two contributing tables in Table G-9, there is a large difference in girder 3 strain gauge readings, being in the entirely wrong direction. Girders 4 and 5 are in the right area, however, values measured in the model are much less than recorded in the field. For completeness, both the axial and rotation degrees of freedom were modeled as fixed, resulting in values offered a lesser correlation than the first run. Deflection differences were only significantly impacted when both degrees are modeled as fixed.

SAP Relative Strain				
	Girder 3 Top	*Girder 4 Top*	*Girder 5 Middle*	*Girder 5 Top*
	u3 46833		***u2 224651.5***	
2001LC1ALL	-107.87	86.14	67.05	86.45
2001LC2ALL	-106.87	87.48	67.97	84.49
2001LC3ALL	-103.93	88.09	64.55	86.26
2001LC4ALL	-101.85	89.06	63.42	88.13
	u3 10000000		***u2 0.0000001***	
2001LC1ALL	-105.13	88.88	74.04	89.23
2001LC2ALL	-104.16	90.19	74.87	87.24
2001LC3ALL	-101.18	90.84	71.54	89.04
2001LC4ALL	-99.09	91.83	70.42	90.93
	u3 70000		***u2 500000***	
2001LC1ALL	-107.59	86.42	68.97	86.73
2001LC2ALL	-106.60	87.75	69.86	84.77
2001LC3ALL	-103.66	88.35	66.46	86.53
2001LC4ALL	-101.60	89.31	65.32	88.38
	u3 fixed		***u2 fixed***	
2001LC1ALL	-154.05	39.94	44.29	40.00
2001LC2ALL	-152.87	41.47	45.26	38.26
2001LC3ALL	-151.44	40.57	40.98	38.48
2001LC4ALL	-151.14	39.76	38.77	38.57
	u3 fixed		***u2 free***	
2001LC1ALL	-105.12	88.89	74.08	89.24
2001LC2ALL	-104.15	90.20	74.90	87.25
2001LC3ALL	-101.17	90.85	71.58	89.06
2001LC4ALL	-99.08	91.84	70.45	90.94

Measured Relative Strain				
	Channel 32 3gc 1002965 Girder 3 Top	*Channel 3 gg1 1003038 Girder 4 Top*	*Channel 5 gg3 1002992 Girder 5 Middle*	*Channel 6 gg4 1003137 Girder 5 Top*
2001LC1ALL	206.73	287.82	302.55	268.29
2001LC2ALL	208.36	290.30	300.04	270.47
2001LC3ALL	211.96	293.58	297.87	274.42
2001LC4ALL	216.54	296.87	297.24	278.93

2001 Runs

Stiffness Value	u3	46833						
	r2	224651.5						
		Strain				Deflection		
		Girder 3 Top	Girder 4 Top	Girder 5 Middle	Girder 5 Top	Girder 3	Girder 4	Girder 5
	2001LC1ALL	314.60	201.68	235.49	181.85	-0.19	-0.32	-0.36
	2001LC2ALL	315.23	202.82	232.07	185.98	-0.22	-0.35	-0.34
	2001LC3ALL	315.89	205.50	233.32	188.16	-0.17	-0.28	-0.23
	2001LC4ALL	318.39	207.81	233.82	190.80	-0.16	-0.11	-0.16

Stiffness Value	u3	10000000						
	r2	0.0000001						
		Strain				Deflection		
		Girder 3 Top	Girder 4 Top	Girder 5 Middle	Girder 5 Top	Girder 3	Girder 4	Girder 5
	2001LC1ALL	311.86	198.94	228.51	179.07	-0.23	-0.35	-0.39
	2001LC2ALL	312.52	200.11	225.17	183.24	-0.26	-0.38	-0.37
	2001LC3ALL	313.14	202.74	226.33	185.37	-0.21	-0.31	-0.26
	2001LC4ALL	315.63	205.04	226.82	188.00	-0.19	-0.15	-0.19

Stiffness Value	u3	70000						
	r2	500000						
		Strain				Deflection		
		Girder 3 Top	Girder 4 Top	Girder 5 Middle	Girder 5 Top	Girder 3	Girder 4	Girder 5
	2001LC1ALL	314.32	201.41	233.58	181.56	-0.23	-0.35	-0.39
	2001LC2ALL	314.96	202.55	230.18	185.71	-0.26	-0.38	-0.37
	2001LC3ALL	315.63	205.23	231.41	187.89	-0.21	-0.31	-0.26
	2001LC4ALL	318.14	207.56	231.92	190.55	-0.19	-0.15	-0.19

Stiffness Value	u3	fixed						
	r2	fixed						
		Strain				Deflection		
		Girder 3 Top	Girder 4 Top	Girder 5 Middle	Girder 5 Top	Girder 3	Girder 4	Girder 5
	2001LC1ALL	360.79	247.88	258.26	228.29	-0.64	-0.77	-0.82
	2001LC2ALL	361.23	248.83	254.78	232.21	-0.67	-0.80	-0.79
	2001LC3ALL	363.40	253.02	256.89	235.93	-0.63	-0.74	-0.70
	2001LC4ALL	367.67	257.11	258.47	240.36	-0.64	-0.59	-0.64

Stiffness Value	u3	fixed						
	r2	free						
		Strain				Deflection		
		Girder 3 Top	Girder 4 Top	Girder 5 Middle	Girder 5 Top	Girder 3	Girder 4	Girder 5
	2001LC1ALL	311.85	198.93	228.47	179.05	-0.28	-0.40	-0.44
	2001LC2ALL	312.51	200.10	225.14	183.23	-0.31	-0.43	-0.42
	2001LC3ALL	313.13	202.73	226.30	185.36	-0.26	-0.36	-0.31
	2001LC4ALL	315.62	205.03	226.79	187.99	-0.24	-0.20	-0.24

Table G-9: 2001 Manual Parameter Estimation Results

Table G-10 shows the results from the 2008 manual parameter estimating runs. As was done in the 2001 data, the first analysis run maintain initially modeled bridge conditions and only the load was changed. This trend is similar to the trend noted in the 2001 data, where Girder 3

modeled and measured response were in different directions, and in this load test Girder 4 also had the different directions. Girder 5 strain values are in the correct orientation, however, are significantly less in the modeled data when compared to the measured response. The 2008 runs, were analyzed using the same protocol as for the previous load tests. The best run seemed to be the fixed axial and free rotation condition. This is what would be expected as the elastomeric bearings begin to experience hardening, after eight years of service. However, the best fit in deflection occurred when the axial and rotational stiffness values were reduced.

SAP Relative Strain				
	Girder 3 Top	*Girder 4 Top*	*Girder 5 Middle*	*Girder 5 Top*
u3 46833		***u2 224651.5***		
2008LC1ALL	-40.12	-23.28	36.50	43.76
2008LC2ALL	-38.53	-21.94	36.99	46.07
2008LC3ALL	-37.11	-21.71	37.25	46.18
2008LC4ALL	-33.33	-19.35	40.35	51.71
u3 5000		***u2 5000***		
2008LC1ALL	-54.39	-37.54	-5.50	29.35
2008LC2ALL	-52.76	-36.16	-4.95	31.70
2008LC3ALL	-51.32	-35.90	-4.63	31.83
2008LC4ALL	-47.41	-33.42	-1.24	37.49
u3 1000000		***u2 1000000***		
2008LC1ALL	-38.00	-21.15	42.98	45.91
2008LC2ALL	-36.46	-19.86	43.43	48.18
2008LC3ALL	-35.07	-19.66	43.67	48.25
2008LC4ALL	-31.43	-17.44	46.64	53.64
u3 fixed		***u2 fixed***		
2008LC1ALL	-44.83	-27.98	39.09	39.04
2008LC2ALL	-44.95	-28.35	38.52	39.63
2008LC3ALL	-44.72	-29.31	38.06	38.55
2008LC4ALL	-45.96	-31.98	38.06	39.04
u3 fixed		***u2 free***		
2008LC1ALL	-37.64	-20.79	43.47	46.28
2008LC2ALL	-36.04	-19.44	43.95	48.61
2008LC3ALL	-34.62	-19.20	44.21	48.71
2008LC4ALL	-30.81	-16.82	47.28	54.27

Measured Relative Strain				
	Channel 32 *3gc* *1002965* *Girder 3* *Top*	*Channel 3* *gg1* *1003038* *Girder 4* *Top*	*Channel 5* *gg3* *1002992* *Girder 5* *Middle*	*Channel 6* *gg4* *1003137* *Girder 5* *Top*
2008LC1ALL	-104.11	123.41	171.79	70.03
2008LC2ALL	-100.22	127.55	176.26	74.74
2008LC3ALL	-97.61	129.98	175.18	78.42
2008LC4ALL	-85.22	142.08	188.29	90.21

2008 Runs

Stiffness Value	**u3**	**46833**						
	r2	**224651.5**						
		Strain				***Deflection***		
		Girder 3 *Top*	*Girder 4* *Top*	*Girder 5* *Middle*	*Girder 5* *Top*	*Girder 3*	*Girder 4*	*Girder 5*
	2008LC1ALL	-63.99	146.69	135.29	26.27	-0.67	-0.69	-0.81
	2008LC2ALL	-61.69	149.49	139.26	28.67	-0.72	-0.63	-0.79
	2008LC3ALL	-60.50	151.68	137.93	32.25	-0.44	-0.66	-0.74
	2008LC4ALL	-51.89	161.43	147.94	38.50	-0.61	-0.71	-0.69
Stiffness Value	**u3**	**5000**						
	r2	**5000**						
		Strain				***Deflection***		
		Girder 3 *Top*	*Girder 4* *Top*	*Girder 5* *Middle*	*Girder 5* *Top*	*Girder 3*	*Girder 4*	*Girder 5*
	2008LC1ALL	-49.73	160.94	177.29	40.68	-0.13	-0.15	-0.27
	2008LC2ALL	-47.46	163.71	181.20	43.05	-0.18	-0.09	-0.25
	2008LC3ALL	-46.29	165.88	179.81	46.59	0.10	-0.12	-0.20
	2008LC4ALL	-37.81	175.50	189.53	52.72	-0.08	-0.17	-0.15
Stiffness Value	**u3**	**1000000**						
	r2	**1000000**						
		Strain				***Deflection***		
		Girder 3 *Top*	*Girder 4* *Top*	*Girder 5* *Middle*	*Girder 5* *Top*	*Girder 3*	*Girder 4*	*Girder 5*
	2008LC1ALL	-66.11	144.56	128.81	24.12	-0.76	-0.78	-0.90
	2008LC2ALL	-63.77	147.41	132.82	26.56	-0.80	-0.71	-0.87
	2008LC3ALL	-62.54	149.64	131.52	30.17	-0.53	-0.74	-0.82
	2008LC4ALL	-53.79	159.53	141.65	36.56	-0.70	-0.79	-0.77
Stiffness Value	**u3**	**fixed**						
	r2	**fixed**						
		Strain				***Deflection***		
		Girder 3 *Top*	*Girder 4* *Top*	*Girder 5* *Middle*	*Girder 5* *Top*	*Girder 3*	*Girder 4*	*Girder 5*
	2008LC1ALL	-59.29	151.39	132.70	30.99	-0.81	-0.83	-0.95
	2008LC2ALL	-55.28	155.90	137.73	35.11	-0.87	-0.78	-0.94
	2008LC3ALL	-52.89	159.29	137.13	39.88	-0.61	-0.82	-0.90
	2008LC4ALL	-39.26	174.06	150.23	51.17	-0.81	-0.91	-0.89
Stiffness Value	**u3**	**fixed**						
	r2	**free**						
		Strain				***Deflection***		
		Girder 3 *Top*	*Girder 4* *Top*	*Girder 5* *Middle*	*Girder 5* *Top*	*Girder 3*	*Girder 4*	*Girder 5*
	2008LC1ALL	-66.48	144.20	128.33	23.75	-0.76	-0.78	-0.90
	2008LC2ALL	-64.19	146.99	132.31	26.14	-0.80	-0.72	-0.88
	2008LC3ALL	-63.00	149.18	130.98	29.71	-0.53	-0.75	-0.83
	2008LC4ALL	-54.41	158.91	141.02	35.94	-0.70	-0.79	-0.77

Table G-10: 2008 Manual Parameter Estimation Results

Conclusions on Manual Parameter Estimating Results

The results from the manual parameter estimation offer a variety of different contributions. Changing attributes in the model does have an effect on the behavior of the bridge model. This can be seen in the 2000 runs and throughout the process as bearing pad stiffness is altered. The analysis of the 2001 data shows that a factor was not accurately captured by the structural model when compared to the bridge response. Reasons for this could be a change in material properties due to the temperature or the abutments and ground conditions changing due to thermal and seasonal effects. The analysis and model updating using the 2008 data produced results that were closer but still not ideal. This shows how much of an effect environmental factors have when conducting bridge tests.

When the model is run through MUSTANG, properties such as moment of inertia and modulus of elasticity will be easily modified to see if those parameters have a larger effect on the response of the model. Including the abutment and ground conditions into the structural model and then performing parameter estimation could also give great insight into the structural response exhibited by the bridge-foundation system in the field. Digital imaging can be used to assess the impact of the abutments on the structural response of the bridge. By collected deflection and rotation throughout the year, the movement of the abutment could be input as boundary condition settlement for structural analysis of the bridge structure for SHM and bridge maintenance. This can then be correlated to change in structural response of the bridge.

Optimal Conditions

As with most research projects, conditions are not always ideal and therefore the desired results are not achieved. If there was enough data to do an empirical correction for all recorded structural response data, it would be interesting to see the results of the manual parameter

estimation. Also, if the initial strain readings were recorded and a benchmark model would be able to be calibrated using that initial data, it is possible that more accurate boundary condition estimation could have been calculated. The parameter estimation using MUSTANG will put a lot of work into getting the 2008 load test model to accurately capture the structural response for all load cases. Once that model is calibrated to that data, it will continue on to the following two years.

APPENDIX H – PAPERS/PRESENTATIONS RELATED TO THIS RESEARCH

1. **Santini-Bell, E. M.** and *Sipple, J.D.* (2009). "Integrating Baseline Structural Modeling, Structural Health Monitoring and Intelligent Transportation Systems for Condition Assessment of In-service Bridges," *Accepted for publication in the Department of Homeland Security: Aging Infrastructure.*

2. **Santini-Bell, E. M.** and *Sipple, J.D.* (2009). "Special Topics Studies for Baseline Structural Modeling for Condition Assessment of In-Service Bridge," Safety and Reliability of Bridge Structures, ed. Khaled M. Mahmoud, CRC Press, pp. 273-289.

3. *Sipple, J.D.* and **Santini-Bell, E. M.** (2009). "Accounting for the Impact of Thermal Loads in Nondestructive Bridge Testing", *Proceedings of the 2009 TRB Annual Meeting*, Washington, DC, January 2009, (09-2002).

Additional Presentation Related To This Research.

4. *Sipple, J.D.* and **Santini-Bell, E. M.** (2009). "Structural Identification for Evaluation of CFRP Reinforcement for use on New Hampshire Bridges", *Proceedings of the 2009 Structures Congress*, ASCE, Austin, Texas, April 30-May 2.
5. **Santini-Bell, E.**, *Sipple, J.*, and Yost, J. (2008). "Long-Term Thermal Performance of a CFRP-Reinforced Bridge Deck," *Proceedings of the Structures Congress*, ASCE, Vancouver, April 24-26, 2008.